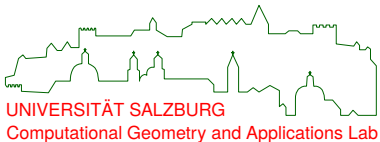


# Computational Geometry (WS 2024/25)

Martin Held

FB Informatik  
Universität Salzburg  
A-5020 Salzburg, Austria  
[held@cs.sbg.ac.at](mailto:held@cs.sbg.ac.at)

October 3, 2024



**Instructor (VO+PS):** M. Held.

**Email:** [held@cs.sbg.ac.at](mailto:held@cs.sbg.ac.at).

**Base-URL:** [www.cosy.sbg.ac.at/~held](http://www.cosy.sbg.ac.at/~held).

**Office:** PLUS, FB Informatik, Rm. 1.20, Jakob-Haringer Str. 2,  
5020 Salzburg-Itzling.

**Phone number (office):** (0662) 8044-6304.

**Phone number (secr.):** (0662) 8044-6300.



**URL of course (VO+PS):** [Base-URL/teaching/compgeo/comp\\_geo.html](#).

**Lecture times (VO):** Friday 12<sup>15</sup>–14<sup>15</sup>.

**Venue (VO):** PLUS, FB Informatik, T03, Jakob-Haringer Str. 2, 5020 Salzburg-Itzling.

**Lecture times (PS):** Friday 11<sup>00</sup>–12<sup>00</sup>.

**Venue (PS):** PLUS, FB Informatik, T03, Jakob-Haringer Str. 2, 5020 Salzburg-Itzling.

**Note** — PS is graded according to continuous-assessment mode!  
— regular attendance is compulsory!

## Electronic Slides and Online Material

In addition to these slides, you are encouraged to consult the WWW home-page of this lecture:

[www.cosy.sbg.ac.at/~held/teaching/compgeo/comp\\_geo.html](http://www.cosy.sbg.ac.at/~held/teaching/compgeo/comp_geo.html).

In particular, this WWW page contains up-to-date information on the course, plus links to online notes, slides and (possibly) sample code.



## A Few Words of Warning

- I hope that these slides will serve as a practice-minded introduction to various aspects of computational geometry. I would like to warn you explicitly not to regard these slides as the sole source of information on the topics of my course. It may and will happen that I'll use the lecture for talking about subtle details that need not be covered in these slides! In particular, the slides won't contain all sample calculations, proofs of theorems, demonstrations of algorithms, or solutions to problems posed during my lecture. That is, by making these slides available to you I do not intend to encourage you to attend the lecture on an irregular basis.
- See also [In Praise of Lectures](#) by T.W. Körner.
- *A basic knowledge of algorithms, data structures and discrete mathematics*, as taught typically in undergraduate courses, should suffice to take this course. It is my sincere intention to start at such a hypothetical level of "typical prior undergrad knowledge". Still, it is obvious that different educational backgrounds will result in different levels of prior knowledge. Hence, you might realize that you do already know some items covered in this course, while you lack a decent understanding of some items which I seem to presuppose. In such a case I do expect you to refresh or fill in those missing items on your own!

## Acknowledgments

These slides are partially based on notes and slides transcribed by various students — most notably Elias Pschernig, Christian Spielberger, Werner Weiser and Franz Wilhelmstötter — for previous courses on “Algorithmische Geometrie”. Some figures were derived from figures originally prepared by students of my lecture “Wissenschaftliche Arbeitstechniken und Präsentation”, while others were taken from papers and slides co-authored with members of my research group, such as Günther Eder, Stefan Huber, Stefan de Lorenzo, Willi Mann, Peter Palfrader, Christian Spielberger. I would like to express my thankfulness to all of them for their help. This revision and extension was carried out by myself, and I am responsible for any errors.

I am also happy to acknowledge that we benefited from material published by colleagues on diverse topics that are partially covered in this lecture. While some of the material used for this lecture was originally presented in traditional-style publications (such as textbooks), some other material has its roots in non-standard publication outlets (such as online documentations, electronic course notes, or user manuals).

Salzburg, July 2024

Martin Held  
  
Computational Geometry and Applications Lab

## Legal Fine Print and Disclaimer

To the best of our knowledge, these slides do not violate or infringe upon somebody else's copyrights. If copyrighted material appears in these slides then it was considered to be available in a non-profit manner and as an educational tool for teaching at an academic institution, within the limits of the "fair use" policy. For copyrighted material we strive to give references to the copyright holders (if known). Of course, any trademarks mentioned in these slides are properties of their respective owners.

Please note that these slides are copyrighted. The copyright holder(s) grant you the right to download and print it for your personal use. Any other use, including non-profit instructional use and re-distribution in electronic or printed form of significant portions of it, beyond the limits of "fair use", requires the explicit permission of the copyright holder(s). All rights reserved.

These slides are made available without warrant of any kind, either express or implied, including but not limited to the implied warranties of merchantability and fitness for a particular purpose. In no event shall the copyright holder(s) and/or their respective employers be liable for any special, indirect or consequential damages or any damages whatsoever resulting from loss of use, data or profits, arising out of or in connection with the use of information provided in these slides.

## Recommended Textbooks

-  F.P. Preparata and M.I. Shamos.  
*Computational Geometry – An Introduction.*  
Springer-Verlag, 3rd edition, Aug 1993. ISBN 978-0387961316.
-  J. O'Rourke.  
*Computational Geometry in C.*  
Cambridge University Press, 2nd edition, 2000. ISBN 978-0521649766.  
<https://doi.org/10.1017/CBO9780511804120>.
-  M. de Berg, O. Cheong, M. van Kreveld, and M. Overmars.  
*Computational Geometry. Algorithms and Applications.*  
Springer-Verlag, 3rd rev. edition, March 2008. ISBN 978-3540779735.
-  F. Aurenhammer, R. Klein and D.-T. Lee.  
*Voronoi Diagrams and Delaunay Triangulations.*  
World Scientific Publ., Aug 2013. ISBN 978-981-4447-63-8.
-  C.D. Toth, J. O'Rourke, J.E. Goodman.  
*Handbook of Discrete and Computational Geometry.*  
CRC Press, Nov 2017. ISBN 9781498711395.

- 1 Introduction
- 2 Geometric Concepts and Paradigms
- 3 Geometric Searching
- 4 Convex Hulls
- 5 Voronoi Diagrams of Points
- 6 Skeletal Structures
- 7 Triangulations
- 8 Robustness Problems and Real-World Issues

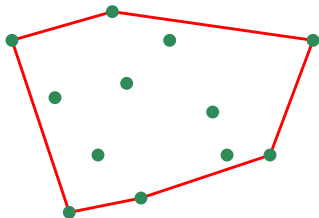
1

## Introduction

- Motivation
- History
- Notation
- Math Basics

## Motivation: Convex Hull

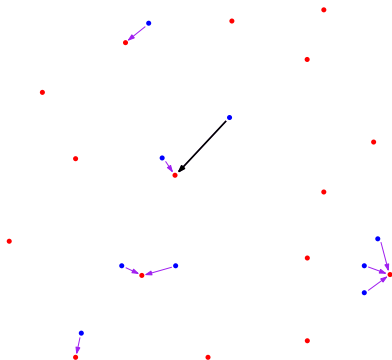
- Given is a set  $S$  of  $n$  points in  $\mathbb{R}^2$ .
- Question: How efficiently can we determine the convex hull of  $S$ ?



- Answer: The convex hull of  $S$  can be computed in  $O(n \log n)$  steps.
- Lower bound: In the worst case,  $\Omega(n \log n)$  steps will be necessary.

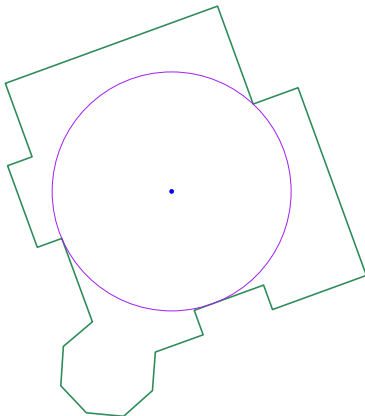
## Motivation: Distance between Point Sets

- Let  $S_1$  and  $S_2$  be sets of blue and red points in  $\mathbb{R}^2$ .
- For each blue point, consider the distance to its closest red point.
- Question: What is the maximum of these distances?
- Answer: This is the so-called directed Hausdorff distance, and it can be obtained in  $O(n \log n)$  time, where  $n := \max\{|S_1|, |S_2|\}$ .



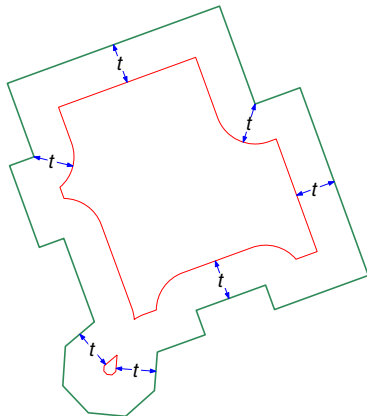
## Motivation: Maximum Inscribed Circle

- Given is a simple polygon  $\mathcal{P}$ . A circle is called inscribed to  $\mathcal{P}$  if it lies completely inside of  $\mathcal{P}$ .
- Question: How efficiently can we determine a maximum inscribed circle?
- Answer: In theory, a maximum inscribed circle can be computed in time linear in the number  $n$  of vertices of  $\mathcal{P}$ . (And  $O(n \log n)$  time is achievable in practice.)



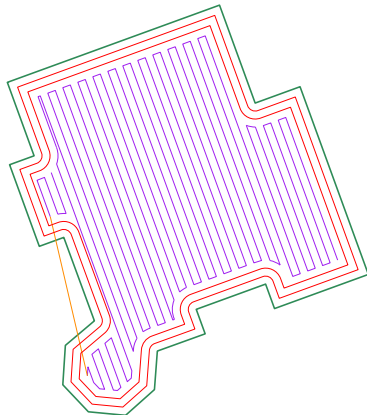
## Motivation: Offset Pattern

- Given is a simple polygon  $\mathcal{P}$ .
- Question: How can we compute offset patterns reliably and efficiently? How can we compute even just one offset?
- Answer: If the Voronoi diagram of the input is known, then all offset curves of one offset can be determined in  $O(n)$  time.



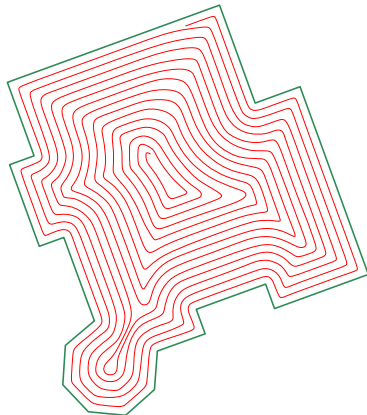
## Motivation: Tool Path

- Given is a simple **polygon**  $\mathcal{P}$ .
- Question: How can we compute a tool path — e.g., for machining or 3D printing — inside of  $\mathcal{P}$  reliably and efficiently?
- Answer: Again, this can be done with the help of Voronoi diagrams.



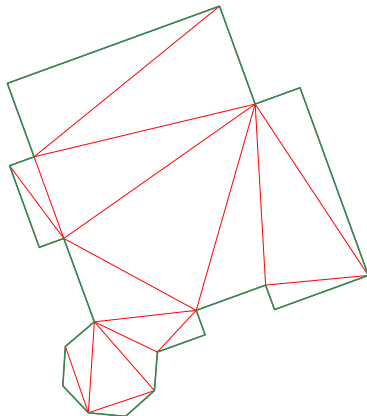
## Motivation: Smooth Tool Path

- Given is a simple polygon  $\mathcal{P}$ .
- Question: How can we compute a smooth tool path — e.g., for high-speed machining — inside of  $\mathcal{P}$  reliably and efficiently?
- Answer: Again, this can be done with the help of Voronoi diagrams.



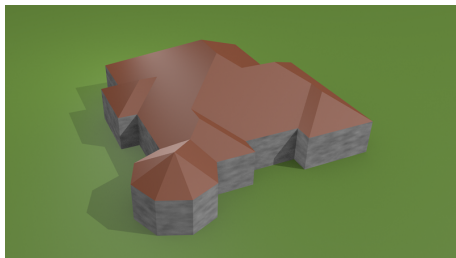
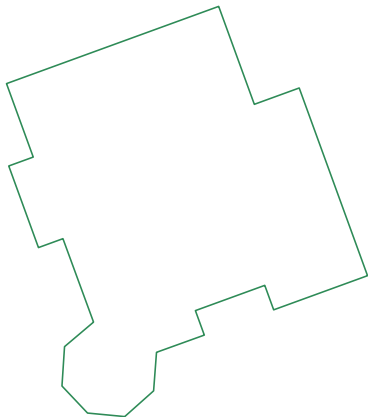
## Motivation: Triangulation

- Given is a simple **polygon**  $\mathcal{P}$ .
- Question: How can we compute a triangulation of  $\mathcal{P}$  reliably and efficiently?
- Answer: In theory, a triangulation can be computed in time linear in the number  $n$  of vertices of  $\mathcal{P}$ . (And slightly super-linear time is achievable in practice.)



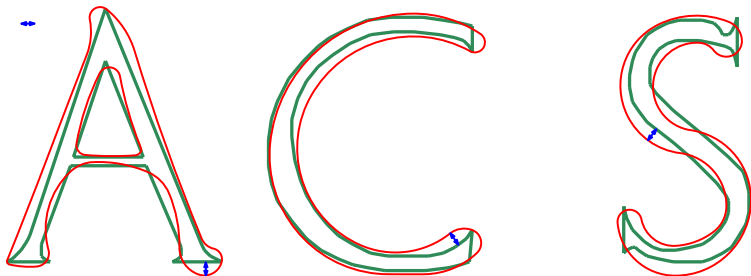
## Motivation: Automatic Roof Construction

- Given is a simple **polygon**  $\mathcal{P}$ , which we consider as the cross-section of a house.
- Question: How can we compute a roof for  $\mathcal{P}$ ?
- Answer: This can be done with the help of straight skeletons.



## Motivation: Approximation of Polygonal Profiles

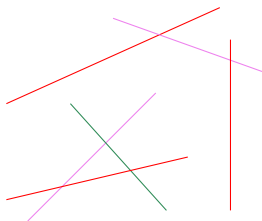
- How can we solve the following approximation problem?
  - For a set of planar (polygonal) profiles,
  - and an approximation threshold given,
  - compute an approximation such that the approximation threshold is not exceeded.



- Approximations can be obtained by biarc or B-spline curves, based on tolerance zones generated by means of Voronoi diagrams.

## Motivation: Minimum Plane Partition

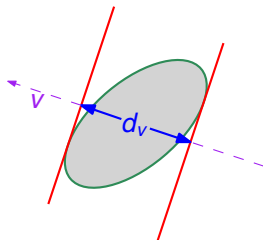
- CG:SHOP Geometric Optimization Challenge 2022: Given is a set  $S$  of  $n$  line segments in the plane.
- We seek a partitioning of  $S$  into a minimum number of  $k$  subsets  $S_1, \dots, S_k$  such that, for all  $1 \leq i \leq k$ , the line segments of  $S_i$  do not intersect pairwise.



- Question: How can we check in  $o(n^2)$  time whether any pair of line segments of  $S$  intersect? How can we determine all intersections efficiently?
- Answer: This can be done with the help of a plane sweep.

## Geometric Intuition: Roundness of a Convex Shape

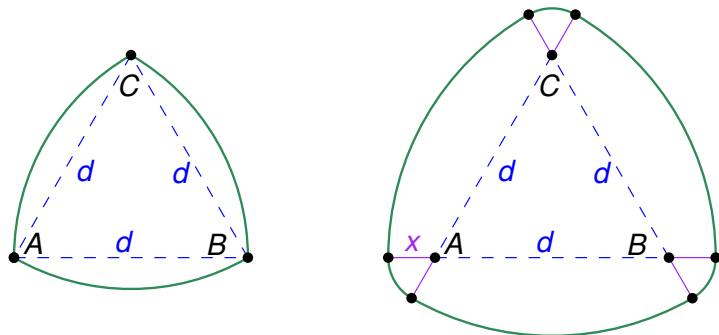
- We define the width of a planar shape relative to a direction vector  $v$  as the minimum distance  $d_v$  of its two parallel lines of support normal to the direction vector such that the shape is enclosed (“caliper probe”).



- Question: Can we conclude that the shape resembles a circle of diameter  $d$  if an arbitrarily large number of caliper probes all yield a uniform width  $d$  (irrespective of the direction vectors chosen)?

## Geometric Intuition: Roundness of a Convex Shape

- Answer: No!! Even an infinite number of caliper probes all would yield a uniform width  $d$  for a Reuleaux triangle!



- Apparently, three caliper probes were applied when checking parts of the Challenger's solid-fuel booster rockets for roundness. (R. Feynman (1988): "What do you care what other people think?")

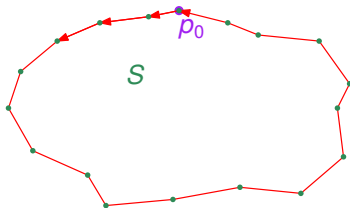
# Geometric Intuition or “It’s Obvious!?”

## Problem: EUCLIDEAN TRAVELING SALESMAN PROBLEM (ETSP)

**Input:** A set  $S$  of  $n$  points in the Euclidean plane.

**Output:** A cycle of minimal length that starts and ends in one point of  $S$  and visits all points of  $S$ .

- Natural strategy to solve an instance of ETSP:
  - 1 Pick a point  $p_0 \in S$ .
  - 2 Find its nearest neighbor  $p' \in S$ , move to  $p'$ , and let  $p := p'$ .
  - 3 Continue from  $p$  to the nearest unvisited neighbor  $p' \in S$  of  $p$ , and let  $p := p'$ .
  - 4 Repeat the last step until all points have been visited, and return back to  $p_0$ .

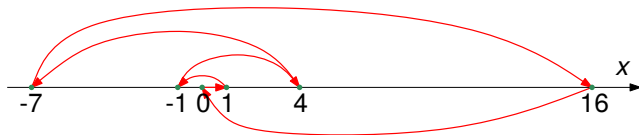


## Geometric Intuition or “It’s Obvious!”

- The strategy to always pick the shortest missing link can be seen as a *greedy* strategy.
- It is obvious that this strategy will always solve ETSP, isn’t it?
- Well . . . The tour computed need not even be close in length to the optimum tour!
- In the example, the tour computed has length 58, while the optimum tour has length 46!

### Geometric intuition . . .

. . . is important, but may not replace formal reasoning. Intuition might misguide, and computational geometry without formal reasoning does not make sense.



# History of Computational Geometry

- 1000 BCE: Length, area and volume are known for simple objects (cube, box, cylinder).
- Antiquity: Move from empirical mathematics to deductive mathematics.
- Thales of Milet ( $\approx 600$  BCE): He proved(!) that the two base angles of an isosceles triangle are identical.
- Euclid of Alexandria ( $\approx 300$  BCE): “The Elements”.
  - definitions,
  - five postulates,
  - five axioms,
  - 115 propositions.

# History of Computational Geometry

- Da Vinci (1452–1519) and others: Introduced perspective and projective geometry.
- Descartes (1596–1650) and P. de Fermat (1607–1665): Coordinates and the foundation of analytical geometry.
- Riemann (1826–1866): Differential geometry.
- Poincaré (1854–1912) and D. Hilbert (1862–1943): Axiom-based mathematics, proved consistency of axioms.
  
- Knuth: “The Art of Computer Programming” published 1968–1973.
  
- Bézier, Forrest, Riesenfeld: Modeling of spline curves and surfaces called “computational geometry”.
- Minsky and Papert: Book entitled “Perceptrons” with chapter on “computational geometry”: Which geometric properties of a figure can be recognized with neural networks?

## Birth of today's computational geometry

Shamos (1978): PhD thesis “Computational Geometry” at Yale University, USA.

- Numbers:
  - The set  $\{1, 2, 3, \dots\}$  of natural numbers is denoted by  $\mathbb{N}$ , with  $\mathbb{N}_0 := \mathbb{N} \cup \{0\}$ .
  - The set  $\{2, 3, 5, 7, 11, 13, \dots\} \subset \mathbb{N}$  of prime numbers is denoted by  $\mathbb{P}$ .
  - The (positive and negative) integers are denoted by  $\mathbb{Z}$ .
  - $\mathbb{Z}_n := \{0, 1, 2, \dots, n-1\}$  and  $\mathbb{Z}_n^+ := \{1, 2, \dots, n-1\}$  for  $n \in \mathbb{N}$ .
  - The reals are denoted by  $\mathbb{R}$ ; the non-negative reals are denoted by  $\mathbb{R}_0^+$ , and the positive reals by  $\mathbb{R}^+$ .
- Open or closed intervals  $I \subset \mathbb{R}$  are denoted using square brackets: e.g.,  $I_1 = [a_1, b_1]$  or  $I_2 = [a_2, b_2[$ , with  $a_1, a_2, b_1, b_2 \in \mathbb{R}$ , where the right-hand “[” indicates that the value  $b_2$  is not included in  $I_2$ .
- The set of all elements  $a \in A$  with property  $P(a)$ , for some set  $A$  and some predicate  $P$ , is denoted by

$$\{x \in A : P(x)\} \quad \text{or} \quad \{x : x \in A \wedge P(x)\}$$

or

$$\{x \in A \mid P(x)\} \quad \text{or} \quad \{x \mid x \in A \wedge P(x)\}.$$

- Bold capital letters, such as  $\mathbf{M}$ , are used for matrices.
- The set of all (real)  $m \times n$  matrices is denoted by  $M_{m \times n}$ .

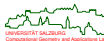
- Points are denoted by letters written in italics:  $p, q$  or, occasionally,  $P, Q$ . We do not distinguish between a point and its position vector.
- The coordinates of a vector are denoted by using indices (or numbers): e.g.,  $v = (v_x, v_y)$  for  $v \in \mathbb{R}^2$ , or  $v = (v_1, v_2, \dots, v_n)$  for  $v \in \mathbb{R}^n$ .
- In order to state  $v \in \mathbb{R}^n$  in vector form we will mix column and row vectors freely unless a specific form is required, such as for matrix multiplication.
- The vector dot product of two vectors  $v, w \in \mathbb{R}^n$  is denoted by  $\langle v, w \rangle$ . That is,  $\langle v, w \rangle = \sum_{i=1}^n v_i \cdot w_i$  for  $v, w \in \mathbb{R}^n$ .
- The vector cross-product (in  $\mathbb{R}^3$ ) is denoted by a cross:  $v \times w$ .
- The length of a vector  $v$  is denoted by  $\|v\|$ .
- The straight-line segment between the points  $p$  and  $q$  is denoted by  $\overline{pq}$ .
- The supporting line of the points  $p$  and  $q$  is denoted by  $\ell(p, q)$ .

## Definition 1 (Polygonal curve, Dt.: Polygonzug)

Consider the sequence of points  $p_0, p_1, p_2, \dots, p_n \in \mathbb{R}^d$ , for some  $d, n \in \mathbb{N}_0$ . The *polygonal curve* (or *polygonal chain*, *polygonal profile*) specified by these points (“vertices”) is given by  $\gamma: [0, n] \rightarrow \mathbb{R}^d$  with

$$\gamma(t) := p_i + (t - i) \cdot (p_{i+1} - p_i) \quad \text{if } t \in [i, i + 1] \text{ for } i \in \{1, 2, \dots, n - 1\}.$$

- Hence, a polygonal curve is a sequence of finitely many vertices connected by straight-line segments such that each segment (except for the first) starts at the end of the previous segment.
- Unless stated otherwise, we will always assume that all vertices of a polygonal curve are co-planar, i.e., that the polygonal curve is plane. The default plane is  $\mathbb{R}^2$ .
- It is common to extend this definition by allowing  $n = 0$ , in which case we get a single point.



## Definition 2 (Polygon)

For  $n \in \mathbb{N}$  with  $n \geq 3$ , a *polygon* with vertices  $p_0, p_1, p_2, \dots, p_n \in \mathbb{R}^d$ , aka *n-gon*, is a polygonal curve such that  $p_0 = p_n$ .

## Definition 3 (Simple polygon, Dt.: einfaches Polygon)

An *n-gon* is *simple* if it admits a simple parametrization.

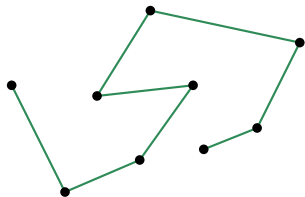
- If a plane polygon  $\mathcal{P}$  is simple then, by the Jordan Curve Theorem, it splits the plane into two regions, one of which is bounded.
- In this case it is common to be a bit liberal and use the term “polygon” for either the (simple) polygonal curve  $\mathcal{P}$  or for the entire region bounded by  $\mathcal{P}$ ; the actual meaning has to be inferred from the context.
- If  $\mathcal{P}$  is regarded to be only the simple polygonal curve then the bounded region (without  $\mathcal{P}$  itself) is called the polygon’s *interior*, and points within that region are said to be *inside* of  $\mathcal{P}$ .

## Definition 4 (Planar straight-line graph)

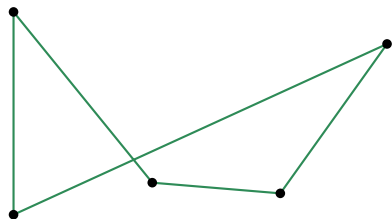
A *planar straight-line graph* (PSLG) is a finite collection of isolated vertices and straight-line segments such that

- each two segments intersect only in vertices shared by both of them,
  - no segment passes through a vertex other than one of its two end-points.
- 
- Hence, a PSLG is an embedding of a planar graph such that all its edges are drawn as straight-line segments.
  - Aka: Plane geometric graph.
  - Hence, simple polygonal curves and simple polygons are special PSLGs.
  - Of course, Euler's Theorem applies to the faces, edges and vertices of a PSLG.

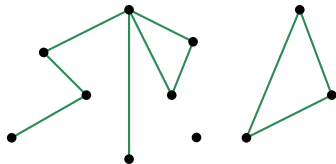
# Sample Polygonal Chains and PSLGs



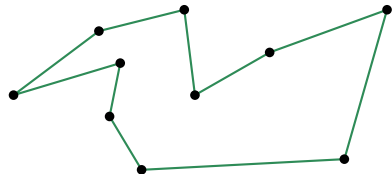
polygonal curve



polygon, not simple



planar straight-line graph



simple polygon

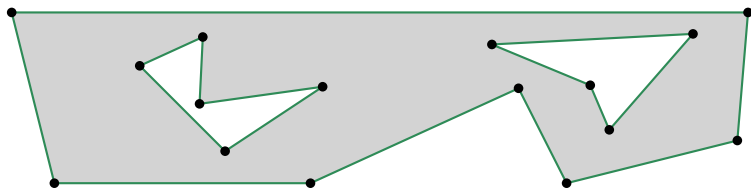
# Polygonal Region

## Definition 5 (Polygonal region)

A *polygonal region* is a (possibly) multiply-connected but connected subset of  $\mathbb{R}^2$  that is bounded by  $k$  simple polygons  $\mathcal{P}_1, \mathcal{P}_2, \dots, \mathcal{P}_k$ , for some  $k \in \mathbb{N}$ , such that

- 1 no pair of polygons (seen as curves) intersect,
- 2 the polygons  $\mathcal{P}_2, \dots, \mathcal{P}_k$  lie in the interior of  $\mathcal{P}_1$ ,
- 3 for  $2 \leq i, j \leq k$ , the polygon  $\mathcal{P}_i$  does not lie in the interior of the polygon  $\mathcal{P}_j$ .

The polygon  $\mathcal{P}_1$  is called *outer polygon* and the polygons  $\mathcal{P}_2, \dots, \mathcal{P}_k$  are called *islands* or *holes*.



## Definition 6 (Polyhedron, Dt.: Polyeder)

A *polyhedron* in  $\mathbb{R}^3$  is either

- a (possibly unbounded) solid given by the intersection of finitely many halfspaces, or
  - a connected bounded solid whose (closed manifold) boundary is formed by a finite collection of plane polygons (“faces”) such that
    - 1 each vertex is incident to at least three edges and faces,
    - 2 each edge is shared by exactly two faces,
    - 3 each two faces intersect only in vertices and edges shared by both of them,
    - 4 the faces that share a vertex form a cyclic chain of polygons in which every pair of consecutive polygons shares an edge.
- Note: Plural of “polyhedron” is “polyhedra”.
- Recall that Euler’s Formula  $v - e + f = 2$  holds for the vertices, edges and faces of a polyhedron.

# Polyhedron

- Unfortunately, even in  $\mathbb{R}^3$  there is no universal agreement over how to define the analogue to a polygon in  $\mathbb{R}^3$  . . .
- The situation gets worse once different fields of mathematics and computer science are considered!

## Grünbaum (1994)

“The Original Sin in the theory of polyhedra goes back to Euclid, . . . and many others, . . . at each stage . . . the writers failed to define what are the polyhedra.”

## Polyhedron versus Polytope

- 1 For convex solids, some authors (in some fields of mathematics) prefer to use the term “polytope” for a bounded polyhedron, whereas “polyhedron” is a generic convex object.
- 2 From this point of view, a polyhedron is the intersection of a finite number of halfspaces and is defined by its faces whereas a polytope is the convex hull of a finite number of points and is defined by its vertices.

## Definition 7 (Logarithm)

The *logarithm* of a positive real number  $x \in \mathbb{R}^+$  with respect to a base  $b$ , which is a positive real number not equal to 1, is the unique solution  $y$  of the equation  $b^y = x$ . It is denoted by  $\log_b x$ .

- Hence, it is the exponent by which  $b$  must be raised to yield  $x$ .
- Common bases:

$$\text{ld } x := \log_2 x \quad \ln x := \log_e x \quad \text{with} \quad e := \lim_{n \rightarrow \infty} \left(1 + \frac{1}{n}\right)^n \approx 2.71828 \dots$$

## Lemma 8

Let  $x, y, p \in \mathbb{R}^+$  and  $b \in \mathbb{R}^+ \setminus \{1\}$ .

$$\log_b(xy) = \log_b(x) + \log_b(y) \quad \log_b\left(\frac{x}{y}\right) = \log_b(x) - \log_b(y)$$

$$\log_b(x^p) = p \log_b(x) \quad \log_b(\sqrt[p]{x}) = \frac{\log_b(x)}{p}$$

## Lemma 9 (Change of base)

Let  $x \in \mathbb{R}^+$  and  $\alpha, \beta \in \mathbb{R}^+ \setminus \{1\}$ . Then  $\log_\alpha(x)$  and  $\log_\beta(x)$  differ only by a multiplicative constant:

$$\log_\alpha(x) = \frac{1}{\log_\beta(\alpha)} \cdot \log_\beta(x)$$

## Convention

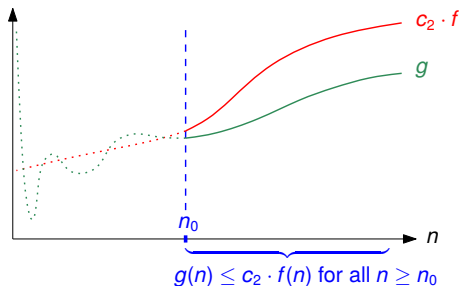
In this course,  $\log n$  will always denote the logarithm of  $n$  to the base 2, i.e.,  $\log n := \log_2 n$ .

# Asymptotic Notation: Big-O

## Definition 10 (Big-O, Dt.: Groß-O)

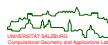
Let  $f: \mathbb{N} \rightarrow \mathbb{R}^+$ . Then the set  $O(f)$  is defined as

$$O(f) := \{g: \mathbb{N} \rightarrow \mathbb{R}^+ \mid \exists c_2 \in \mathbb{R}^+ \exists n_0 \in \mathbb{N} \forall n \geq n_0 \quad g(n) \leq c_2 \cdot f(n)\}.$$



- Equivalent definition used by some authors:

$$O(f) := \left\{ g: \mathbb{N} \rightarrow \mathbb{R}^+ \mid \exists c_2 \in \mathbb{R}^+ \exists n_0 \in \mathbb{N} \forall n \geq n_0 \quad \frac{g(n)}{f(n)} \leq c_2 \right\}.$$

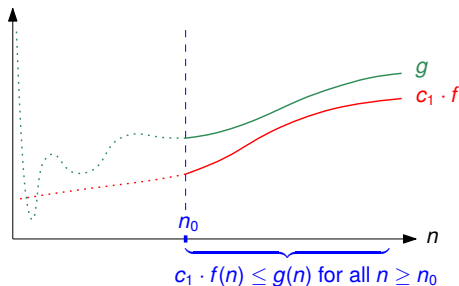


# Asymptotic Notation: Big-Omega

## Definition 11 (Big-Omega, Dt.: Groß-Omega)

Let  $f: \mathbb{N} \rightarrow \mathbb{R}^+$ . Then the set  $\Omega(f)$  is defined as

$$\Omega(f) := \left\{ g: \mathbb{N} \rightarrow \mathbb{R}^+ \mid \exists c_1 \in \mathbb{R}^+ \quad \exists n_0 \in \mathbb{N} \quad \forall n \geq n_0 \quad c_1 \cdot f(n) \leq g(n) \right\}.$$



- Equivalently,

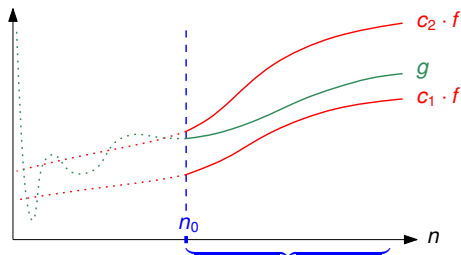
$$\Omega(f) := \left\{ g: \mathbb{N} \rightarrow \mathbb{R}^+ \mid \exists c_1 \in \mathbb{R}^+ \quad \exists n_0 \in \mathbb{N} \quad \forall n \geq n_0 \quad c_1 \leq \frac{g(n)}{f(n)} \right\}.$$

# Asymptotic Notation: Big-Theta

## Definition 12 (Big-Theta, Dt.: Groß-Theta)

Let  $f: \mathbb{N} \rightarrow \mathbb{R}^+$ . Then the set  $\Theta(f)$  is defined as

$$\Theta(f) := \{g: \mathbb{N} \rightarrow \mathbb{R}^+ \mid \exists c_1, c_2 \in \mathbb{R}^+ \exists n_0 \in \mathbb{N} \forall n \geq n_0 \\ c_1 \cdot f(n) \leq g(n) \leq c_2 \cdot f(n)\}.$$



$$c_1 \cdot f(n) \leq g(n) \leq c_2 \cdot f(n) \text{ for all } n \geq n_0$$

which is equivalent to  $c_1 \leq \frac{g(n)}{f(n)} \leq c_2$  for all  $n \geq n_0$

## Asymptotic Notation: Small-Oh and Small-Omega

### Definition 13 (Small-Oh, Dt.: Klein-O)

Let  $f: \mathbb{N} \rightarrow \mathbb{R}^+$ . Then the set  $o(f)$  is defined as

$$o(f) := \{g: \mathbb{N} \rightarrow \mathbb{R}^+ \mid \forall c \in \mathbb{R}^+ \exists n_0 \in \mathbb{N} \forall n \geq n_0 \quad g(n) \leq c \cdot f(n)\}.$$

### Definition 14 (Small-Omega, Dt.: Klein-Omega)

Let  $f: \mathbb{N} \rightarrow \mathbb{R}^+$ . Then the set  $\omega(f)$  is defined as

$$\omega(f) := \{g: \mathbb{N} \rightarrow \mathbb{R}^+ \mid \forall c \in \mathbb{R}^+ \exists n_0 \in \mathbb{N} \forall n \geq n_0 \quad g(n) \geq c \cdot f(n)\}.$$

- We can extend Defs. 10–14 such that  $\mathbb{N}_0$  rather than  $\mathbb{N}$  is taken as the domain (Dt.: Definitionsmenge). We can also replace the codomain (Dt.: Zielbereich)  $\mathbb{R}^+$  by  $\mathbb{R}_0^+$  (or even  $\mathbb{R}$ ) provided that all functions are eventually positive.

### Warning

The use of the equality operator “=” instead of the set operators “ $\in$ ” or “ $\subseteq$ ” to denote set membership or a subset relation is a *common abuse of notation*.

## Theorem 15

Consider constants  $n_0 \in \mathbb{N}$  and  $a \in \mathbb{N}$ ,  $b \in \mathbb{R}$  with  $b > 1$ , and a function  $f: \mathbb{N} \rightarrow \mathbb{R}_0^+$ . Let  $T: \mathbb{N} \rightarrow \mathbb{R}_0^+$  be an eventually non-decreasing function such that

$$T(n) = a \cdot T\left(\frac{n}{b}\right) + f(n)$$

for all  $n \in \mathbb{N}$  with  $n \geq n_0$ , where we interpret  $T(\frac{n}{b})$  as (a combination of)  $T(\lceil \frac{n}{b} \rceil)$  or  $T(\lfloor \frac{n}{b} \rfloor)$ .

Then we have

$$T \in \begin{cases} \Theta(f) & \text{if } \begin{cases} f \in \Omega(n^{(\log_b a)+\varepsilon}) \text{ for some } \varepsilon \in \mathbb{R}^+, \\ \text{and if the following regularity condition holds} \\ \text{for some } 0 < s < 1 \text{ and all sufficiently large } n: \\ a \cdot f(n/b) \leq s \cdot f(n), \end{cases} \\ \Theta(n^{\log_b a} \log n) & \text{if } f \in \Theta(n^{\log_b a}), \\ \Theta(n^{\log_b a}) & \text{if } f \in O(n^{(\log_b a)-\varepsilon}) \text{ for some } \varepsilon \in \mathbb{R}^+. \end{cases}$$

- This is a simplified version of the Akra-Bazzi Theorem [Akra&Bazzi 1998].

# Fibonacci Numbers

## Definition 16 (Fibonacci numbers)

For all  $n \in \mathbb{N}_0$ ,

$$F_n := \begin{cases} n & \text{if } n \leq 1, \\ F_{n-1} + F_{n-2} & \text{if } n \geq 2. \end{cases}$$

$n$	0	1	2	3	4	5	6	7	8	9	10	11	12	13	14	15
$F_n$	0	1	1	2	3	5	8	13	21	34	55	89	144	233	377	610

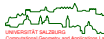
## Lemma 17

For  $n \in \mathbb{N}$  with  $n \geq 2$ :

$$F_n = \frac{1}{\sqrt{5}} \cdot \left( \frac{1 + \sqrt{5}}{2} \right)^n - \frac{1}{\sqrt{5}} \cdot \left( \frac{1 - \sqrt{5}}{2} \right)^n \geq \left( \frac{1 + \sqrt{5}}{2} \right)^{n-2}$$

- Lots of interesting mathematical properties. For instance,

$$\lim_{n \rightarrow \infty} \frac{F_{n+1}}{F_n} = \phi, \quad \text{where } \phi := \frac{1 + \sqrt{5}}{2} = 1.618 \dots \text{ is the } \textit{golden ratio}.$$



## Definition 18 (Catalan numbers)

For  $n \in \mathbb{N}_0$ ,

$$C_0 := 1 \quad \text{and} \quad C_{n+1} := \sum_{i=0}^n C_i \cdot C_{n-i}.$$

$n$	0	1	2	3	4	5	6	7	8	9	10	11
$C_n$	1	1	2	5	14	42	132	429	1430	4862	16796	58786

## Lemma 19

For  $n \in \mathbb{N}_0$ ,

$$C_n = \frac{1}{n+1} \sum_{i=0}^n \binom{n}{i}^2 = \frac{1}{n+1} \binom{2n}{n} \in \Theta\left(\frac{4^n}{n^{1.5}}\right).$$

# Harmonic Numbers

## Definition 20 (Harmonic numbers)

For  $n \in \mathbb{N}$ ,

$$H_n := 1 + \frac{1}{2} + \frac{1}{3} + \cdots + \frac{1}{n} = \sum_{k=1}^n \frac{1}{k}.$$

## Lemma 21

The sequence  $s: \mathbb{N} \rightarrow \mathbb{R}$  with

$$s_n := H_n - \ln n$$

is monotonically decreasing and convergent. Its limit is the Euler-Mascheroni constant

$$\gamma := \lim_{n \rightarrow +\infty} (H_n - \ln n) \approx 0.5772 \dots,$$

and we have

$$\ln n < H_n - \gamma < \ln(n+1), \quad \text{i.e. } H_n \in \Theta(\ln) = \Theta(\log).$$

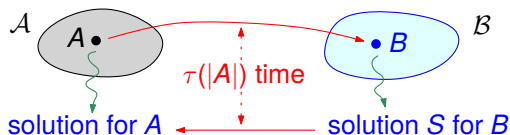


## Reduction of a Problem

### Definition 22 (Reduction)

A problem  $\mathcal{A}$  can be *reduced* (or *transformed*) to a problem  $\mathcal{B}$  if

- 1 every instance  $A$  of  $\mathcal{A}$  can be converted to an instance  $B$  of  $\mathcal{B}$ ,
- 2 a solution  $S$  for  $B$  can be computed, and
- 3  $S$  can be transformed back into a correct solution for  $A$ .



### Definition 23

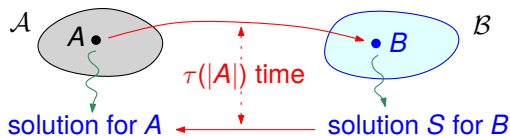
A problem  $\mathcal{A}$  is  $\tau$ -*reducible* to  $\mathcal{B}$ , denoted by  $\mathcal{A} \leq_{\tau} \mathcal{B}$ , if

- 1  $\mathcal{A}$  can be reduced to  $\mathcal{B}$ ,
- 2 for any instance  $A$  of  $\mathcal{A}$ , steps 1 and 3 of the reduction can be carried out in at most  $\tau(|A|)$  time, where  $|A|$  denotes the input size of  $A$ .

# Transfer of Complexity Bounds

## Lemma 24 (Upper bound via reduction)

Suppose that  $\mathcal{A}$  is  $\tau$ -reducible to  $\mathcal{B}$  such that the order of the input size is preserved. If problem  $\mathcal{B}$  can be solved in  $O(T)$  time, then  $\mathcal{A}$  can be solved in at most  $O(T + \tau)$  time.



## Lemma 25 (Lower bound via reduction)

Suppose that  $\mathcal{A}$  is  $\tau$ -reducible to  $\mathcal{B}$  such that the order of the input size is preserved. If problem  $\mathcal{A}$  is known to require  $\Omega(T)$  time, then  $\mathcal{B}$  requires at least  $\Omega(T - \tau)$  time.

## 2 Geometric Concepts and Paradigms

- Plane Sweep
- Arrangements
- Point-Line Duality

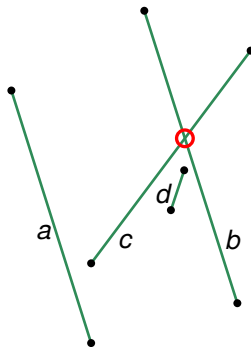
# Line Segment Intersection

## Problem: LINESEGMENTINTERSECTION

**Given:** A set  $S$  of line segments in  $\mathbb{R}^2$ .

**Decide:** Do any two segments of  $S$  intersect?

- LINESEGMENTINTERSECTION does not require us to find and report one or all intersections.
- Still, we explain how all intersections can be found.
- Stopping the algorithm at the first intersection (if one exists) yields an answer to the original problem.



# Line Segment Intersection

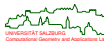
## Theorem 26 (Bentley&Ottmann (1979))

All  $k$  intersections among  $n$  line segments in  $\mathbb{R}^2$  can be detected in  $O((n + k) \log n)$  time and  $O(n)$  space, using a plane-sweep algorithm.

## Corollary 27

LINESEGMENTINTERSECTION can be solved in optimal  $O(n \log n)$  time and  $O(n)$  space for  $n$  line segments.

- Note that  $n$  line segments may yield  $\Theta(n^2)$  many intersections. Hence,  $k \in O(n^2)$ , and in the worst case the Bentley-Ottmann algorithm runs in  $\Theta(n^2 \log n)$  time.
- [Chazelle&Edelsbrunner (1992)] explain how to detect all  $k$  intersections in  $O(k + n \log n)$  time, using  $O(n + k)$  space.
- [Balaban (1995)] improves this to  $O(k + n \log n)$  time and  $O(n)$  space.



# Line Segment Intersection: General Position Assumed

## General position assumed

For the sake of descriptiveness, we assume that

- no two end-points or intersections of line segments of  $S$  have the same  $y$ -coordinate;
  - no two line segments overlap;
  - no three line segments intersect at the same point;
  - no segment is horizontal.
- 
- A GPA assumption makes perfect sense since it allows to avoid special cases and, thus, to focus on the essential ideas of a (geometric) algorithm.
  - Different GPA assumptions might be made depending on the actual application. (See the slides on Voronoi diagrams later in this course!)

## Caveat

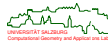
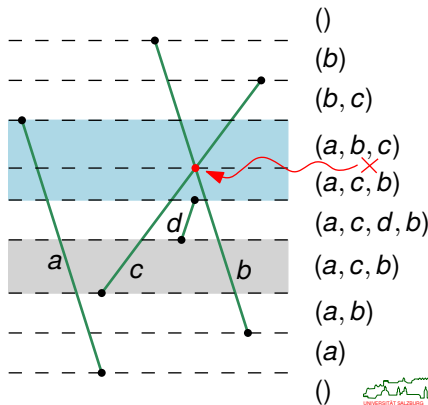
A GPA assumption will not hold for most real-world data. Thus, a GPA assumption may make it necessary to work out all the (possibly subtle) details and to close all (possibly non-trivial) gaps on one's own prior to an actual implementation . . .

# Line Segment Intersection: Plane Sweep

- Suppose that we draw horizontal lines through all  $2n$  end-points of the line segments and all  $k$  intersection points.
- These  $2n + k$  lines split  $\mathbb{R}^2$  into  $2n + k + 1$  horizontal slabs.
- Note that the left-to-right order of the line segments does not change within a slab. And this observation holds for all slabs!
- Question: When does the relative order of two line segments change?
- Answer: The relative order of two line segments  $l_1, l_2$  changes at the border line of two adjacent slabs if that border line passes through the point of intersection of  $l_1$  and  $l_2$ .

## Lemma 28

Two line segments  $l_1, l_2$  intersect if and only if there exist two adjacent slabs such that  $l_1, l_2$  are neighbors in the left-to-right orders and such that the relative order of  $l_1, l_2$  within the two slabs is different.



# Line Segment Intersection: Plane Sweep

- Basic idea:
  - Sweep a horizontal line over the line segments and keep track of their left-to-right orders.
  - Halt and update these left-to-right orders whenever necessary.

## Plane-sweep algorithm (aka: “sweep-line algorithm”)

A *plane-sweep algorithm* uses two data structures:

- 1 *Event-point schedule*: Sequence of halting positions to be assumed by the sweep line.
- 2 *Sweep-line status*: Description of the intersection of the sweep line with the geometric object(s) being swept at the current event.

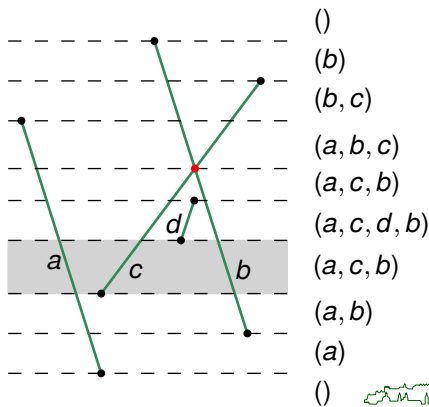
## Sweep for line-segment intersection

Plane sweep applied to line-segment intersection detection:

- 1 **Event-point schedule**: End-points of all line segments of  $S$  and all intersection points, arranged according to ascending  $y$ -coordinates. (The sweep is bottom-to-top.)
- 2 **Sweep-line status**: Left-to-right sequence of the line segments of  $S$  that intersect the sweep line.

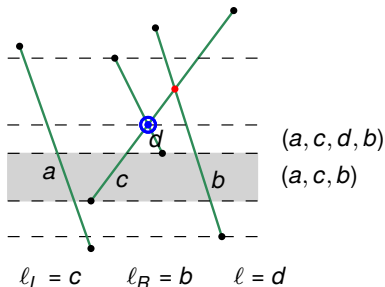
# Line Segment Intersection: Plane Sweep

- 1 Initialize a priority queue  $Q$  of future events:
  - Every event is associated with a point in  $\mathbb{R}^2$  and with the up to two line segments on which it lies.
  - The events are prioritized according to the points'  $y$ -coordinates.
- 2 Insert all  $2n$  end-points of the  $n$  line segments into  $Q$ .
- 3 Initialize a binary search tree  $T$  that will contain those line segments of  $S$  which are crossed by the sweep line:
  - The segments are ordered according to the  $x$ -coordinates of the crossing points.
  - Initially,  $T$  is empty.



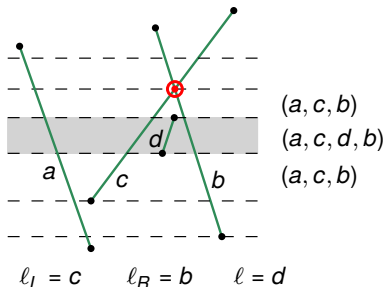
## Line Segment Intersection: Plane Sweep

- ④ While  $Q$  is not empty, fetch and remove the next event from  $Q$ . Let  $p$  be the point associated with that event, and let  $y_p$  be its  $y$ -coordinate:
  - a If  $p$  is the lower end-point of a line segment  $l$ :
    - i Insert  $l$  into  $T$ .
    - ii Let  $l_L$  and  $l_R$  be the line segments that are immediately to the left and right of  $l$ , if they exist. (Use  $T$  to locate  $l_L, l_R$ .)
    - iii If  $l_L, l_R$  intersect above  $y_p$  then remove the intersection from  $Q$ .
    - iv If  $l_L, l$  or  $l, l_R$  intersect above  $y_p$  then insert the intersection(s) into  $Q$ .



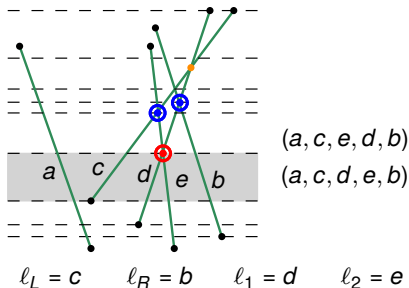
## Line Segment Intersection: Plane Sweep

- 4 While  $Q$  is not empty, fetch and remove the next event from  $Q$ . Let  $p$  be the point associated with that event, and let  $y_p$  be its  $y$ -coordinate:
  - b If  $p$  is the upper end-point of a line segment  $l$ :
    - i Let  $l_L$  and  $l_R$  be the line segments that are immediately to the left and right of  $l$ , if they exist. (Use  $T$  to locate  $l_L, l_R$ .)
    - ii Remove  $l$  from  $T$ .
    - iii If  $l_L, l_R$  intersect above  $y_p$  then insert the intersection into  $Q$ .



# Line Segment Intersection: Plane Sweep

- iv While  $Q$  is not empty, fetch and remove the next event from  $Q$ . Let  $p$  be the point associated with that event, and let  $y_p$  be its  $y$ -coordinate:
  - c If  $p$  is a point of intersection of  $l_1$  and  $l_2$ :
    - i Let  $l_L$  and  $l_R$  be the line segments that are immediately to the left of  $l_1$  and right of  $l_2$ , if they exist. (Use  $T$  to locate  $l_L, l_R$ .)
    - ii If  $l_L, l_1$  or  $l_2, l_R$  intersect above  $y_p$  then remove the intersection(s) from  $Q$ .
    - iii If  $l_1, l_R$  or  $l_L, l_2$  intersect above  $y_p$  then insert the intersection(s) into  $Q$ .
    - iv Trade the order of  $l_1$  and  $l_2$  in  $T$ .



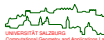
# Line Segment Intersection: Plane Sweep

## Correctness:

- Whenever two line segments  $\ell_1, \ell_2$  are neighbors in the sorted left-to-right order of segments, the point of intersection of  $\ell_1, \ell_2$  is present in  $Q$ , if it exists and has a higher  $y$ -coordinate.
- Hence, no future event and, in particular, no point of intersection is missed.

## Complexity:

- The algorithm processes a sequence of  $2n + k$  events.
- Since future intersections between line segments are maintained in the priority queue  $Q$  if and only if the line segments currently are neighbors in the left-to-right order, at any given point in time we will never need to do maintain more than  $3n - 1$  events in  $Q$ .
- The algorithm stores up to  $n$  line segments in left-to-right order in  $T$ .
- Every event requires a constant number of updates of  $Q$  and  $T$ .
- If  $Q$  and  $T$  allow insertions, deletions and searches in logarithmic time then every event is handled in  $O(\log n)$  time.
- Any standard balanced binary search tree (e.g., AVL-tree, red-black tree) and any logarithmic-time priority queue (e.g., binary heap) suffices.
- Summarizing, the Bentley-Ottmann algorithm finds all intersections among  $n$  line segments in  $O((n + k) \log n)$  time, using  $O(n)$  space.



# Generalizations of the Sweep Paradigm

## Rotational sweep:

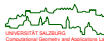
- A line (or ray) rotates about a point.

## Space sweep:

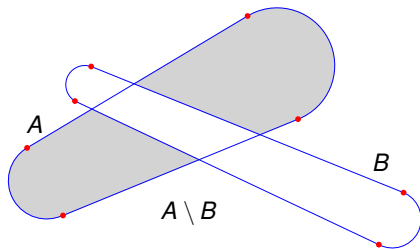
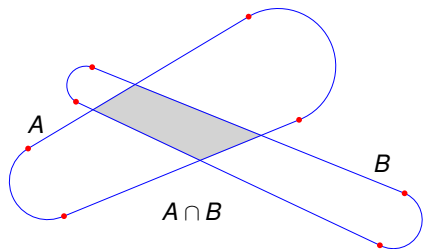
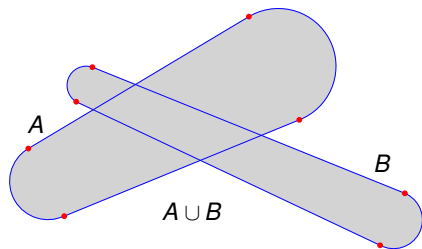
- A plane (which is parallel to one of the coordinate planes) sweeps through 3D space.
- A recursive application of this idea sometimes allows to replace a  $d$ -dimensional problem by a series of  $(d - 1)$ -dimensional problems.

## Topological sweep:

- Edelsbrunner&Guibas (1991).
- A “topological” line is used instead of a straight line.

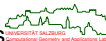


# Computing Boolean Operations on Curvilinear Polygons



# Sweep-Line Algorithm for Boolean Operations

- Consider a vertical line  $\ell$  that sweeps from left to right. Study
  - (1) its intersection with the union of the curvilinear polygons,
  - (2) the top-to-bottom order of the segments/arcs intersected by  $\ell$ .
- Q: At which events does the intersection of  $\ell$  with the union change topologically?  
A: Whenever  $\ell$  enters or leaves a curvilinear polygon.
- Q: At which events does the top-to-bottom order of the segments/arcs intersected by  $\ell$  change?  
A: Whenever  $\ell$  moves through a vertex or an intersection point.
- Put events into a priority queue and process in left-to-right order.
- Intersection points can be detected on the fly between segments/arcs that are neighbors in the top-to-bottom order!
- Handling of circular arcs on the same circle requires some care.
- Complexity:  $O((n + k) \log n)$  for  $n$  segments/arcs and  $k$  intersection points.



# Line Arrangement

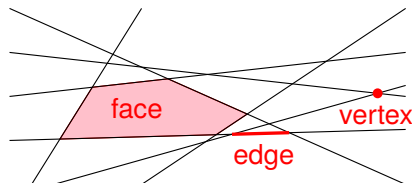
## Definition 29 (Arrangement)

Consider a set  $L$  of lines in the plane. The (line) arrangement  $\mathcal{A}(L)$  induced by  $L$  is the subdivision of the plane that consists of

- vertices:** points of intersection of two or more lines of  $L$ ,
- edges:** connected components of all lines of  $L$  without all vertices,
- faces:** the connected components of the subset of the plane not intersected by any line of  $L$ . Aka: cells.

An arrangement is *simple* if no more than two lines of  $L$  intersect at a vertex.

- Arrangements can also be induced by other primitives (e.g., circles) and studied in higher dimensions.



# Line Arrangement: Combinatorial Complexity

## Lemma 30

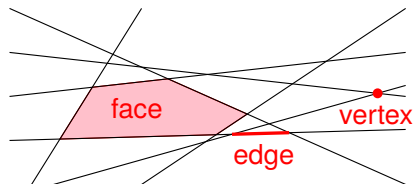
Every face of an arrangement is convex.

## Lemma 31

The arrangement induced by a set of  $n$  lines has

- at most  $\binom{n}{2}$  vertices,
- at most  $n^2$  edges,
- at most  $\binom{n+1}{2} + 1$  faces,

i.e., its combinatorial complexity is  $O(n^2)$ . Equality holds for simple arrangements.



# Line Arrangement: Combinatorial Complexity

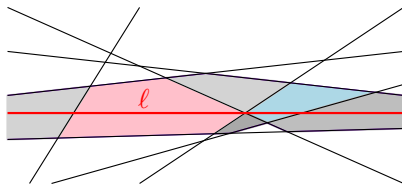
## Definition 32

The *zone* of a line  $\ell \notin L$  in an arrangement  $\mathcal{A}(L)$  of a set  $L$  of lines is the set of all faces of  $\mathcal{A}(L)$  whose closure is intersected by  $\ell$ .

## Theorem 33 (Zone theorem)

The complexity of the zone of a line in an arrangement of  $n$  lines is  $O(n)$ .

*Sketch of Proof:* Assume that  $\ell$  is horizontal and construct the zone by inserting the lines of  $L$  from left to right along  $\ell$ . Then one can show by induction that each new line adds at most 6 new zone edges. □



# Line Arrangement: Construction

## Problem: LINEARRANGEMENT

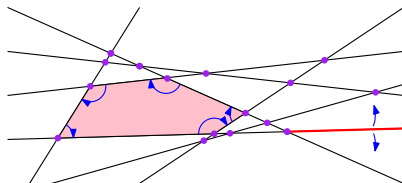
**Given:** A set  $L$  of lines in the plane.

**Compute:** A (combinatorial) representation of the arrangement  $\mathcal{A}(L)$  that allows to traverse  $\mathcal{A}(L)$ .

## Theorem 34

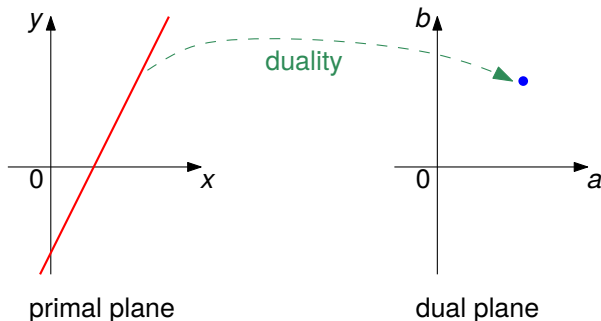
A combinatorial representation of the arrangement  $\mathcal{A}(L)$  of a set  $L$  of  $n$  lines in the plane can be computed incrementally in time  $O(n^2)$ .

*Sketch of Proof:* The Zone Theorem 33 implies  $O(n)$  complexity per insertion of a line of  $L$ . □



# Point-Line Duality

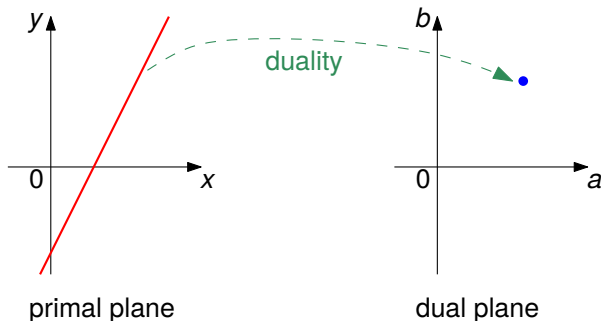
- We study two incarnations of the plane, both with right-handed Cartesian coordinate systems:
  - the *primal plane* with coordinates  $x, y$ , and
  - the *dual plane* with coordinates  $a, b$ .
- We will identify a line in one plane with a point in the other plane, and vice versa.
- Remember: A (non-vertical) line  $l$  has the equation  $y = l_a x - l_b$ , where  $l_a$  models the slope and  $l_b$  models the  $y$ -intercept of  $l$ .



# Point-Line Duality: Motivation

## Goal

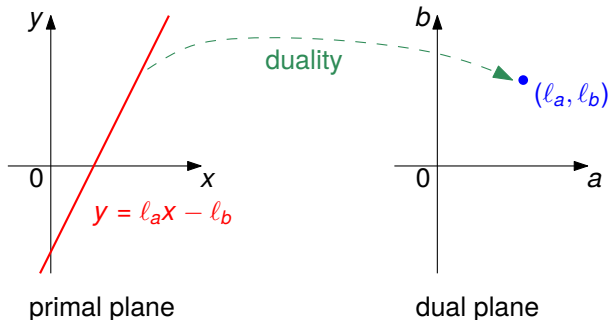
A duality mapping between points and lines in the plane shall allow us to translate theorems and algorithms about points and lines into theorems and algorithms about lines and points.



# Point-Line Duality

## Definition 35 (Point-line duality)

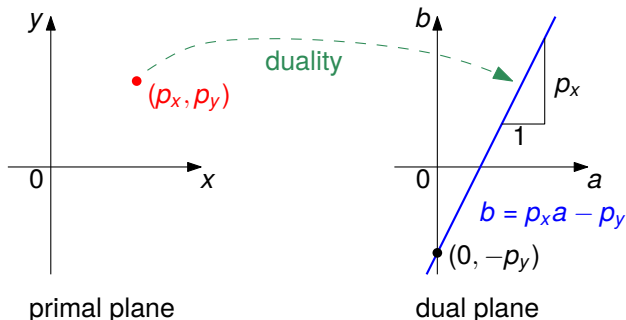
- Let  $l$  be a line in primal space with equation  $y = l_a x - l_b$ . We associate with  $l$  the point  $l^*$  in the dual plane with coordinates  $(l_a, l_b)$ .



# Point-Line Duality

## Definition 35 (Point-line duality)

- 1 Let  $\ell$  be a line in primal space with equation  $y = \ell_a x - \ell_b$ . We associate with  $\ell$  the point  $\ell^*$  in the dual plane with coordinates  $(\ell_a, \ell_b)$ .
- 2 Let  $p$  be a point in the primal space with coordinates  $(p_x, p_y)$ . We associate with  $p$  the line  $p^*$  in the dual plane with equation  $b = p_x a - p_y$ .



## Point-Line Duality: Properties

- Of course, we can apply the same duality mapping  $\star$  to points and lines in the dual plane, and map them to lines and points in the primal plane.

### Lemma 36 (Self-inverse mapping)

The duality mapping  $\star$  is self-inverse:

- (1) For every point  $p$  in the primal plane:  $(p^\star)^\star = p$ .
- (2) For every line  $\ell$  in the primal plane:  $(\ell^\star)^\star = \ell$ .

*Proof:* (1) For  $p$  with coordinates  $(p_x, p_y)$  we get the dual line  $p^\star$  with equation  $b = p_x a - p_y$ . This line dualizes to a point  $(p^\star)^\star$  with coordinates  $(p_x, -(-p_y))$ , i.e., to  $p$ .

(2) A line  $\ell$  with equation  $y = \ell_a x - \ell_b$  dualizes to the point  $\ell^\star$  with coordinates  $(\ell_a, \ell_b)$ , which in turn dualizes to the line  $(\ell^\star)^\star$  with equation  $y = \ell_a x - \ell_b$ , i.e., to  $\ell$ .  $\square$

# Point-Line Duality: Properties

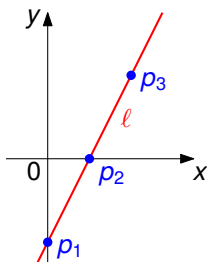
## Lemma 37 (Incidence-preserving mapping)

For every point  $p$  and every line  $l$  in primal space:  $p \in l$  if and only if  $l^* \in p^*$ .

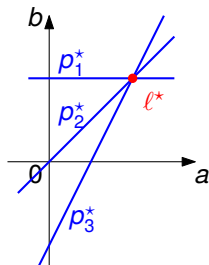
*Proof:* Assume that  $p \in l$ , with point coordinates  $(p_x, p_y)$  and line equation  $y = l_a x - l_b$ . Then  $p_y = l_a p_x - l_b$ . Hence,  $l_b = p_x l_a - p_y$ , and  $l^* = (l_a, l_b) \in p^*$ . Now assume that  $l^* \in p^*$ . We get  $(p^*)^* \in (l^*)^*$ , and by Lem. 36,  $p \in l$ . □

## Corollary 38

The points  $p_1, p_2, p_3$  lie on the line  $l$  if and only if the lines  $p_1^*, p_2^*, p_3^*$  intersect in the common point  $l^*$ .



primal plane



dual plane



# Point-Line Duality: Properties

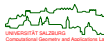
## Lemma 39

The signed vertical distance from a point  $p$  to a line  $l$  equals the signed vertical distance from the point  $l^*$  to the line  $p^*$ .

- This lemma implies Lem. 37.

## Corollary 40

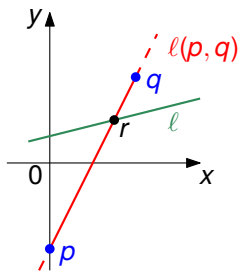
A point  $p$  lies above a line  $l$  if and only if the point  $l^*$  lies above the line  $p^*$ .



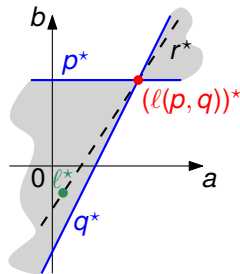
# Point-Line Duality: Properties

## Corollary 41

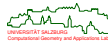
A line  $l$  intersects the line segment  $\overline{pq}$  if and only if the point  $l^*$  lies in the “horizontal” double wedge defined by the lines  $p^*$  and  $q^*$ . (I.e., the double wedge which does not contain the vertical line through the intersection point of  $p^*$  and  $q^*$ .)



primal plane



dual plane



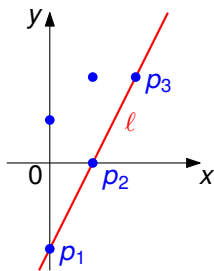
## Detecting Collinearity

### Problem: COLLINEARITY

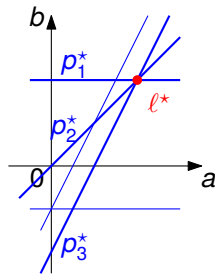
**Given:** A set  $S$  of  $n$  points in the plane.

**Decide:** Are any three points of  $S$  collinear?

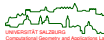
- Naïve algorithm: Check all triples of points of  $S$  in  $O(n^3)$  time.
- Better: Recall duality (Cor. 38) and compute the arrangement of the dual lines of the points of  $S$  in  $O(n^2)$  time.



primal plane



dual plane



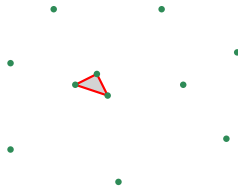
# Smallest Triangle

## Problem: MINIMUMAREATRIANGLE

**Given:** A set  $S$  of  $n$  points in the plane.

**Find:** The triangle with smallest area whose three vertices are in  $S$ .

- A naïve solution evaluates all triples of points of  $S$  and, thus, runs in  $O(n^3)$  time.
- General position assumed: No three points are collinear.

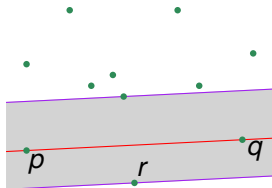


# Smallest Triangle: Characterization of Solution

## Lemma 42

Let  $p, q \in S$  with  $p \neq q$ . Then the point  $r \in S$  which forms the smallest triangle  $\Delta(p, q, r)$  with fixed base edge  $\overline{pq}$  is a point of  $S$  which lies on the boundary of the largest empty corridor along the line  $\ell(p, q)$ .

- Let  $\ell$  be the line through  $p, q$ .
- Then  $r$  lies on a line  $\ell_r$  such that
  - $\ell_r$  is parallel to  $\ell$ ,
  - there is no other line with the same slope through a point of  $S$  that lies strictly between  $\ell$  and  $\ell_r$ .



## Smallest Triangle: Interpretation in Dual Space

- This implies for the dual space:
  - $l_r^*$  is on  $r^*$ ,
  - $l_r^*$  and  $l^*$  have the same  $x$ -coordinate (since  $l_r$  and  $l$  have the same slope),
  - no line  $s^*$ , for  $s \in S$ , crosses the line segment with endpoints  $l^*$  and  $l_r^*$  (since then  $s$  would lie between  $l$  and  $l_r$ ).
- Hence,
  - $l^*$  is a vertex of  $\mathcal{A}(S^*)$ ,
  - $l_r^*$  lies on the boundary of the same cell of  $\mathcal{A}(S^*)$  as  $l^*$ ,
  - $l_r^*$  lies vertically below or above  $l^*$ .
- This implies that we have only two candidate lines parallel to  $l$  for any fixed pair  $p, q$ , namely the duals of the two points  $u, v$  on  $\mathcal{A}(S^*)$  right below or above  $l^*$ .
- Thus, it suffices to determine  $u, v$  for every vertex  $w$  of  $\mathcal{A}(S^*)$ .
- Since all faces of  $\mathcal{A}(S^*)$  are convex, this can be done on a face-by-face basis for all vertices of  $\mathcal{A}(S^*)$ , in total  $O(n^2)$  time.

### Theorem 43

MINIMUMAREATRIANGLE can be solved in  $O(n^2)$  time for  $n$  points.

## 3 Geometric Searching

- Introduction
- Point Inclusion

# Introduction to Geometric Searching

**Point-Inclusion Query:** In which “cell” (of, e.g., a map) does a query point lie?

## Range Searching:

- **Report Query:** Which points are within a query object (rectangle, circle)?
- **Count Query:** Only the number of points within an object matters.
- Another way to distinguish geometric searching queries:

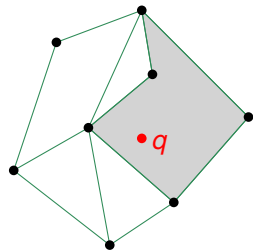
**Single-Shot Query:** Only one query per data set.

**Repetitive-Mode Query:** Many queries per data set; preprocessing may make sense.

- The complexity of a query is determined relative to four cost measures:
  - query time,
  - preprocessing time,
  - memory consumption,
  - update time (in the case of dynamic data sets).

## Point Inclusion

- Given: Decomposition of the plane into polygonal regions, as induced by a PSLG  $\mathcal{G}$ , and a query point  $q$ .
- Problem: Which face of  $\mathcal{G}$  contains  $q$ ?
- Aka “point location”. Obviously, point-inclusion problems can also be studied in higher dimensions.



### Theorem 44

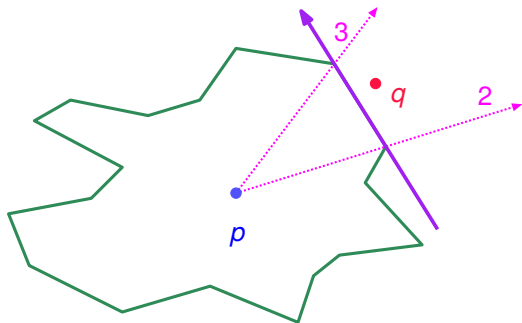
A brute-force point location within an  $n$ -vertex planar subdivision can be carried out in  $O(n)$  time, using  $O(n)$  space.

*Sketch of Proof:* An “even-odd” test can be used for the individual point-in-face tests. □

- This is not an efficient solution for repetitive-mode queries!
- Goal: Create geometric data structure that supports some kind of binary search.

## Point-in-Polygon Query for Star-Shaped Polygons

- 1 Preprocessing: Find point  $p$  within kernel of polygon.
- 2 Preprocessing: Shoot rays starting at  $p$  through each vertex.
- 3 For a query point  $q$ : Perform binary search.
- 4 Determine sidedness relative to one edge of the polygon.

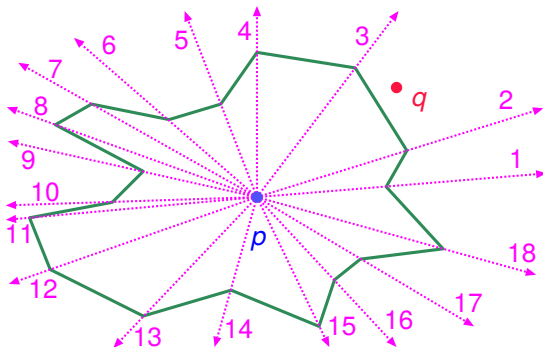


# Point-in-Polygon Query for Star-Shaped Polygons

## Theorem 45

For an  $n$ -vertex star-shaped polygon, a point-location query can be answered in  $O(\log n)$  query time, after  $O(n)$  preprocessing and within  $O(n)$  space.

*Sketch of Proof:* Determining a point  $p$  within the kernel can be seen as a solution of an LP, which can be obtained in  $O(n)$  time [Megiddo (1983)]. □



# Triangulation Refinement Technique

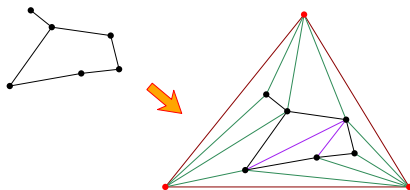
- Aka: Dobkin-Kirkpatrick Hierarchy [1990] in 3D, based on Kirkpatrick [1983].
- For a given  $n$ -vertex PSLG  $\mathcal{G}$ , generate a PSLG  $\mathcal{G}'$  with the following properties:
  - 1  $\mathcal{G}'$  is a super-graph of  $\mathcal{G}$ ,
  - 2  $\mathcal{G}'$  is a triangulation,
  - 3  $\mathcal{G}'$  has a triangular boundary, and, by Euler's formula,
  - 4  $\mathcal{G}'$  has exactly  $3n - 6$  edges.

## Triangulation refinement in a nutshell

- Construct hierarchy of triangulations above  $\mathcal{G}'$ , and set up a directed acyclic search graph  $\mathcal{T}$ , in time  $O(n \log n)$  and space  $O(n)$ .
- Perform point-location queries within  $\mathcal{T}$  in time  $O(\log n)$ .

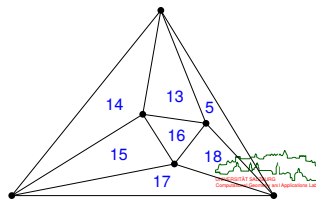
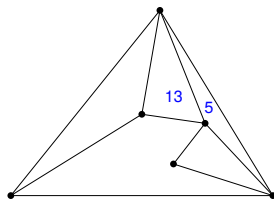
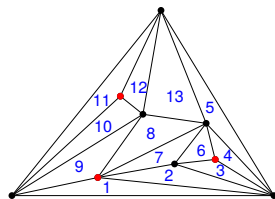
# Triangulation Refinement Technique

- Convert  $\mathcal{G}$  into a triangulation  $\mathcal{G}'$  with triangular outer face.

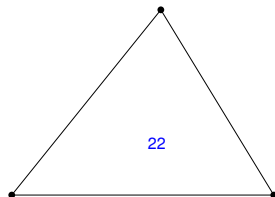
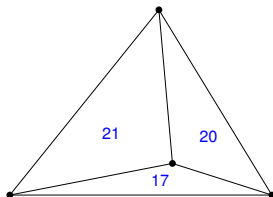
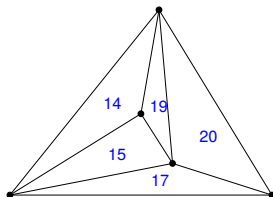
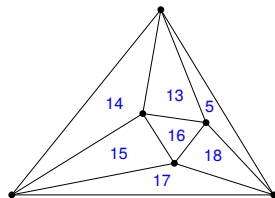
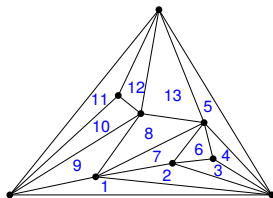
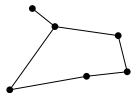


## Triangulation Refinement: Hierarchy of Triangulations

- Consider a triangulated PSLG  $\mathcal{G}'$  (with triangular outer face) on  $n$  vertices.
- We construct a hierarchy of triangulations  $S_1, S_2, \dots, S_{h(n)}$ , where  $S_1 := \mathcal{G}'$  and  $S_i$  is obtained from  $S_{i-1}$  as follows:
  - **Step 1:** Select and remove a maximal independent set of non-boundary vertices of  $S_{i-1}$  together with their incident edges.
  - **Step 2:** Re-triangulate the holes arising from the removal of those vertices and edges.
- The final triangulation in the hierarchy,  $S_{h(n)}$ , is just one triangle.

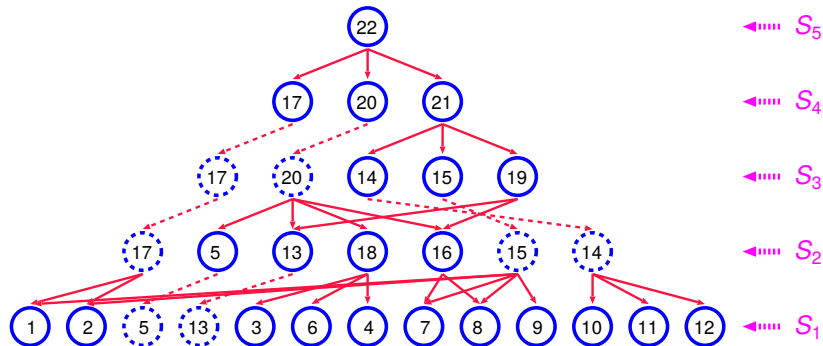


# Triangulation Refinement: Hierarchy of Triangulations



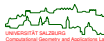
# Triangulation Refinement: Directed Acyclic Search Graph

- We set up a directed acyclic search graph  $\mathcal{T}$  on  $S_1, S_2, \dots, S_{h(n)}$ .
- The graph  $\mathcal{T}$  contains an edge from triangle  $\Delta_k$  to triangle  $\Delta_j$  if, when constructing triangulation  $S_i$  from triangulation  $S_{i-1}$ , we have:
  - 1  $\Delta_j$  is removed from  $S_{i-1}$  in **Step 1**.
  - 2  $\Delta_k$  is created in  $S_i$  in **Step 2**.
  - 3  $\Delta_j \cap \Delta_k \neq \emptyset$ .



## Triangulation Refinement Technique: Query

- For a query point  $q$ , perform a point-in-triangle test of  $q$  relative to the root triangle of  $\mathcal{T}$ .
- If  $q$  is
  - **outside** then  $q$  lies in the unbounded (exterior) face.
  - **inside** then  $q$  is tested for triangle inclusion with each of the descendants of the current node.
- This scheme is applied recursively until a leaf of  $\mathcal{T}$  is reached.
- What is the complexity of a query? This depends on
  - the height  $h(n)$  of  $\mathcal{T}$ ,
  - the maximum number  $m$  of point-in-triangle tests needed per node.
- Both terms seem to depend on how we select those vertices of  $S_{i-1}$  that will not be part of  $S_i$ .
- Goal: Construct  $\mathcal{T}$  such that  $m = O(1)$  and  $h(n) = O(\log n)$ .



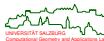
# Analysis of Triangulation Refinement Technique

- Let  $N_i$  denote the number of vertices of triangulation  $S_i$ .
- Criterion for selecting vertices that are to be removed:  
*Remove a set of non-adjacent vertices of degree less than  $K$ ,*  
where  $K := 12$ .
- Easy to prove: This criterion allows us to delete at least

$$\frac{1}{12} \left( \frac{N_{i-1}}{2} - 3 \right)$$

vertices within  $S_{i-1}$ .

- We get:
  - $N_i \leq \alpha N_{i-1}$ , where  $\alpha \approx \frac{23}{24}$ .
  - $h(n) \leq \lceil \log_{1/\alpha} n \rceil \approx 16 \log n$ , and only  $O(n)$  triangles need to be stored.
  - Finally,  $m = (K - 1) - 2 = 9$ .
- Other choices for  $K$  yield tighter bounds! E.g.,  $K := 9$  yields the slightly better bounds  $\alpha \approx \frac{17}{18}$  and  $12 \log n$  per query, and more elaborate choices for the vertices to be deleted bring down the query complexity to roughly  $\frac{9}{2} \log n$ .



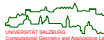
## Analysis of Triangulation Refinement Technique

- The key step in the preprocessing is the initial triangulation of the PSLG, which takes  $O(n \log n)$  time (or  $O(n)$  time if the PSLG is connected and Chazelle's linear-time triangulation algorithm is used).
- All other triangulation operations can easily be carried out in time linear in the number of vertices involved.

### Theorem 46 (Kirkpatrick (1983))

For a connected  $n$ -vertex PSLG, triangulation refinement supports point-location queries in  $O(\log n)$  query time, after  $O(n)$  preprocessing and within  $O(n)$  space.

- Although this point-inclusion algorithm is optimum in terms of the  $O$ -notation, it is not very practical and better (but more elaborate) algorithms are known.



## Convex Hulls

- Basics
- Algorithms
- Convex Hull of Polygons
- Convex Hulls in 3D
- Applications of Convex Hulls

# Linear Combination and Convex Combination

## Definition 47 (Linear combination, Dt.: Linearkombination)

Let  $p_1, p_2, \dots, p_k$  be  $k$  points in  $\mathbb{R}^n$ . A *linear combination* of  $p_1, \dots, p_k$  is given by

$$\sum_{i=1}^k \lambda_i p_i$$

where  $\lambda_1, \lambda_2, \dots, \lambda_k \in \mathbb{R}$  are scalars.

## Definition 48 (Convex combination, Dt.: Konvexkombination)

Let  $p_1, p_2, \dots, p_k$  be  $k$  points in  $\mathbb{R}^n$ . A *convex combination* of  $p_1, \dots, p_k$  is given by

$$\sum_{i=1}^k \lambda_i p_i \quad \text{with} \quad \sum_{i=1}^k \lambda_i = 1 \quad \text{and} \quad \forall (1 \leq i \leq k) \lambda_i \geq 0,$$

where  $\lambda_1, \lambda_2, \dots, \lambda_k \in \mathbb{R}$  are scalars.

## Definition 49 (Convex hull, Dt.: konvexe Hülle)

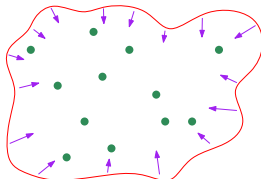
Let  $p_1, p_2, \dots, p_k$  be  $k$  points in  $\mathbb{R}^n$ . The *convex hull* of  $p_1, \dots, p_k$  is the set

$$\left\{ \sum_{i=1}^k \lambda_i p_i : \lambda_1, \dots, \lambda_k \in \mathbb{R}_0^+ \text{ and } \sum_{i=1}^k \lambda_i = 1 \right\}.$$

For a set  $S \subseteq \mathbb{R}^n$  (with possibly infinitely many points), the *convex hull* of  $S$  is the set

$$\left\{ \sum_{i=1}^k \lambda_i p_i : k \in \mathbb{N} \text{ and } p_1, p_2, \dots, p_k \in S \text{ and } \lambda_1, \dots, \lambda_k \in \mathbb{R}_0^+ \text{ and } \sum_{i=1}^k \lambda_i = 1 \right\}.$$

The convex hull of  $S$  is commonly denoted by  $CH(S)$ .



## Definition 50 (Convex set, Dt.: konvexe Menge)

A set  $S \subseteq \mathbb{R}^n$  is called *convex* if for all  $p, q \in S$

$$\overline{pq} \subseteq S$$

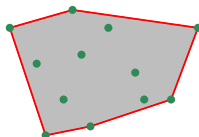
where  $\overline{pq}$  denotes the straight-line segment between  $p$  and  $q$ .

## Lemma 51

For  $S \subseteq \mathbb{R}^n$ , the convex hull  $CH(S)$  of  $S$  is a convex set.

## Lemma 52

For a set  $S$  of  $n$  points in  $\mathbb{R}^2$ , the convex hull  $CH(S)$  is a convex polygon.



## Definition 53 (Convex superset)

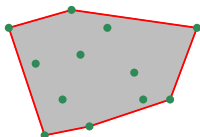
A set  $B \subseteq \mathbb{R}^n$  is called a *convex superset* of a set  $A \subseteq \mathbb{R}^n$  if

$$A \subseteq B \quad \text{and} \quad B \text{ is convex.}$$

## Lemma 54

For  $A \subseteq \mathbb{R}^n$ , the following definitions are equivalent to Def. 49:

- $CH(A)$  is the smallest convex superset of  $A$ .
- $CH(A)$  is the intersection of all convex supersets of  $A$ .
- The definition of a convex hull (and of convexity) is readily extended from  $\mathbb{R}^n$  to other vector spaces over  $\mathbb{R}$ .



# Complexity of Computing Convex Hulls

## Problem: CONVEXHULL

**Given:** A set  $S$  of  $n$  points in the plane.

**Compute:** The convex hull  $CH(S)$ , as an ordered list of vertices.

- Question: Can we state a worst-case lower bound on the time complexity of CONVEXHULL, i.e., for computing  $CH(S)$ ?

## Theorem 55

SORTING is linear-time transformable to CONVEXHULL.

## Corollary 56

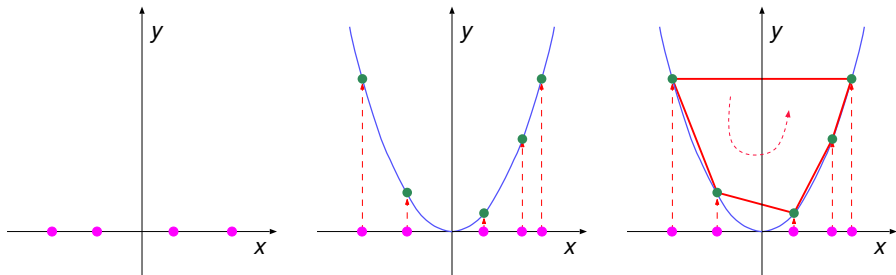
Solving CONVEXHULL for  $n$  points requires at least  $\Omega(n \log n)$  time.



# Reduction From Sorting to Convex Hulls

*Sketch of Proof:* of Theorem 55

- Suppose the instance of SORTING is the set of  $S' := \{x_1, x_2, \dots, x_n\} \subset \mathbb{R}$ .
- We transform  $S'$  into an instance of CONVEXHULL by mapping each real number  $x_i$  to the point  $(x_i, x_i^2)$ . All points of the resulting set  $S$  of points lie on the parabola  $y = x^2$ .
- The convex hull of  $S$  contains a list of vertices sorted by  $x$ -coordinates.
- One pass through this list will find the smallest element. The sorted numbers can be obtained by a second pass through this list.

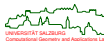


## Complexity of Computing Convex Hulls

- The  $\Omega(n \log n)$  lower bound also applies if only the unordered set of hull vertices is sought. (But the proof becomes a bit trickier . . .)
- If also the size  $h$  of the output is considered (in addition to the input size  $n$ ), then one can prove the lower bound  $\Omega(n \log h)$ .
- This lower bound is matched by a “marriage-before-conquest” algorithm (Kirkpatrick&Seidel) and by Chan’s algorithm. Chan’s algorithm is simpler and also extends to 3D.

### Theorem 57 (Kirkpatrick&Seidel (1986), Chan (1996))

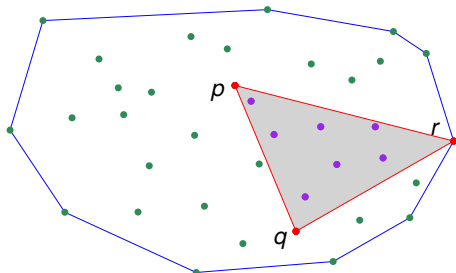
The convex hull of  $n$  points in the plane can be computed in  $O(n \log h)$  time and within  $O(n)$  storage, where  $h$  denotes the number of vertices of  $CH(S)$ .



## Discarding Internal Points

### Lemma 58

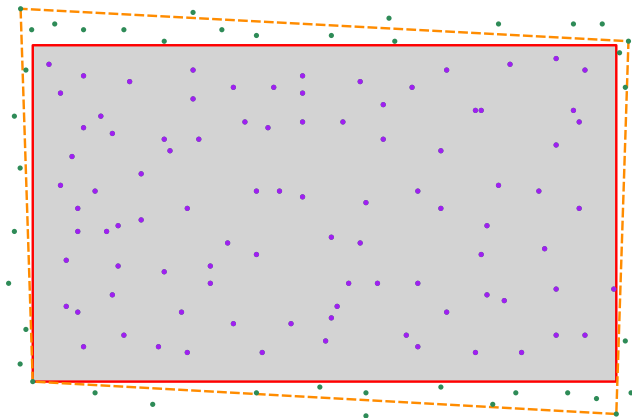
Consider three points  $p, q, r \in CH(S)$ . Then every point  $q$  that lies strictly within  $\Delta(p, q, r)$  is internal to  $CH(S)$ .



- In particular, no point strictly within  $\Delta(p, q, r)$  can be a vertex of the convex hull.
- This lemma can be generalized to any convex quadrangle (or polygon) whose vertices lie within  $CH(S)$ .

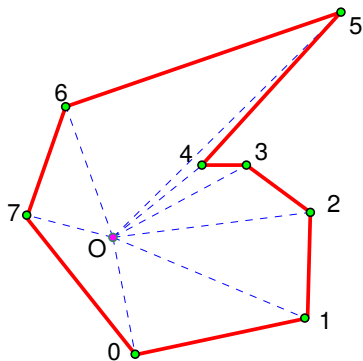
## Discarding Internal Points: Interior Elimination

- Discard all points within a large (axis-aligned) rectangle.
- Heuristic improvement; does not change worst-case complexity.



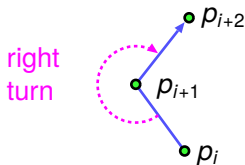
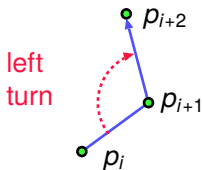
# Graham's Scan

- Find a point  $O$  internal to  $CH(S)$ , e.g, the center of three points of  $S$ .
- Sort the  $n$  points of  $S$  lexicographically on
  - 1 polar angle relative to  $O$ ,
  - 2 distance from  $O$ .
- Choose a point  $p_0 \in S$  guaranteed to be a vertex of  $CH(S)$ , and re-number the points.



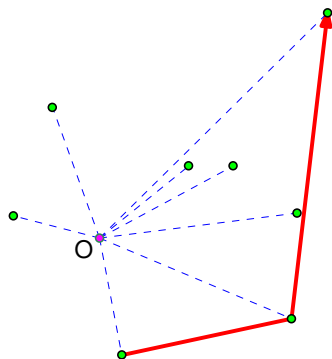
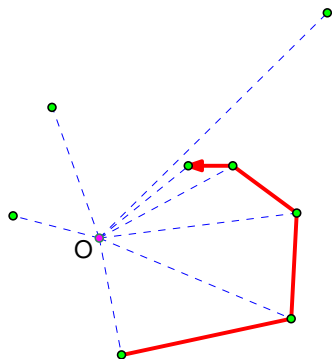
# Graham's Scan

- CCW scan algorithm: The algorithm repeatedly examines triangles defined by triples of consecutive points  $\triangle(p_i, p_{i+1}, p_{i+2})$ :
  - If  $\triangle(p_i, p_{i+1}, p_{i+2})$  is a left turn, advance to  $\triangle(p_{i+1}, p_{i+2}, p_{i+3})$ .
  - If  $\triangle(p_i, p_{i+1}, p_{i+2})$  is a right turn, eliminate  $p_{i+1}$  from  $S$  and backtrack to  $\triangle(p_{i-1}, p_i, p_{i+2})$ .
  - If  $p_i, p_{i+1}, p_{i+2}$  are collinear then eliminate  $p_{i+1}$  and advance to  $\triangle(p_i, p_{i+2}, p_{i+3})$ .
  - Scan ends when it returns to  $p_0$ .

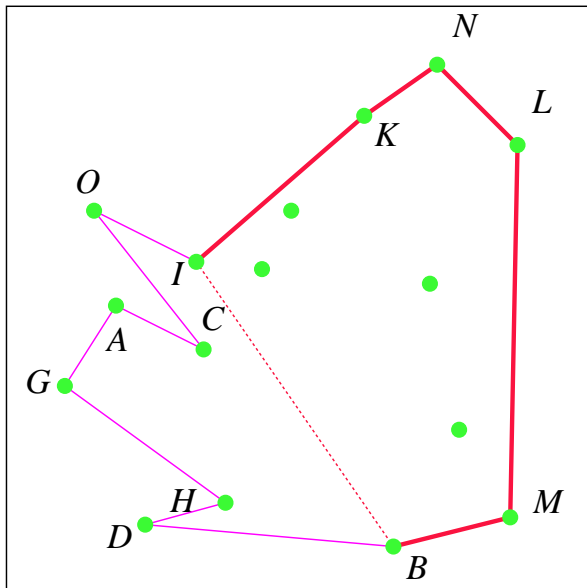


## Graham's Scan: Advancing and Backtracking

- Backtracking may occur more than once in succession, eliminating a sequence of points.
- Backtracking sure to stop at  $p_0$ .



# Animation of Graham's Scan



## Theorem 59 (Complexity of Graham's Scan)

Graham's Scan computes the convex hull of  $n$  points in the plane in  $O(n \log n)$  time and within  $O(n)$  storage.

*Proof:*

- 1 Find a point  $O$  within  $CH(S)$ :  $O(1)$ .
- 2 Sort the points relative to  $O$  in polar coordinates:  $O(n \log n)$ .
- 3 Find a point on  $CH(S)$ :  $O(n)$ .
- 4 Scan algorithm: Use amortized analysis to argue  $O(n)$ .

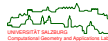
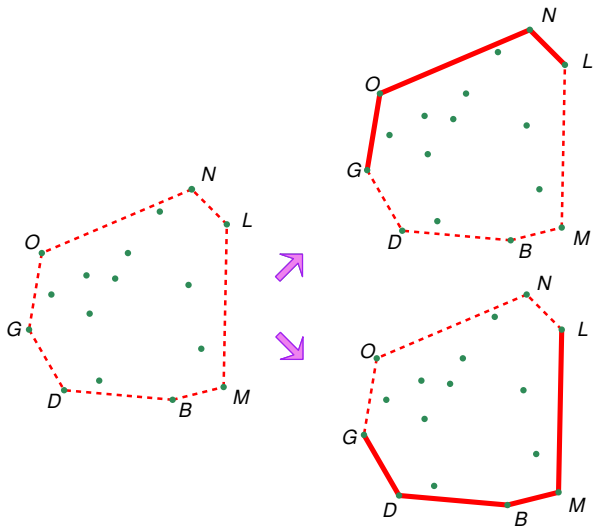


## Corollary 60

Graham's Scan computes the convex hull of a star-shaped polygon in linear time.

## Practice-Minded Simplification of Graham's Scan

- Compute upper and lower convex hull separately: Then a conventional lexicographical sort with respect to x-coordinates (and y-coordinates) suffices.

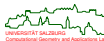


# Divide-and-Conquer Convex Hull

- 1 If  $|S| \leq k_0$ , where  $k_0$  is a small integer (e.g.,  $k_0 = 3$ ), then construct the convex hull  $CH(S)$  directly by some method and stop, else go to Step 2.
- 2 Partition the set  $S$  arbitrarily into two subsets  $S_1$  and  $S_2$  of approximately equal sizes.
- 3 Recursively find the convex hulls  $CH(S_1)$  and  $CH(S_2)$ .
- 4 Merge the two hulls together to form  $CH(S)$ .

## Observations

- The convex hull of the union of the two subsets is the same as the convex hull of the union of the convex hulls of the two subsets.
- Computing the convex hull of  $CH(S_1) \cup CH(S_2)$  is relatively simple since  $CH(S_1)$  and  $CH(S_2)$  are convex polygons  $P_1, P_2$  and, thus, have a natural ordering of their vertices.

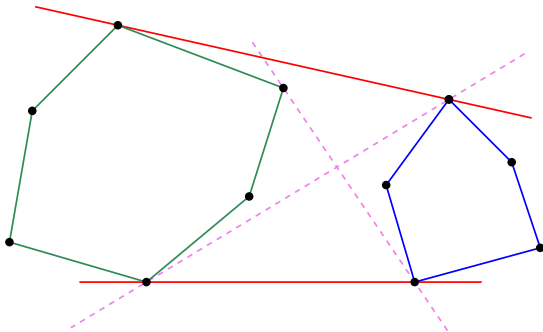


## Divide-and-Conquer Convex Hull: Supporting Lines

### Definition 61 (Supporting line, Dt.: Stützgerade)

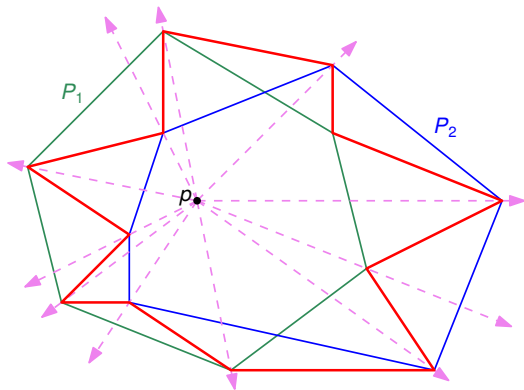
A *supporting line* of a convex polygon  $P$  is a straight line  $\ell$  passing through a vertex of  $P$  such that the interior of  $P$  lies entirely to one side of  $\ell$ .

- This definition is readily generalized to general convex sets.
- Two convex polygons  $P_1$  and  $P_2$ , where no polygon is entirely contained within the other polygon, have up to four *common supporting lines*.



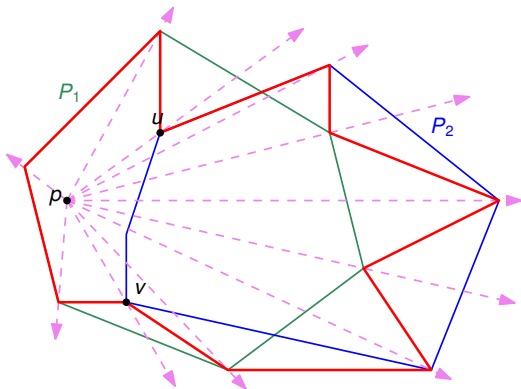
## Divide-and-Conquer Convex Hull: Merge

- 1 Find a point  $p$  that is internal to  $P_1$ ; e.g., the centroid. Note that this point  $p$  will be internal to  $CH(P_1 \cup P_2)$ .
- 2 Determine whether or not  $p$  is internal to  $P_2$ .
- 3 Case: Point  $p$  is internal to  $P_2$ :  
Merge  $P_1$  and  $P_2$  into one polygon that is star-shaped, with  $p$  within its kernel.
- 4 Apply Graham's Scan to the resulting polygon.



## Divide-and-Conquer Convex Hull: Merge

- 3 Case: Point  $p$  is not internal to  $P_2$ :
  - (a) Find vertices  $u$  and  $v$  on  $P_2$  such that  $\overline{pu}$  and  $\overline{pv}$  are supporting lines of  $P_2$ .
  - (b) Split  $P_2$  into two chains at  $u$  and  $v$ .
  - (c) Merge  $P_1$  and one chain of  $P_2$  into one polygon that is star-shaped, with  $p$  within its kernel.
- 4 Apply Graham's Scan to the resulting polygon.



## Divide-and-Conquer Convex Hull: Analysis

- If polygon  $P_1$  has  $n_1$  vertices and polygon  $P_2$  has  $n_2$  vertices, then the merge algorithm computes  $CH(P_1 \cup P_2)$  in  $O(n_1 + n_2)$  time.
- Obviously, an  $O(n)$  merge yields an  $O(n \log n)$  time bound for this divide-and-conquer algorithm.

### Theorem 62 (Complexity of divide&conquer convex hull)

The divide&conquer algorithm computes the convex hull of  $n$  points in the plane in  $O(n \log n)$  time and within  $O(n)$  storage.

## Convex Hull of a Simple Polygon

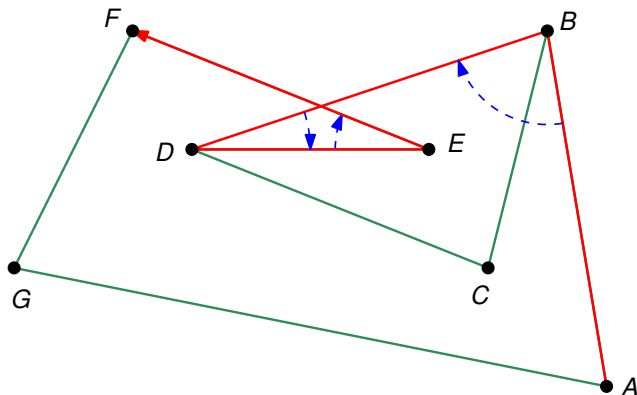
- Given is the sequence  $(p_1, p_2, \dots, p_n)$  of  $n$  points in  $\mathbb{R}^2$  which form the vertices of a simple polygon  $P$ .
- Obviously,  $CH(P)$  can be computed in  $O(n \log n)$  time.
- Can we do any better? Note: The lower bound for computing the convex hull of  $n$  points does not carry over to this problem!
- Recall that Graham's Scan runs in linear time when applied to a star-shaped polygon.
- Thus, the fact that the points are vertices of a polygon can be expected to help when designing a linear-time algorithm.

### Caveats

- 1 Several invalid linear-time “algorithms” were published in the early days of computational geometry.
- 2 Graham's Scan does not work properly for arbitrary simple polygons!

# Convex Hull of a Simple Polygon

- Graham's Scan does not work properly for arbitrary simple polygons!



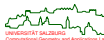
## Convex Hull of a Simple Polygon: Melkman's Algorithm

- Melkman's algorithm (1987) operates on a double-ended queue ("deque")  $\langle d_b, \dots, d_t \rangle$ , with  $d_b = d_t$ ; the  $d_i$ 's will represent vertices of the convex hull.
- Deque operations:
  - $\text{Push}(v)$  increments  $t$  by one, and inserts  $v$  at the new top;
  - $\text{Pop}(d_t)$  deletes the top element and decrements  $t$  by one;
  - $\text{Insert}(v)$  decrements  $b$  by one, and inserts  $v$  at the new bottom;
  - $\text{Delete}(d_b)$  deletes the bottom element and increments  $b$  by one.
- Melkman's algorithm incrementally computes the convex hull of the polygon by adding one vertex at a time.
- A deque  $D$  is used to maintain the vertices of the convex hull constructed so far in CW order.
- The input polygon needs to be oriented CW.
- In the pseudo-code the vertices are retrieved online from "input", and an actual implementation needs to check for an end of the input data.

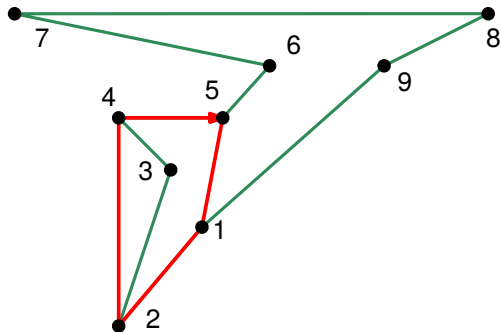
# Convex Hull of a Simple Polygon: Melkman's Algorithm

## Algorithm *Melkman's Algorithm*

1.  $t \leftarrow -1; b \leftarrow 0;$  (\* The current convex hull is maintained in the deque  $D$  \*)
2.  $v_1 \leftarrow \text{input}; v_2 \leftarrow \text{input}; v_3 \leftarrow \text{input};$  (\* Obtain vertices in CW order \*)
3. **if**  $\det(v_1, v_2, v_3) < 0$  **then** (\* Initialize  $D$  \*)
4.   Push( $v_1$ ); Push( $v_2$ );
5. **else**
6.   Push( $v_2$ ); Push( $v_1$ );
7.   Push( $v_3$ ); Insert( $v_3$ );
8. **repeat**
9.   **repeat**
10.      $v \leftarrow \text{input};$
11.     **until**  $\det(d_b, d_{b+1}, v) > 0$  **or**  $\det(d_{t-1}, d_t, v) > 0$  (\* Skip  $v$  if interior to  $D$  \*)
12.     **while**  $\det(d_{t-1}, d_t, v) > 0$  **do**
13.       Pop( $d_t$ ); (\* Delete interior vertices from top of  $D$  \*)
14.       Push( $v$ ); (\* Insert  $v$  at top of  $D$  \*)
15.       **while**  $\det(d_b, d_{b+1}, v) > 0$  **do**
16.         Delete( $d_b$ ); (\* Delete interior vertices from bottom of  $D$  \*)
17.       Insert( $v$ );
18.     **until** input is empty.



# Animation of Melkman's Algorithm



	$b$		$t$			
	←		→			
	-2	-1	0	1	2	3
		3	1	2	3	
4	3	1	2	4		
		5	1	2	4	5

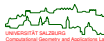
# Convex Hull of a Simple Polygon: Analysis of Melkman's Algorithm

## Theorem 63 (Melkman (1987))

Melkman's algorithm computes the convex hull of a simple  $n$ -vertex polygon in  $O(n)$  time.

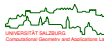
*Proof:* Similar to the analysis of Graham's Scan:

- Each vertex of the polygon is classified as either interior or exterior to the current hull in  $O(1)$  time.
- If vertex  $v_i$  is exterior to the current hull then  $k_i$  other vertices may end up being deleted, with  $O(1)$  time per each vertex that is deleted.
- Since  $\sum_{i=1}^n k_i \leq n - 3$ , the entire algorithm runs in  $O(n)$  time. □
- The first correct linear-time convex-hull algorithm for polygons is due to McCallum&Avis (1979).



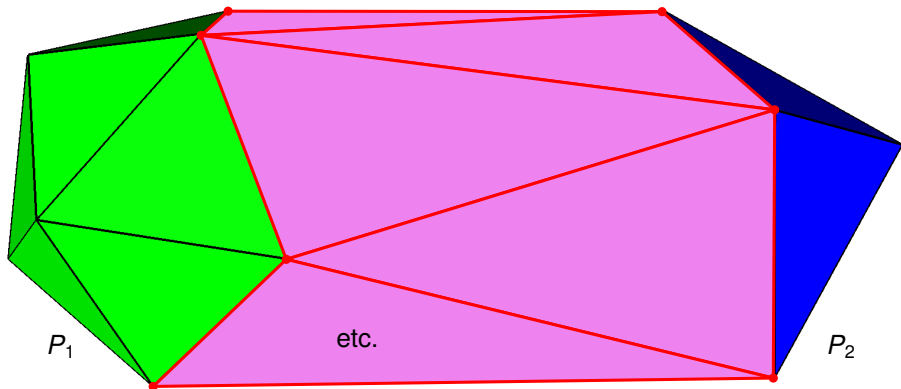
## Convex Hulls in 3D

- Consider a set  $S$  of  $n$  points  $\{p_1, p_2, \dots, p_n\} \subset \mathbb{R}^3$ . We want to compute  $CH(S)$ .
- Easy to prove:  $CH(S)$  is a convex polyhedron with at most  $3n - 6$  edges.
- The  $\Omega(n \log n)$  lower bound extends trivially from 2D to 3D.
- Divide-and-conquer algorithm for computing convex hulls in 3D:
  - 1 Sort (and re-number) the points of  $S$  according to their  $x$ -coordinates.
  - 2 Partition the set  $S$  into two subsets:  
 $S_1 := \{p_1, p_2, \dots, p_{\lfloor n/2 \rfloor}\}$ , and  
 $S_2 := \{p_{\lfloor n/2 \rfloor + 1}, \dots, p_n\}$ .
  - 3 Recursively find the convex hulls  $P_1 := CH(S_1)$  and  $P_2 := CH(S_2)$ .
  - 4 Merge  $P_1$  and  $P_2$  together to form  $CH(S)$ .
- In order to assist the merge, during all steps of the divide-and-conquer algorithm we maintain convex hulls of the point sets projected to 2D.



## Convex Hulls in 3D: Divide-and-Conquer Algorithm

- The key idea of the merge step is similar to “gift wrapping”:
  - 1 Find a supporting edge  $e$  of the projections of  $P_1$  and  $P_2$  to 2D.
  - 2 Construct the first merge facet of the hull by “wrapping” a 2D plane through  $e$  around  $P_1$  and  $P_2$ .
  - 3 Find a neighboring facet of the hull, again by “wrapping”.
  - 4 Continue from each facet to its neighbor until all merge facets are found.



# Convex Hulls in 3D: Divide-and-Conquer Algorithm

## Lemma 64

The merge step of the divide&conquer algorithm for computing the convex hull of  $n$  points in  $\mathbb{R}^3$  can be carried out in  $O(n)$  time.

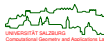
*Sketch of Proof:* Each new facet runs through the last constructed edge  $e$  and through an endpoint of another edge  $e'$  either on  $P_1$  or on  $P_2$ , where  $e$  and  $e'$  share a common endpoint. □

## Theorem 65

The full convex hull of  $n$  points in  $\mathbb{R}^3$  can be computed in  $O(n \log n)$  time.

## Theorem 66 (Seidel (1984))

The computation of the convex hull of a star-shaped polyhedron in  $\mathbb{R}^3$  with  $n$  vertices requires  $\Omega(n \log n)$  time in the worst case.



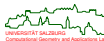
# Convex Hulls in Higher Dimensions

## Theorem 67 (Seidel (1981))

The convex hull of  $n$  points in  $\mathbb{R}^d$  can have  $\Omega(n^{\lfloor d/2 \rfloor})$  facets.

## Theorem 68 (Chazelle (1993))

The convex hull of  $n$  points in  $\mathbb{R}^d$  can be computed in  $O(n \log n + n^{\lfloor d/2 \rfloor})$  time.



## Sample Application of Convex Hulls: Lower Envelope

### Definition 69 (Lower envelope)

Let  $L$  be a set of  $n$  lines with equations

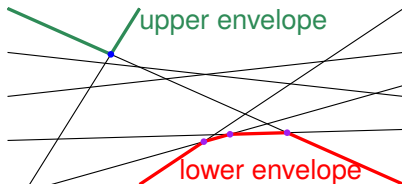
$$y = k_1x - d_1, \quad y = k_2x - d_2, \quad \dots, \quad y = k_nx - d_n.$$

Then the *lower envelope*  $\mathcal{L}_L$  of  $L$  is the function  $\mathcal{L}_L: \mathbb{R} \rightarrow \mathbb{R}$  with

$$\mathcal{L}_L(x) := \min_{1 \leq i \leq n} (k_i x - d_i).$$

Similarly for the upper envelope  $\mathcal{U}_L$ .

- Note that a line of  $L$  may belong to both the lower and the upper envelope.

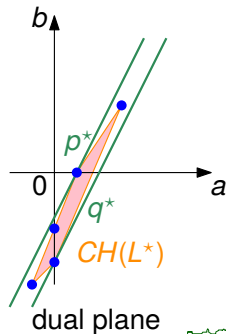
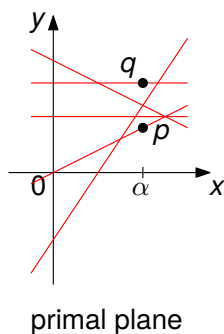


## Sample Application of Convex Hulls: Lower Envelope

### Lemma 70

Let  $L$  be a set of lines. For  $\alpha \in \mathbb{R}$  arbitrary but fixed let  $\beta^- := \mathcal{L}_L(\alpha)$  and  $\beta^+ := \mathcal{U}_L(\alpha)$ . Let  $(\alpha, \beta^-)$  be the coordinates of the point  $p$  and  $(\alpha, \beta^+)$  be the coordinates of the point  $q$ . Then the lines  $p^*$  and  $q^*$  support  $CH(L^*)$ .

*Proof:* By Cor. 40, all points of  $L^*$  are below or on the line  $p^*$ . Furthermore, since  $p$  is on the lower envelope and, thus, on a line of  $L$ , the line  $p^*$  must pass through one of the points of  $L^*$ . Hence,  $p^*$  supports  $CH(L^*)$  and lies above it. Similarly for  $q^*$ .  $\square$

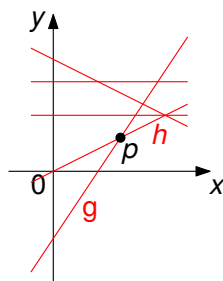


## Sample Application of Convex Hulls: Lower Envelope

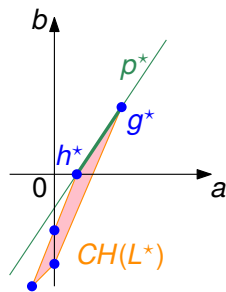
### Lemma 71

Let  $L$  be a set of lines. Then  $p$  is a vertex of the lower envelope of  $L$  if and only if  $p^*$  contains an edge on the (upper) convex hull  $CH(L^*)$ .

*Proof:* If  $p$  is a vertex of the lower envelope of  $L$ , then it is given by the intersection of two lines  $g$  and  $h$ . By Lem 70, all points of  $L^*$  lie below or on  $p^*$ . Furthermore,  $p^*$  passes through  $g^*$  and  $h^*$ . Hence,  $p^*$  contains an edge of  $CH(L^*)$ . The other direction is argued similarly.  $\square$



primal plane



dual plane

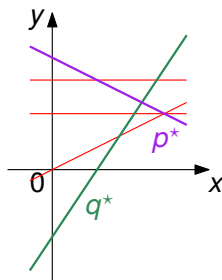


# Sample Application of Convex Hulls: Lower Envelope

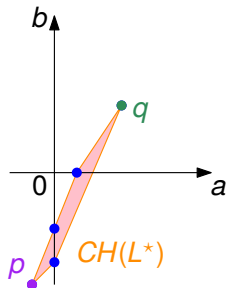
## Theorem 72

The lower (or upper) envelope of a set  $L$  of  $n$  lines in the plane can be computed in  $O(n \log n)$ .

- The  $y$ -extreme points  $p, q$  of  $CH(L^*)$  correspond to the two lines which appear on both the upper and lower envelope of  $L$  and which contain the four infinite rays of these envelopes.



primal plane

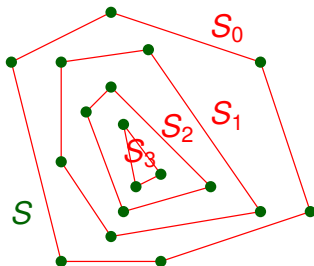


dual plane



## Sample Application of Convex Hulls: Onion Layers

- Consider a set  $S$  of  $n$  points in  $\mathbb{R}^2$ , with general position assumed.
- Let  $S_0 \subseteq S$  be the set of all vertices of  $CH(S)$ .
- The points of  $S_0$  are said to have *depth* 0.



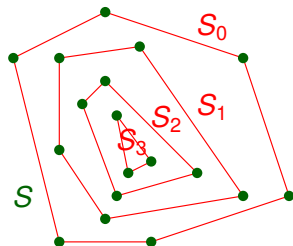
- Now let  $S := S \setminus S_0$ , and re-consider  $CH(S)$ .
- All points of  $S$  that are on  $CH(S)$  are said to have *depth* 1, and are assigned to  $S_1$ .
- Similarly for depths 2, 3,  $\dots$ ,  $k$ , where  $S_k \neq \emptyset$  and  $S_{k+1} = \emptyset$ .
- The sets  $S_0, S_1, S_2, \dots$  are called *shells* or *onion layers* or *convex layers* of  $S$ .



# Sample Application of Convex Hulls: Onion Layers

## Lemma 73

It takes  $\Omega(n \log n)$  time to compute all depths of  $n$  points in  $\mathbb{R}^2$ .



## Theorem 74 (Chazelle (1985))

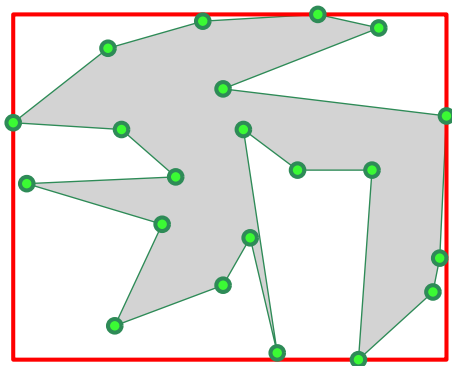
All depths of  $n$  points in  $\mathbb{R}^2$ , together with their onion layers, can be computed in time  $O(n \log n)$ .

- Statistics: The points of  $S_k, S_{k-1}, S_{k-2}, \dots$  lie close to the “center” of  $S$ , and computing their mean tends to discard “outliers”, thus yielding a more robust statistical estimator of the mean of  $S$  than the mean of all point samples.
- Rendering: Onion layers can be used to generate Hamiltonian triangulations.

## Sample Application of Convex Hulls: Kinetic AABB

### Definition 75 (AABB)

The (*axis-aligned*) bounding box (AABB) of a set  $S \subset \mathbb{R}^d$ , denoted by  $AABB(S)$ , is the smallest box (with sides parallel to the coordinate planes) which contains  $S$ .

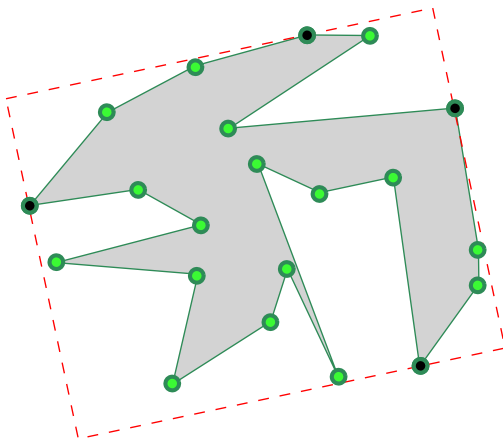


- If  $S$  can be described by a set of  $n$  vertices then  $AABB(S)$  can be computed in  $O(d \cdot n)$  time in a straightforward manner.



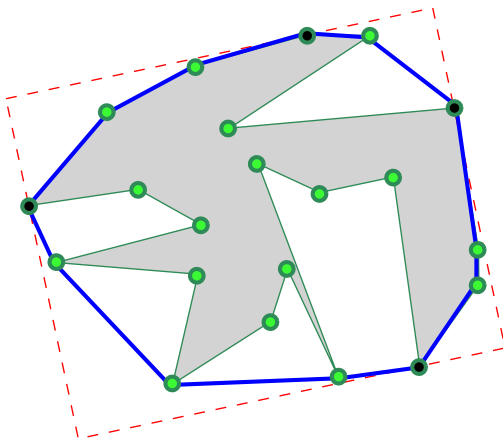
## Sample Application of Convex Hulls: Kinetic AABB

- What happens if  $S$  moves? We observe that  $AABB(S)$  equals  $AABB(CH(S))$ : up to six vertices  $v_1, v_2, \dots, v_6$  of  $CH(S)$  determine  $AABB(S)$  in  $\mathbb{R}^3$ .
- Goal: Avoid re-scanning all vertices of  $S$  in order to re-compute the axis-aligned bounding box from scratch.



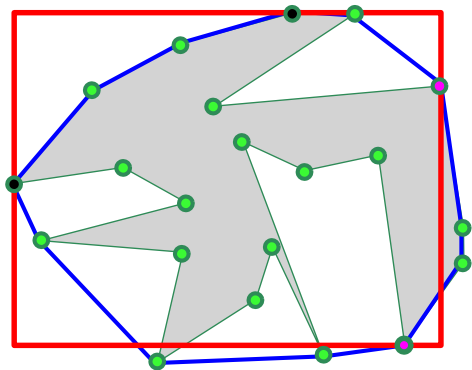
## Sample Application of Convex Hulls: Kinetic AABB

- What happens if  $S$  moves? We observe that  $AABB(S)$  equals  $AABB(CH(S))$ : up to six vertices  $v_1, v_2, \dots, v_6$  of  $CH(S)$  determine  $AABB(S)$  in  $\mathbb{R}^3$ .
- We can exploit coherence by applying a hill-climbing algorithm, starting at each of these six vertices (resp. four vertices in 2D).



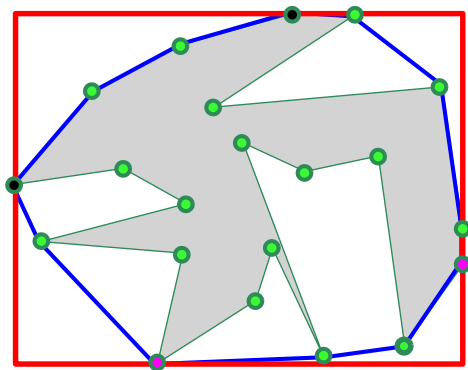
## Sample Application of Convex Hulls: Kinetic AABB

- What happens if  $S$  moves? We observe that  $AABB(S)$  equals  $AABB(CH(S))$ : up to six vertices  $v_1, v_2, \dots, v_6$  of  $CH(S)$  determine  $AABB(S)$  in  $\mathbb{R}^3$ .
- Hill-climbing means to move from one vertex to a neighboring vertex of  $CH(S)$  if it has a smaller/larger  $x$ -coordinate,  $y$ -coordinate,  $\dots$



## Sample Application of Convex Hulls: Kinetic AABB

- What happens if  $S$  moves? We observe that  $AABB(S)$  equals  $AABB(CH(S))$ : up to six vertices  $v_1, v_2, \dots, v_6$  of  $CH(S)$  determine  $AABB(S)$  in  $\mathbb{R}^3$ .
- If  $S$  has moved only a little then few steps of the hill-climbing algorithm will suffice. Of course, this scheme can be extended to  $k$ -dops.



## 5 Voronoi Diagrams of Points

- Definition and Properties
- Algorithms
- Generalizations
- Applications

# A Set of Proximity Problems

## Problem: PROXIMITY

**Given:** A set  $S := \{p_1, p_2, \dots, p_n\}$  of  $n$  points in  $\mathbb{R}^2$  under the Euclidean metric.

**CLOSESTPAIR:** Determine two points of  $S$  whose mutual distance is smallest.

**ALLNEARESTNEIGHBORS:** Determine the “nearest neighbor” (point of minimum distance within  $S$ ) for each point in  $S$ .

**EUCLIDEANMINIMUMSPANNINGTREE (EMST):** Construct a tree of minimum total (Euclidean) length whose vertices are the points of  $S$ . (No Steiner points allowed.)

**MAXIMUMEMPTYCIRCLE:** Find a circle with largest radius which does not contain a point of  $S$  in its interior and whose center lies within  $CH(S)$ .

**TRIANGULATION:** Join the points in  $S$  by non-intersecting straight-line segments so that every region internal to the convex hull of  $S$  is a triangle.

**NEARESTNEIGHBORSEARCH:** Given a query point  $q$ , determine which point  $p \in S$  is closest to  $q$ .

- Unless stated explicitly otherwise, we will always deal with the Euclidean metric

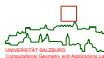


### Theorem 76

NEARESTNEIGHBORSEARCH among  $n$  points in  $\mathbb{R}^2$  has an  $\Omega(\log n)$  lower bound; CLOSESTPAIR, ALLNEARESTNEIGHBORS, EMST, MAXIMUMEMPTYCIRCLE and TRIANGULATION all have  $\Omega(n \log n)$  lower bounds (in the ACT model of computation).

#### *Sketch of Proof:*

- NEARESTNEIGHBORSEARCH: standard information-theoretic arguments yield  $\Omega(\log n)$  comparisons.
- CLOSESTPAIR: ELEMENTUNIQUENESS, which requires  $\Omega(n \log n)$  time (in the ACT model of computation), is linearly reducible to CLOSESTPAIR.
- ALLNEARESTNEIGHBORS: CLOSESTPAIR is linearly reducible to ALLNEARESTNEIGHBORS.
- EMST: CLOSESTPAIR is linearly reducible to EMST. (Also, SORTING can be reduced linearly to EMST.)
- MAXIMUMEMPTYCIRCLE in 1D solves MAXGAP, which establishes the  $\Omega(n \log n)$  lower bound.
- TRIANGULATION: CONVEXHULL is linearly reducible to TRIANGULATION.

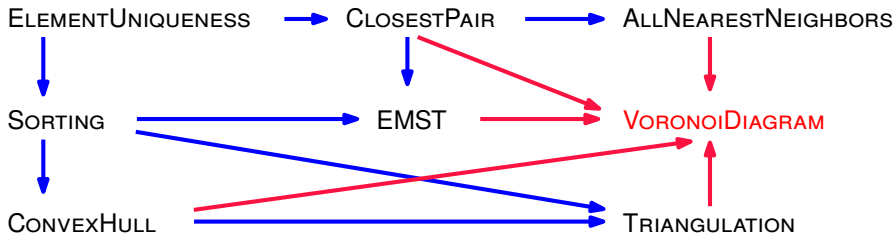


## Lower Bounds: Summary of Reductions

- Thus, we have  $\Omega(n \log n)$  lower bounds due to a variety of reductions.
- If Voronoi diagram is available then these problems can be solved in  $O(n)$  time!

### Theorem 77

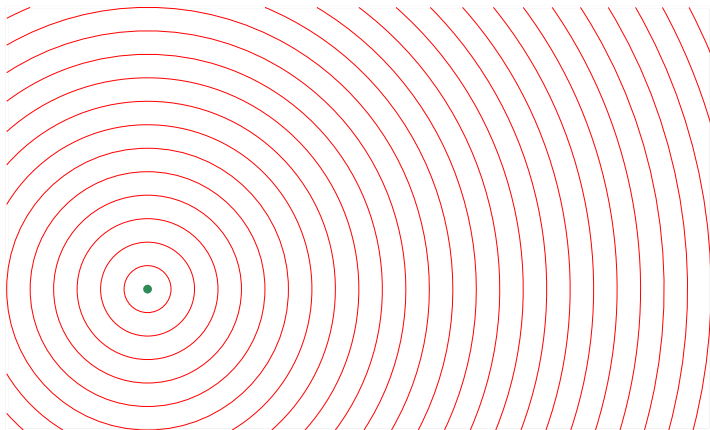
The computation of the Voronoi diagram of  $n$  points in  $\mathbb{R}^2$  requires  $\Omega(n \log n)$  time.



# Voronoi Diagram: Motivation

## Prairie fire

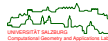
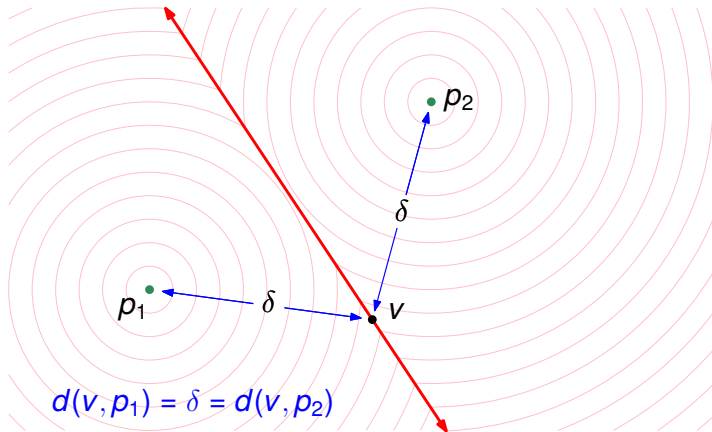
Let's ignite a fire in a grassland, and watch it spread out. In an idealized setting — uniform grassland, no wind — the fire **wavefronts** will form concentric circles!



# Voronoi Diagram of Points

## Prairie fire

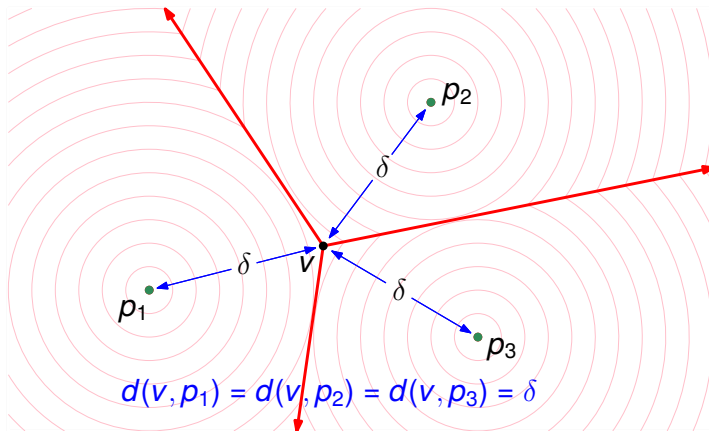
Now ignite two fires simultaneously: As the fire wavefronts meet — which propagate at the same speeds! — the **bisector line** between the two fire sites is traced out.



# Voronoi Diagram of Points

## Prairie fire

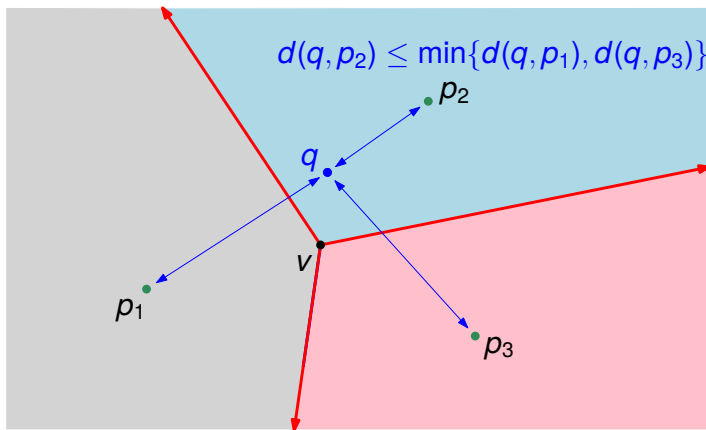
We repeat the experiment with three fires ignited simultaneously: Again, the fire wavefronts trace out the bisectors between the fire sites as they meet.



# Voronoi Diagram: Motivation

## Voronoi regions

The red bisectors defined by the three fires partition the plane into Voronoi regions: Each region is the loci of points  $q$  closer to its defining fire site than to any other fire.



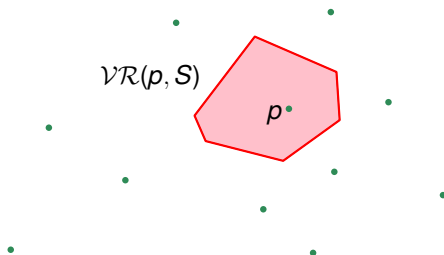
## Voronoi Diagram: Definition

- Consider a set  $S := \{p_1, p_2, \dots, p_n\}$  of  $n$  distinct points in  $\mathbb{R}^2$  and denote the Euclidean distance by  $d(\cdot, \cdot)$ , with  $d(q, S) := \min\{d(q, p) : p \in S\}$ .

### Definition 78 (Voronoi region, Dt.: Voronoi-Zelle)

The *Voronoi region* (VR, aka “Voronoi cell”) of a point  $p \in S$  is the locus of points of  $\mathbb{R}^2$  whose distance to  $p$  is not greater than the distance to any other point of  $S$ :

$$\mathcal{VR}(p, S) := \{q \in \mathbb{R}^2 : d(q, p) \leq d(q, S)\}.$$



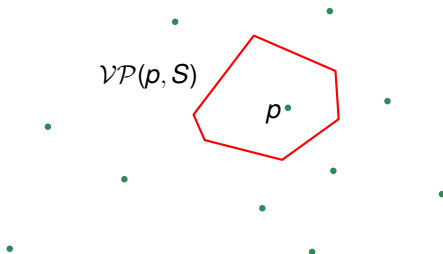
## Voronoi Diagram: Definition

### Definition 79 (Voronoi polygon)

The *Voronoi polygon* (VP) of  $p \in S$  is defined as

$$\mathcal{VP}(p, S) := \partial \mathcal{VR}(p, S).$$

The segments of a Voronoi polygon are called *Voronoi edges*.

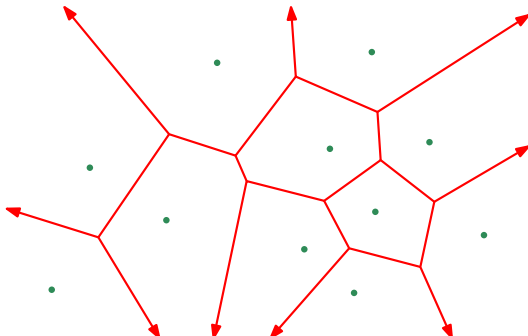


# Voronoi Diagram: Definition

## Definition 80 (Voronoi diagram)

The *Voronoi diagram* (VD) of  $S$  is defined as

$$\mathcal{VD}(S) := \bigcup_{1 \leq i \leq n} \mathcal{VP}(p_i, S).$$

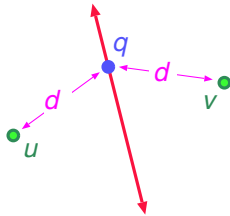


## Voronoi Diagram: Definition

### Definition 81 (Bisector)

The *bisector* of two points  $u, v \in \mathbb{R}^2$  is the set of points of  $\mathbb{R}^2$  which are equidistant to  $u$  and  $v$ :

$$b(u, v) := \{q \in \mathbb{R}^2 : d(u, q) = d(v, q)\}.$$



- A Voronoi edge always lies on a bisector. Thus, points on a Voronoi edge are equidistant to two points of  $S$ .

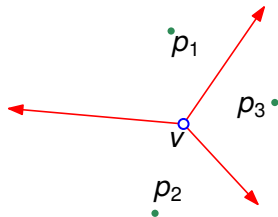
### Lemma 82

For  $p \in S$  we get  $\mathcal{VP}(p, S) = \{q \in \mathbb{R}^2 : d(q, p) = d(q, S \setminus \{p\})\}$ .

## Voronoi Diagram: Definition

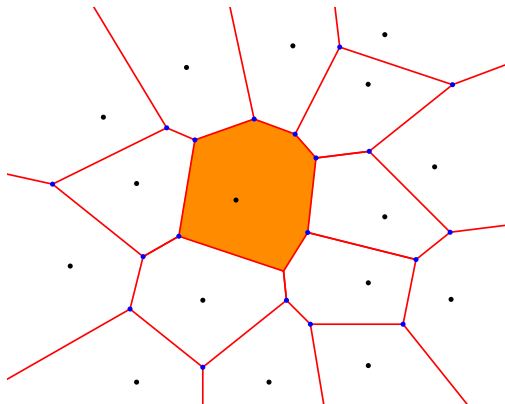
### Definition 83 (Voronoi node, Dt.: Voronoi-Knoten)

Intersections of Voronoi edges are called *Voronoi nodes*.



# Sample Voronoi Diagram

- Input set  $S$  of points, Voronoi diagram and one Voronoi region, Voronoi nodes.



## Historical Remarks

- René Descartes (1596–1650) drew Voronoi-like diagrams to illustrate the subdivision of space by celestial bodies [Descartes 1644].
- Gustav Lejeune Dirichlet (1805–1859) provided the first formal definition of Voronoi diagrams in two dimensions [Dirichlet 1850].
- Georgy Feodosevich Voronoi (1868–1908) generalized them to  $n$  dimensions [Voronoi 1908].
  - Several other Latin spellings of his name: Voronoï, Voronoy, Woronoi.
  - Born at Zhuravky (near Kyiv).
  - Studied at Saint Petersburg University as a student of Andrey Markov.
  - Professor at the University of Warsaw.
  - Students (among others): Boris Delaunay (Kyiv) and Wacław Sierpiński (Warsaw).



# Voronoi Diagram: Properties

## Lemma 84

The Voronoi region  $\mathcal{VR}(p_i, S)$  is the intersection of half-planes defined by bisectors between  $p_i \in S$  and the other points of  $S$ :

$$\mathcal{VR}(p_i, S) = \bigcap_{\substack{1 \leq j \leq n \\ j \neq i}} H(p_i, p_j),$$

where  $H(p_i, p_j)$  is the half-plane that contains  $p_i$  and is bounded by  $b(p_i, p_j)$ .

## Corollary 85

Every Voronoi region is a convex polygonal area.

## Lemma 86

Every point of  $S$  has its own Voronoi region that is not empty.

## Lemma 87

The (topological) interiors of Voronoi regions of distinct points of  $S$  are disjoint.

# Voronoi Diagram: Properties

## General position assumed (GPA)

No four points of  $S$  are co-circular!

## Lemma 88

A Voronoi node is the common intersection of exactly three Voronoi edges. It is equidistant to the three points of  $S$  which lie in the Voronoi regions it belongs to.

## Corollary 89

A Voronoi diagram is a 3-regular (plane) graph.

## Lemma 90

The disk  $D$  centered at a Voronoi node  $v$  that passes through the node's three equidistant points  $p_1, p_2, p_3 \in S$  contains no other points of  $S$  in its interior.

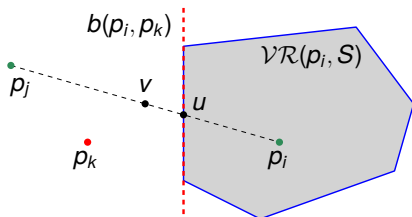
# Voronoi Diagram: Properties

## Lemma 91

For  $p_i \in S$ , every nearest neighbor of  $p_i$  defines an edge of  $\mathcal{VP}(p_i, S)$ .

*Proof:*

- Let  $p_j \in S$  be a nearest neighbor of  $p_i$ , and let  $v$  be their midpoint.
- Suppose that  $v$  does not lie on the boundary of  $\mathcal{VR}(p_i, S)$ . Then it has to lie outside of  $\mathcal{VP}(p_i, S)$ !



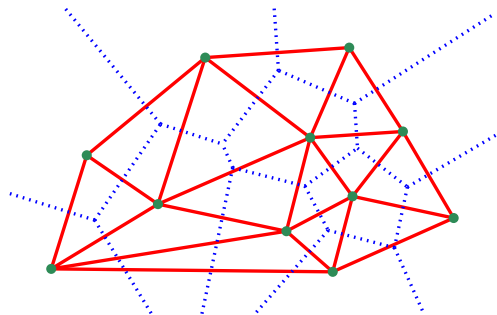
- Then the line segment  $\overline{p_i v}$  would intersect some edge of  $\mathcal{VP}(p_i, S)$ . Assume that it intersects the bisector of  $\overline{p_i p_k}$  in the point  $u$ . Now  $|\overline{p_i u}| < |\overline{p_i v}|$ , and therefore  $|\overline{p_i p_k}| \leq 2|\overline{p_i u}| < 2|\overline{p_i v}| = |\overline{p_i p_j}|$ , and we would have  $p_k$  closer to  $p_i$  than  $p_j$ , which is a contradiction.

# Delaunay Triangulation: Definition and Properties

## Definition 92 (Delaunay triangulation)

A *Delaunay triangulation* (DT),  $DT(S)$ , of  $S$  is a plane geometric graph that is *dual* to the Voronoi diagram of  $S$ :

- The nodes of the graph are given by the points of  $S$ .
- Two points are connected by a line segment, and form an edge of  $DT(S)$ , exactly if they share a Voronoi edge of  $VD(S)$ .



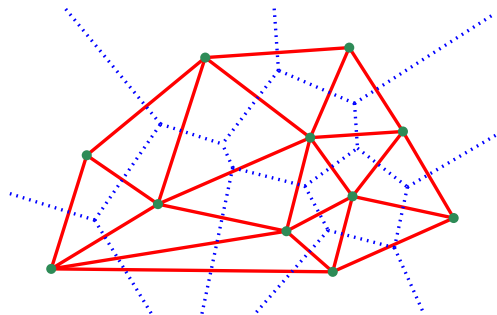
- Named after Boris Nikolaevich Delaunay (1890–1980).

# Delaunay Triangulation: Definition and Properties

## Lemma 93

The structure  $DT(S)$  does indeed form a triangulation of  $S$ .

- Thus, the interior faces of  $DT(S)$  are triangles that are defined by triples of  $S$ , with each face corresponding to exactly one node of  $\mathcal{VD}(S)$ .
- By definition, every edge of the Delaunay triangulation has a corresponding edge in the Voronoi diagram.
- $DT(S)$  is called the *straight-line dual* of  $\mathcal{VD}(S)$ .



- Note: An edge of  $DT(S)$  need not intersect its dual Voronoi edge.
- If no four points of  $S$  are co-circular then its Delaunay triangulation is unique.

# Complexity of Voronoi Diagram and Delaunay Triangulation

## Lemma 94

The Delaunay triangulation of  $n$  points has at most  $3n - 6$  edges and at most  $2n - 4$  faces (for all  $n \geq 3$ ).

*Proof:* Recall that a Delaunay triangulation forms a connected planar graph on  $n$  nodes, where every bounded face is bounded by exactly three edges. Hence, Euler's formula  $V - E + F = 2$  can be applied, with  $V := n$ , and we get

$$E \leq 3V - 6 \quad \text{and} \quad F \leq 2V - 4 \quad \text{and} \quad F \leq \frac{2}{3}E. \quad \square$$

- We conclude that

$$\begin{array}{ll} DT: & \leq 3n - 6 \text{ edges} \quad \text{and thus} \quad \mathcal{VD}: & \leq 3n - 6 \text{ edges,} \\ DT: & \leq 2n - 4 \text{ faces} \quad \text{and thus} \quad \mathcal{VD}: & \leq 2n - 5 \text{ nodes.} \end{array}$$

## Lemma 95

The Voronoi diagram of  $n$  points has at most  $3n - 6$  edges and at most  $2n - 5$  nodes.

## Corollary 96

A Voronoi polygon has at most  $n - 1$  edges, but only six edges on average.

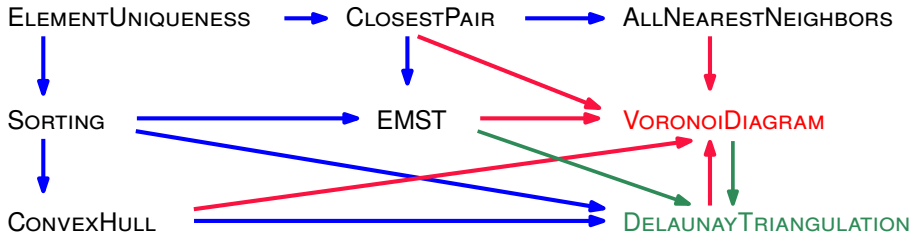
## Proximity Problems Solved by Voronoi Diagrams

- The fact that the Voronoi polygons of nearest neighbors always have a Voronoi edge in common implies that it is sufficient to check all points in adjacent Voronoi regions to find a nearest neighbor of a point  $p_i \in S$ .
- Thus, knowledge of the Voronoi diagram helps to solve CLOSESTPAIR and ALLNEARESTNEIGHBORS in  $O(n)$  time.
- The Voronoi polygon of  $p_i \in S$  is unbounded if and only if  $p_i$  is a vertex of the convex hull of the set  $S$ . (Proof: See Preparata&Shamos.) This means that the vertices of  $CH(S)$  are those points of  $S$  which have unbounded Voronoi polygons.
- Thus, knowledge of the Voronoi diagram allows to solve CONVEXHULL in  $O(n)$  time.
- A MAXIMUMEMPTYCIRCLE can be found in  $O(n)$  time by scanning all nodes of the Voronoi diagram; see later.
- After  $O(n)$  preprocessing for building a search data structure of size  $O(n)$  on top of the Voronoi diagram, NEARESTNEIGHBORSEARCH queries can be handled in  $O(\log n)$  time. (However, the constants are high — better techniques are known for point sites!)

# Reductions Among Proximity Problems

## Lemma 97

The Voronoi diagram of  $n$  points in  $\mathbb{R}^2$  can be obtained in  $O(n)$  time from the Delaunay triangulation, and the Delaunay triangulation can be obtained in  $O(n)$  time from the Voronoi diagram.

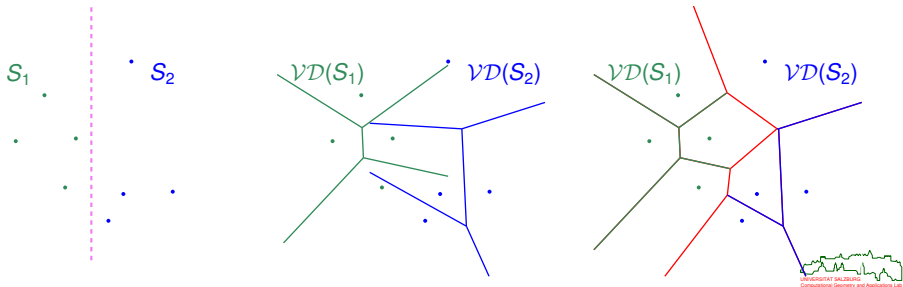


## Theorem 98 (Chazelle 1993)

The Voronoi diagram of  $n$  points in  $\mathbb{R}^d$  can be computed in optimal  $O(n \log n + n^{\lceil \frac{d}{2} \rceil})$  time.

# Divide&Conquer Algorithm

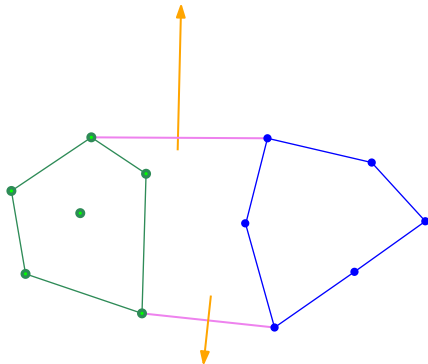
- Preprocessing: Sort the points of  $S$  by  $x$ -coordinates. This takes  $O(n \log n)$  time.
- Divide:
  - Divide  $S$  into two subsets  $S_1$  and  $S_2$  of roughly equal size such that the points in  $S_1$  lie to the left and the points in  $S_2$  lie to the right of a vertical line.
  - This step can be carried out in  $O(n)$  time.
- Conquer (aka “Merge”):
  - Assume that  $\mathcal{VD}(S_1)$  and  $\mathcal{VD}(S_2)$  are known.
  - Clip those parts of  $\mathcal{VD}(S_1)$  that lie to the “right” of a so-called *dividing chain*.
  - Analogously for  $\mathcal{VD}(S_2)$ .



# Divide&Conquer Algorithm: Merge

1 Find upper and lower supporting edges of  $CH(S_1)$  and  $CH(S_2)$  in order to form the convex hull  $CH(S)$ .

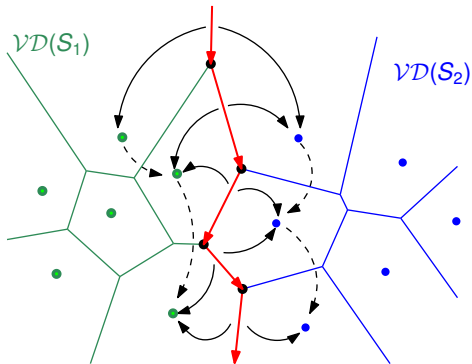
- Bisector (ray) defined by upper bridge of convex hull is part of the dividing chain.
- Bisector (ray) defined by lower bridge of convex hull is part of the dividing chain.



# Divide&Conquer Algorithm: Merge

2 Build dividing chain from top to bottom:

- Start by walking down along the upper ray.
- Intersect the ray with  $\mathcal{VD}(S_1)$  and  $\mathcal{VD}(S_2)$ .
- Pick the first intersection as new Voronoi node.
- The next ray is the new bisector originating at this node.
- Continue this jagged walk until the lower ray is reached.



# Divide&Conquer Algorithm: Complexity Analysis

## Lemma 99

The merge can be carried out in  $O(n)$  time, based on the Shamos-Hoey scanning scheme that prevents Voronoi edges from being searched for an intersection for more than a constant number of times.

- If the merge is carried out in linear time then we get a familiar recurrence relation for the time  $T$ :

$$T(n) = 2T\left(\frac{n}{2}\right) + O(n),$$

and therefore

$$T \in O(n \log n).$$

## Theorem 100

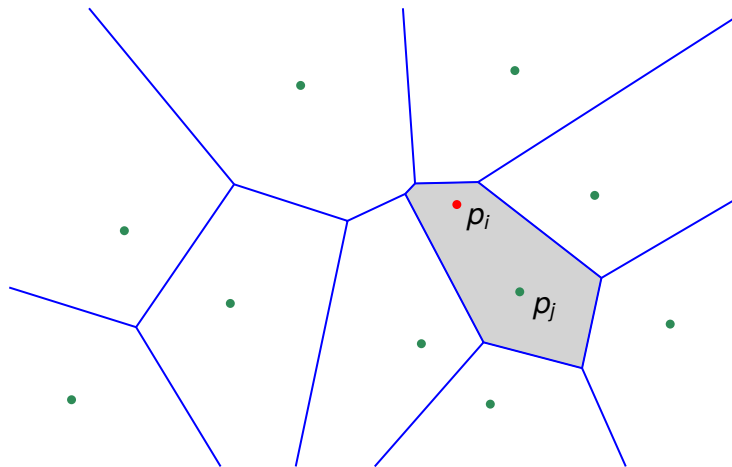
The divide&conquer algorithm computes  $\mathcal{VD}(S)$  for a set  $S$  of  $n$  points in optimal  $O(n \log n)$  time.

## Incremental Construction

- We compute the Voronoi diagram  $\mathcal{VD}(S)$  of a set  $S := \{p_1, p_2, \dots, p_n\}$  of  $n$  points by inserting the  $i$ -th point  $p_i$  into  $\mathcal{VD}(\{p_1, p_2, \dots, p_{i-1}\})$ , for  $1 \leq i \leq n$ .
- If we could achieve constant complexity per insertion then a linear algorithm would result:
  - Best case:  $O(n)$ .
- An insertion could, however, affect all other sites:
  - Worst case:  $O(n^2)$ , or even worse.
- Since, on average, every Voronoi region is bounded by six Voronoi edges there is reason to hope that a close-to-linear time complexity can be achieved.
- Let  $S' := \{p_1, p_2, \dots, p_{i-1}\}$ .

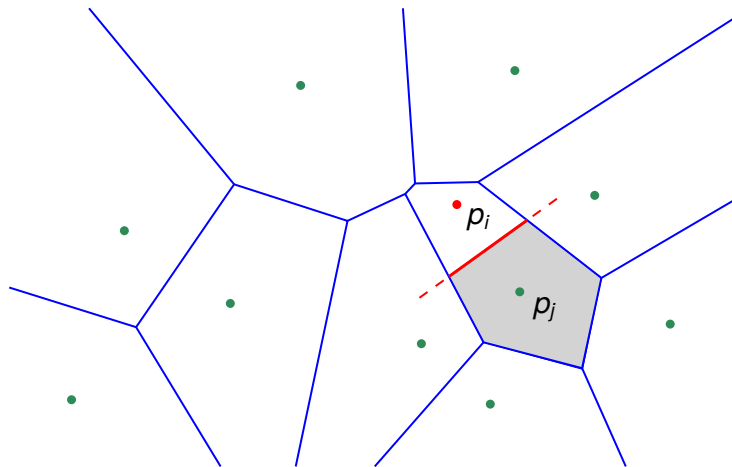
## Incremental Construction: Basic Algorithm

- 1 Nearest-neighbor search among  $S'$ : Determine  $1 \leq j < i$  such that the **new point**  $p_i$  lies in  $\mathcal{VR}(p_j, S')$ .



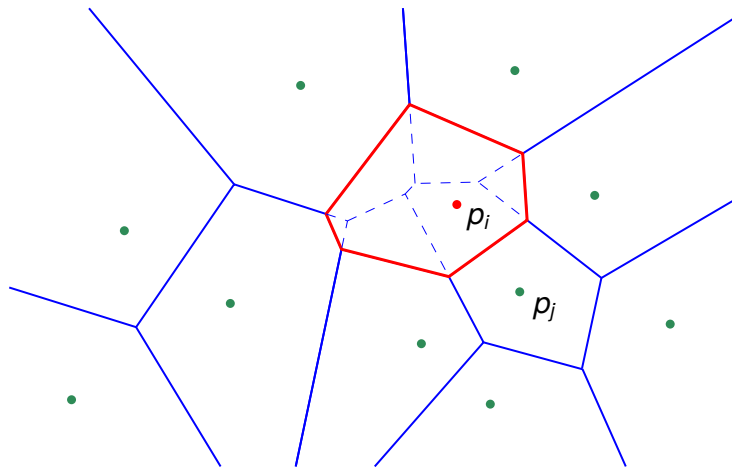
## Incremental Construction: Basic Algorithm

- 2 Construct the bisector  $b(p_i, p_j)$  between  $p_i$  and  $p_j$ , intersect it with  $\mathcal{VP}(p_j, S')$ , and clip that portion of  $\mathcal{VP}(p_j, S')$  which is closer to  $p_i$  than to  $p_j$ .



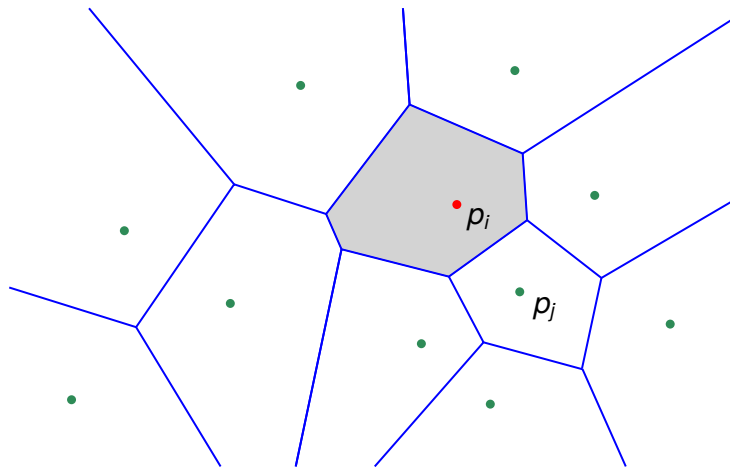
## Incremental Construction: Basic Algorithm

- 3 Generate  $\mathcal{VP}(p_i, \{p_1, p_2, \dots, p_i\})$  by a circular scan around  $p_i$ , similar to the construction of the dividing chain in the divide&conquer algorithm.



## Incremental Construction: Basic Algorithm

- The scan is finished once it returns to  $\mathcal{VR}(p_j, S')$ .



## Incremental Construction: Complexity

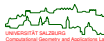
- The complexity mainly depends on the complexity of the nearest-neighbor search and on the number of edges generated/deleted during the scan.
- It is fairly easy to pick  $n$  points and number them “appropriately” such that the insertion of the  $i$ -th point requires the generation of  $O(i)$  Voronoi edges!
- But randomization comes to our rescue, and one can prove the following result.

### Theorem 101

Randomized incremental construction allows to compute the Voronoi diagram of  $n$  points in  $O(n \log n)$  expected time.

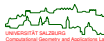
*Sketch of Proof:* A search data structure (“history DAG”) can be maintained that has  $O(n)$  expected size, and supports nearest-neighbor queries in  $O(\log n)$  expected time. Updates can be done in  $O(1)$  expected time. □

- The actual proof of these claims relies on backwards analysis.
- This result is independent of the point distribution, as long as the insertion order is random!
- This is a nice result seen from a theoretical point of view, but an actual implementation of the search structure would require a bit of work . . .



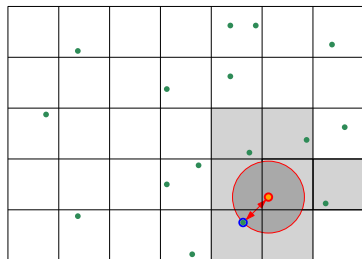
# Geometric Hashing for Nearest-Neighbor Searching

- The bounding box of  $S$  (or of a slightly larger region that contains  $S$ ) is partitioned into rectangular cells of uniform size by means of a regular grid.
- For every cell  $c$ , all points of  $\{p_1, p_2, \dots, p_{i-1}\}$  that lie in  $c$  are stored with  $c$ . (Alternatively, only one point is stored per cell.)



# Geometric Hashing for Nearest-Neighbor Searching

- To find the point  $p_j$  closest to point  $p_i$ :
  - Determine the cell  $c$  in which  $p_i$  lies.
  - By searching in  $c$  (and possibly in its neighboring cells, if  $c$  is empty), we find a first candidate for the nearest neighbor.
  - Let  $\delta$  be the distance from  $p_i$  to this point.
  - We continue searching in  $c$  and in those cells around  $c$  which are intersected by a disk  $D$  with radius  $\delta$  centered at  $p_i$ .
  - Whenever a point of  $\{p_1, p_2, \dots, p_{i-1}\}$  that is closer to  $p_i$  is found, we reduce  $\delta$  appropriately.
  - The search stops once no unsearched cell exists that is intersected by  $D$ .

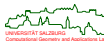


# Geometric Hashing for Nearest-Neighbor Searching

- What is a suitable resolution of the grid? There is no universally valid answer. In any case, the grid should not use more than  $O(n)$  memory!

## Personal experience

- Grids of the form  $(w \cdot \sqrt{n}) \times (h \cdot \sqrt{n})$  seem to work nicely, with  $w \cdot h = c$  for some constant  $c$ .
- The parameters  $w, h$  are chosen to adapt the resolution of the grid to the aspect ratio of the bounding box of the points.
- By experiment:  $1 \leq c \leq 2$ .
- This basic scheme can be tuned considerably:
  - Switch to multi-level hashing or to kd-trees if a small sample of the points indicates that the points are distributed highly non-uniformly.
  - Adapt the grid resolution and re-hash if the number of points stored changes significantly due to insertions and deletions of points.
- Hash-based nearest-neighbor searching will work best for points that are distributed uniformly, and will fail miserably if all points end up in one cell!
- Still, personal experience tells me that (tuned) geometric hashing works extremely well even for point sets that are distributed highly irregularly!

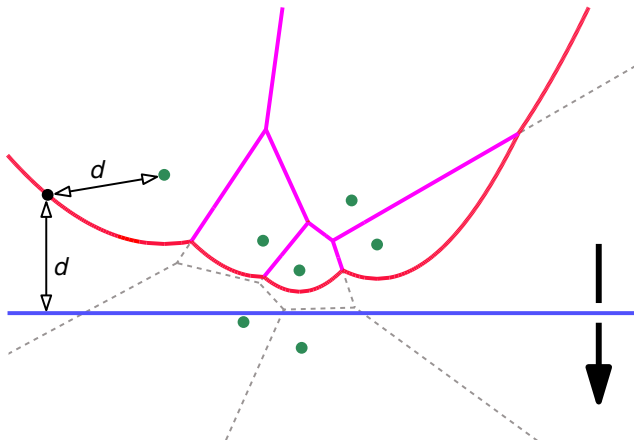


# Sweep-Line Algorithm

- Can a sweep-line algorithm be applied to compute the Voronoi diagram?
- Principal problem: When a top-down sweep line reaches the top-most vertex of  $\mathcal{VP}(p_i, S)$ , then it has not yet moved over  $p_i$ !
- Thus, the information on the corresponding point site is missing when a Voronoi polygon is first encountered and Voronoi nodes are to be computed.
- This problem is independent of the sweep direction chosen.
- Hence, for quite some time it was assumed that the sweep-line paradigm is not applicable to Voronoi diagrams.
- W.l.o.g., we move the sweep line  $\ell$  from top to bottom.
- Remarkable idea (by S. Fortune): Rather than keeping the actual intersection of the Voronoi diagram with  $\ell$ , we maintain information on that part of the Voronoi diagram of the points above  $\ell$  that is guaranteed not to be affected by points below  $\ell$ .

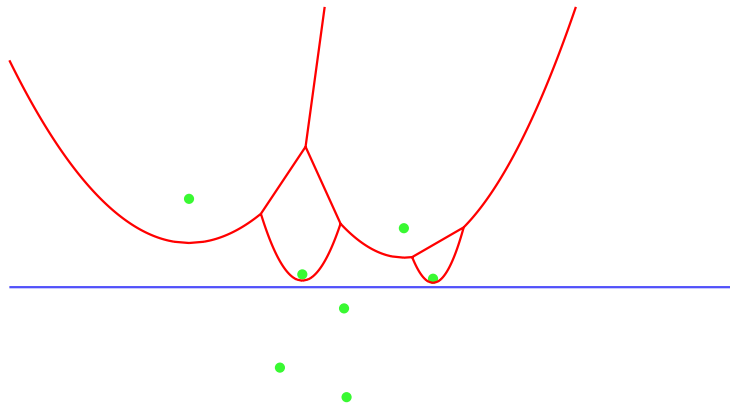
## Sweep-Line Algorithm: Beach Line

- The part of the Voronoi diagram that will not change any more as the sweep line continues to move downwards lies above the so-called *beach line* formed by the lower envelope of parabolic arcs: Each parabolic arc is defined by  $\ell$  and by a point above  $\ell$ .



# Animation of Sweep-Line Algorithm

- The beach line moves downwards as the sweep-line is moved from top to bottom. A full sweep reveals the complete Voronoi diagram.

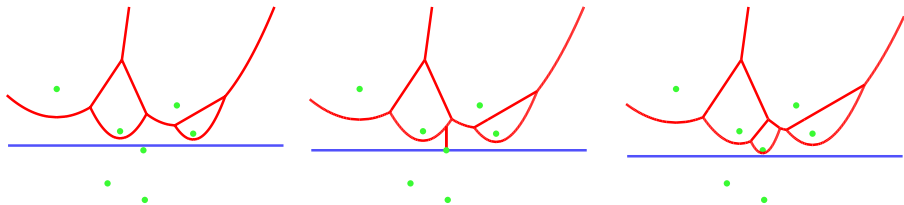


# Sweep-Line Algorithm: Events

- The following two events need to be considered for the event-point schedule:
  - 1 Site event:
    - The sweep line  $\ell$  passes through an input point, and a new parabolic arc needs to be inserted into the beach line.
  - 2 Circle event:
    - A parabolic arc of the beach line vanishes, i.e., degenerates to a point  $v$ , and a new Voronoi node has to be inserted at  $v$ .
    - What does this mean for the sweep line  $\ell$ ? What is the appropriate  $y$ -position of  $\ell$  to catch this event?

## Sweep-Line Algorithm: Site Event

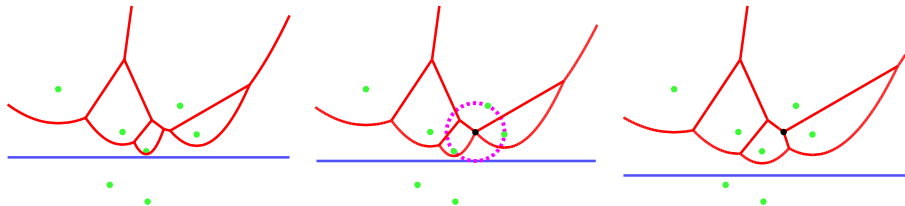
- If the sweep line  $\ell$  passes through an input point then a new parabolic arc needs to be inserted into the beach line. Initially, this arc is degenerate.



- This event occurs whenever the sweep line  $\ell$  passes through an input point  $p_i$ .
- It is responsible for the initialization of a new Voronoi region that will become  $\mathcal{VR}(p_i, S)$ .

## Sweep-Line Algorithm: Circle Event

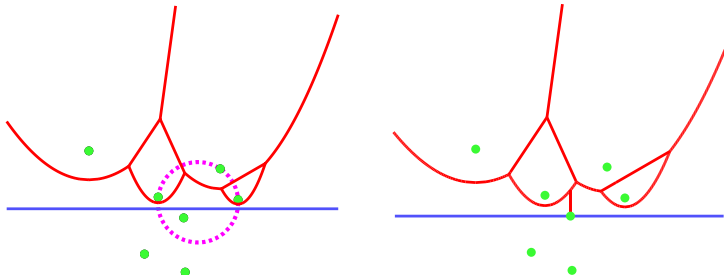
- If a parabolic arc of the beach line degenerates to a point  $v$  then a new Voronoi node needs to be inserted at  $v$ .



- A circle event occurs when the sweep line  $\ell$  passes over the south pole of a circle through the three defining input points  $p_i, p_j, p_k$  of three consecutive parabolic arcs of the beach line.
- The center  $v$  of such a circle is equidistant to  $p_i, p_j, p_k$  and also to  $\ell$ ; it becomes a new node of the Voronoi diagram.

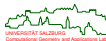
## Sweep-Line Algorithm: False Alarms

- Not all scheduled circle events correspond to valid new Voronoi nodes: A circle event has to be processed only if its defining three parabolic arcs still are consecutive members of the beach line at the time when the sweep line  $\ell$  passes over the south pole of the circle.



## Sweep-Line Algorithm: Event-Point Schedule and Sweep-Line Status

- All input points are stored in sorted order (according to  $y$ -coordinates) in the event-point schedule.
- Whenever three parabolic arcs become consecutive for the first time — when a site event occurs — the  $y$ -coordinate of the corresponding circle event is inserted into the event-point schedule at the appropriate place.
- Parabolic arcs have to be inserted into the beach line when processing site events, and have to be deleted when processing circle events.
- Both structures are best represented as balanced binary search trees, since this allows logarithmic insertion/deletion.



# Sweep-Line Algorithm: Analysis

## Lemma 102

The beach line is monotone with respect to the  $x$ -axis.

## Lemma 103

An arc can appear on the beach line only through a site event.

## Corollary 104

The beach line is a sequence of at most  $2n - 1$  parabolic arcs.

## Lemma 105

An arc can disappear from the beach line only through a circle event.

## Theorem 106 (Fortune (1986))

A sweep-line algorithm computes the Voronoi diagram of  $n$  points in  $O(n \log n)$  time, using  $O(n)$  storage.

## Construction via Lifting to 3D

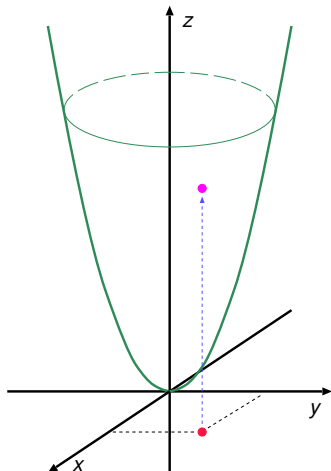
- Consider the transformation that maps a point  $p = (p_x, p_y)$  to the non-vertical plane  $h(p) \equiv z = 2p_x x + 2p_y y - (p_x^2 + p_y^2)$  in  $\mathbb{R}^3$ .
- This plane is tangent to the unit paraboloid  $z = x^2 + y^2$  at the point  $(p_x, p_y, p_x^2 + p_y^2)$ .
- Let  $h^+(p)$  be the half-space induced by  $h(p)$  which contains the unit paraboloid.

### Theorem 107

For  $S := \{p_1, p_2, \dots, p_n\}$ , consider the convex polyhedron  $\mathcal{P} := \bigcap_{1 \leq i \leq n} h^+(p_i)$ . The normal projection of the vertices and edges of  $\mathcal{P}$  onto the  $xy$ -plane yields  $\mathcal{VD}(S)$ .

### Corollary 108

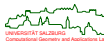
This lifting allows to construct Voronoi diagrams in  $O(n \log n)$  time.



# Voronoi Diagram as Minimization Diagram

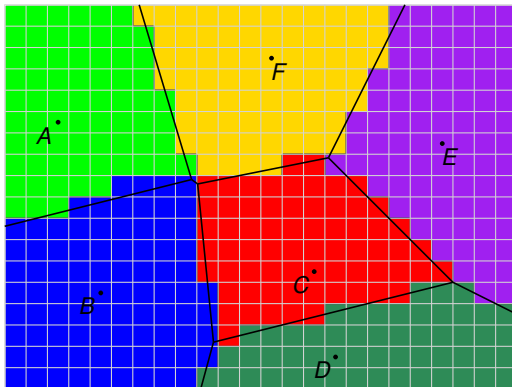
## Edelsbrunner&Seidel (1986)

- 1 For each site: Construct (in  $\mathbb{R}^3$ ) one upside-down, infinitely tall, right pyramid whose apex coincides with the site's location.
- 2 Every cross-section of a site's pyramid corresponds to a wavefront of the site: A point  $p \in \mathbb{R}^3$  with coordinates  $(x, y, t)$  lies on the pyramid of site  $s$  if the point  $p_{xy} \in \mathbb{R}^2$  with coordinates  $(x, y)$  is at weighted distance  $t$  from  $s$ .
- 3 Then the minimization diagram of all pyramids matches the Voronoi diagram.



# Discrete Voronoi Diagram

- For a input points given, a regular grid is constructed over a super-set of their bounding box.
- Then discrete Voronoi regions are determined by deciding on a cell-by-cell basis which input point is closest.
- The Voronoi diagram is extracted from the grid.



## Approximate Voronoi Diagram by Means of Graphics Hardware

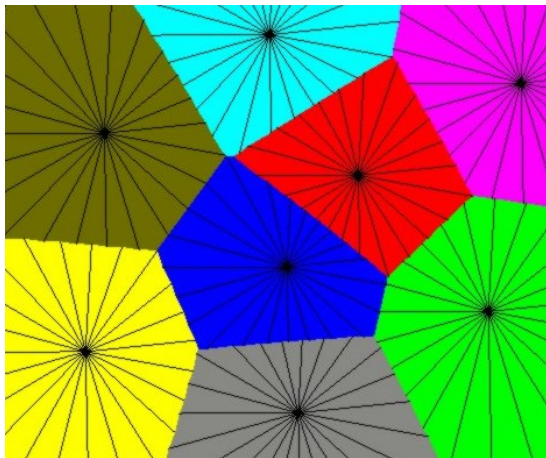
- Regard  $\mathbb{R}^2$  as the  $xy$ -plane of  $\mathbb{R}^3$ , and construct upright circular unit cones at every point of  $S$ . (All cones point upwards, are of the same size and form the same angle with the  $xy$ -plane!) Assign a unique color to every cone.



# Approximate Voronoi Diagram by Means of Graphics Hardware

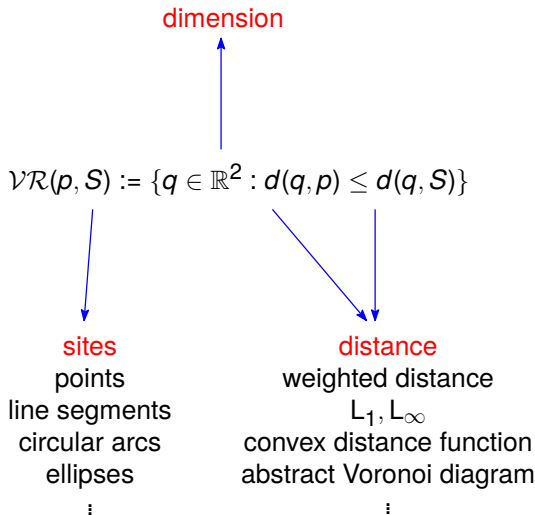
Hoff et al. (1999)

Look at the cones from below the  $xy$ -plane, and use graphics hardware to render them. This yields a subdivision of the  $xy$ -plane into approximate Voronoi regions.



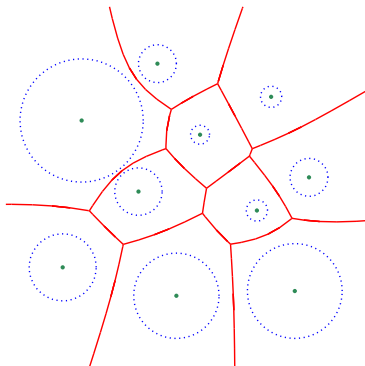
# Generalizations of Voronoi Diagrams

- The definition of a Voronoi region allows **generalizations** in three different directions.



## Additively-Weighted Voronoi Diagram

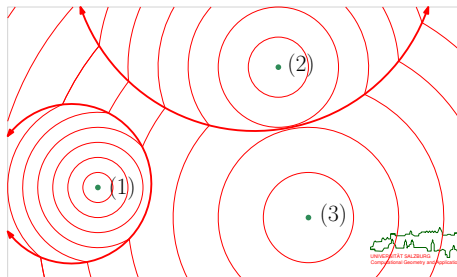
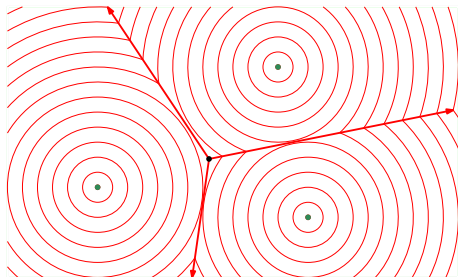
- We define the distance of a point  $q$  to a site  $p_i$  as  $d(q, p_i) - w_i$ , where  $d(\cdot, \cdot)$  denotes the standard Euclidean distance and where  $w_i$  is non-negative.
- The resulting diagram is called *Apollonius diagram* or *additively-weighted VD*.
- It can be seen as the Voronoi diagram of circles with radii  $w_i$ ; all its edges are hyperbolic arcs (and straight-line segments).



# Multiplicatively-Weighted Voronoi Diagram of Points

## Weighted Prairie fire

- Unweighted: Each wavefront propagates at the same speed.
- Weighted: The speed of a wavefront is proportional to the weight of the fire site.



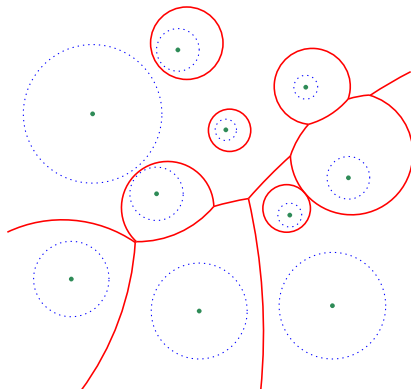
# Multiplicatively-Weighted Voronoi Diagram

- We define the weighted distance of a point  $q$  to a site  $p$  as

$$d_w(p, q) := \frac{d(p, q)}{w(p)},$$

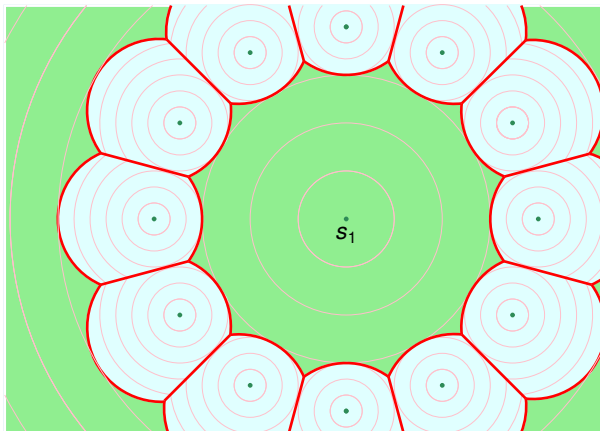
where  $d(\cdot, \cdot)$  denotes the standard Euclidean distance and where  $w(p) \in \mathbb{R}^+$ .

- The resulting diagram is called the *multiplicatively-weighted Voronoi diagram*.
- All its edges are circular arcs (and straight-line segments).



## Multiplicatively-Weighted Voronoi Diagram of Points

- Note that the Voronoi regions of (higher-weighted) sites may be disconnected.



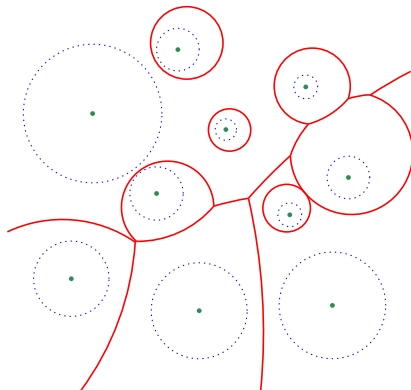
# Multiplicatively-Weighted Voronoi Diagram of Points

Aurenhammer&Edelsbrunner (1984)

The multiplicatively-weighted VD of  $n$  points is computed in  $\Theta(n^2)$  time.

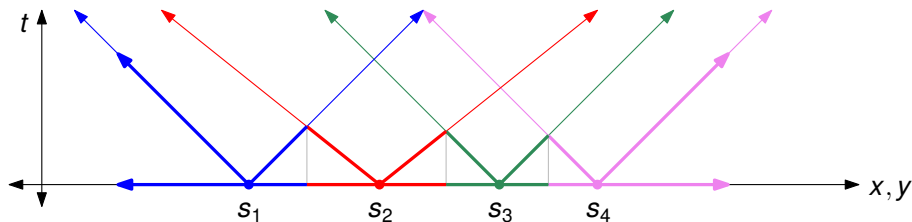
Held&de Lorenzo (2020)

The multiplicatively-weighted VD of  $n$  points is computed in  $O(n \log^4 n)$  expected time.

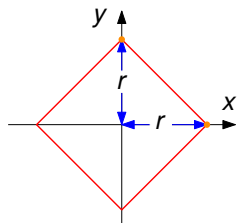


# Multiplicatively-Weighted Voronoi Diagram as Minimization Diagram

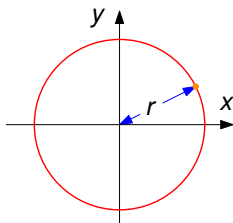
- The approach by Edelsbrunner&Seidel (1986) is also applicable to multiplicatively-weighted Voronoi diagrams: The inclinations of the lateral surfaces are chosen indirectly proportional to the weights of the points.



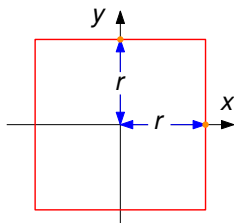
# $L_1$ and $L_\infty$ Voronoi Diagram



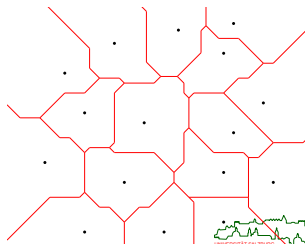
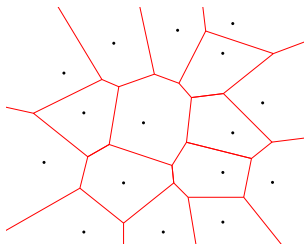
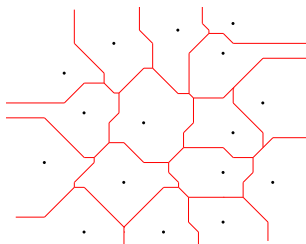
$$L_1: |x| + |y| = r$$



$$L_2: \sqrt{x^2 + y^2} = r$$



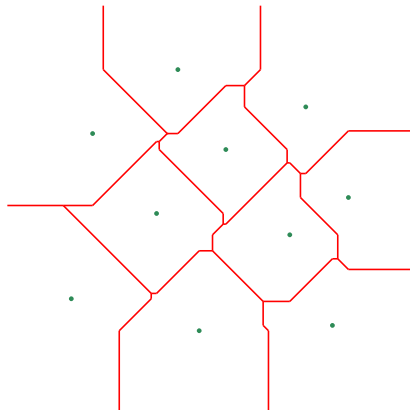
$$L_\infty: \max\{|x|, |y|\} = r$$



# $L_1$ Voronoi Diagram

Eder&Held (2019)

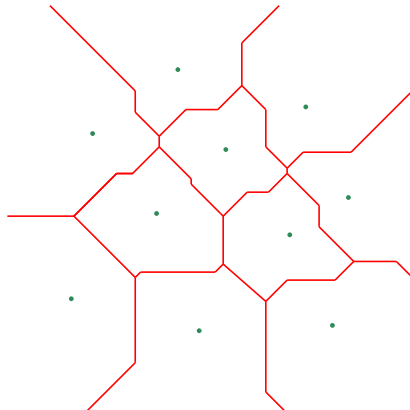
The combinatorial complexity of the VD of  $n$  multiplicatively-weighted points in the  $L_1$  norm has a  $\Theta(n^2)$  worst-case bound. All its bisectors are polygonal curves of constant complexity. It can be computed by an incremental algorithm in  $O(n^2 \log n)$  time.



# $L_\infty$ Voronoi Diagram

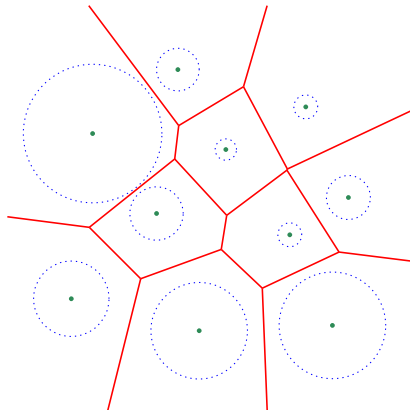
Eder&Held (2019)

The combinatorial complexity of the Voronoi diagram of  $n$  multiplicatively-weighted points, axis-aligned rectangular boxes and straight-line segments in the  $L_\infty$  norm has a tight  $\Theta(n^2)$  worst-case bound. All its bisectors are polygonal curves of constant complexity. It can be computed by an incremental algorithm in  $O(n^2 \alpha(n) \log n)$  time.



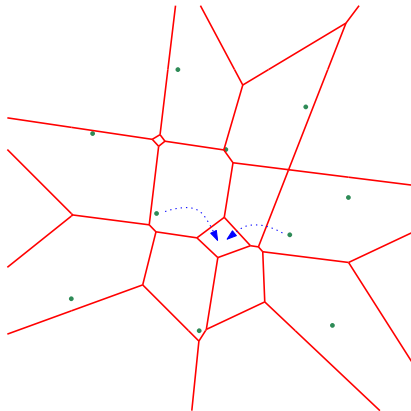
# Power Diagram

- We are again given a set of sites  $p_i$  with non-negative weights  $w_i$ . Then the power of a point  $q$  from  $p_i$  is defined as  $d(q, p_i)^2 - w_i^2$ .
- The resulting diagram is called *power diagram*.
- All its edges are straight-line segments.



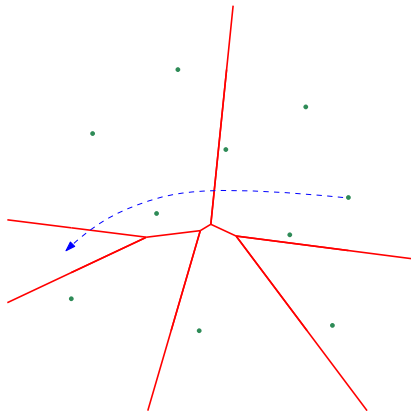
# Higher-Order Voronoi Diagram

- We are given a set  $S$  of  $n$  points  $p_1, p_2, \dots, p_n$ , and consider the standard Euclidean distance.
- The *second-order Voronoi diagram* is a partition of the plane such that each Voronoi region is the locus of points closer to two distinct sites  $p_i, p_j$  than to any other site of  $S$ . Similar for higher orders.



## Farthest-Point Voronoi Diagram

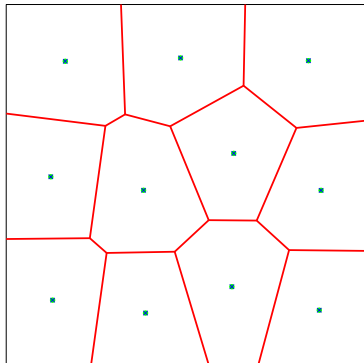
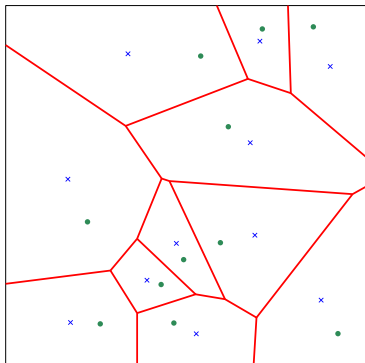
- Again we are given a set  $S$  of  $n$  points  $p_1, p_2, \dots, p_n$ .
- The *farthest-point Voronoi diagram* is a partition of the plane such that each Voronoi region is the locus of points which have the same point of  $S$  as the farthest point. The farthest-point VD is the  $(n - 1)$ -st order VD. A point  $p_i$  of  $S$  has a region in the farthest-point VD if and only if  $p_i$  is a vertex of  $CH(S)$ .
- It can be computed in  $O(n \log n)$  time.



# Centroidal Voronoi Diagram

## Definition 109 (Centroidal Voronoi Diagram (CVD))

A Voronoi diagram of a set of points is called *centroidal* if the **points** are also **centroids** of the Voronoi regions, i.e., centers of mass with respect to a given density function.

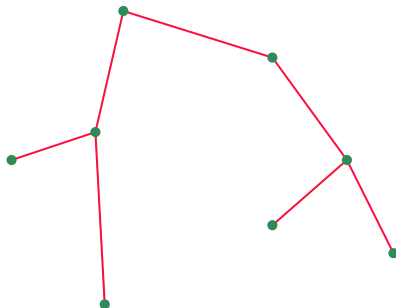


- Applications of CVDs: data compression, image segmentation, mesh generation, modeling of territorial behavior of animals, etc.

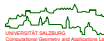


# Euclidean Minimum Spanning Tree

- Consider a set  $S := \{p_1, p_2, \dots, p_n\} \subset \mathbb{R}^2$  of  $n$  points, and assume that we want to compute a Euclidean minimum spanning tree (EMST) of  $S$ .



- Note: An EMST is unique if all inter-point distances on  $S$  are distinct.



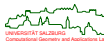
## Euclidean Minimum Spanning Tree

- Obviously, we could apply standard techniques of graph theory by computing an EMST on the weighted graph  $\mathcal{G} := (V, E)$ , where  $V := S$  and  $E := S \times S$ , and where the Euclidean length of an edge is taken as its weight.

### Lemma 110 (Jarnik (1930), Prim (1957), Dijkstra (1959))

Assume that  $\mathcal{G}$  is connected, and let  $V_1, V_2$  be a partition of  $V$ . There is a minimum spanning tree of  $\mathcal{G}$  which contains the shortest of the edges with one terminal in  $V_1$  and the other in  $V_2$ .

- *Prim's algorithm* starts with a small tree  $\mathcal{T}$  and grows it until it contains all nodes of  $\mathcal{G}$ . Initially,  $\mathcal{T}$  contains just one arbitrary node of  $V$ . At each stage one node not yet in  $\mathcal{T}$  but closest to (a node of)  $\mathcal{T}$  is added to  $\mathcal{T}$ . Prim's algorithm can be implemented to run in  $O(|V|^2)$  time.
- *Kruskal's algorithm* begins with a spanning forest, where each forest is initialized with one node of  $V$ . It repeatedly joins two trees together by picking the shortest edge between them until a spanning tree of the entire graph is obtained. Kruskal's algorithm can be implemented to run in  $O(|E| \log |E|)$  time.
- Can we do any better than  $O(n^2)$  when computing EMSTs?

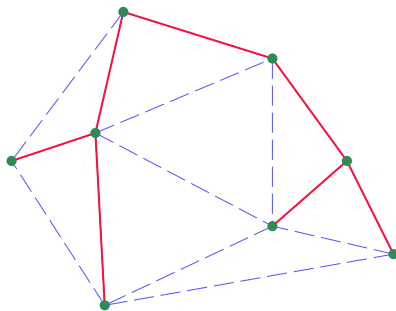


# Euclidean Minimum Spanning Tree

- Can we do any better than  $O(n^2)$  when computing EMSTs?

## Lemma 111

The EMST of a set  $S$  of points is a sub-graph of  $\mathcal{DT}(S)$ .



# Euclidean Minimum Spanning Tree

- Thus, there is no need to consider the complete graph,  $K_n$ , on  $S$ .
- Rather, we can apply Kruskal's algorithm to  $\mathcal{DT}(S)$ , and obtain an  $O(n \log n)$  algorithm for computing EMSTs.

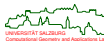
## Lemma 112

An EMST of  $S$  can be computed in time  $O(n \log n)$ .

## Theorem 113

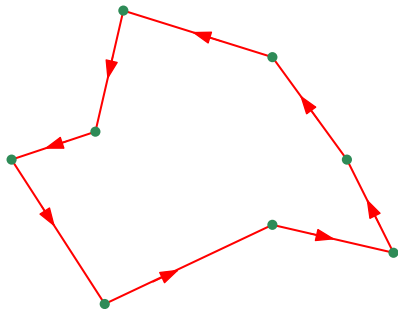
An EMST of  $S$  can be computed from the Delaunay triangulation of  $S$  in time  $O(n)$ .

*Sketch of Proof:* Observe that  $\mathcal{DT}(S)$  is a planar graph, and use Cheriton and Tarjan's "clean-up refinement" of Kruskal's algorithm. □



## Approximate Traveling Salesman Tour

- The EUCLIDEAN TRAVELING SALESMAN PROBLEM (ETSP) asks to compute a shortest closed path on  $S \subset \mathbb{R}^2$  that visits all  $n$  points of  $S$ .



## Theorem 114

TSP is  $\mathcal{NP}$ -complete, and ETSP is  $\mathcal{NP}$ -hard.

- Intuitively, ETSP ought to be  $\mathcal{NP}$ -complete, too.
- And, indeed, the  $\mathcal{NP}$ -completeness of ETSP is claimed in many publications . . .
- However, this claim is wrong! (The title of [Papadimitriou (1977)] is misleading!) ETSP, and several other optimization problems involving Euclidean distance, are not known to be in  $\mathcal{NP}$  due to a “technical twist”: For ETSP, the length of a tour on  $n$  points is a sum of  $n$  square roots. Comparing this sum to a number  $c$  may require very high precision, and no polynomial-time algorithm is known for solving this problem. (E.g., repeated squaring of  $n$  square roots may lead to numbers that need  $2^n$  bits to store.)
- Open problem: Can the sum of  $n$  square roots of integers be compared to another integer in polynomial time?

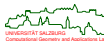
# Approximate Solution for Euclidean Traveling Salesman Problem

- Let  $OPT$  be the true length of a TSP tour, and let  $APX$  be the length of an approximate solution.

## Definition 115 (Constant-factor approximation)

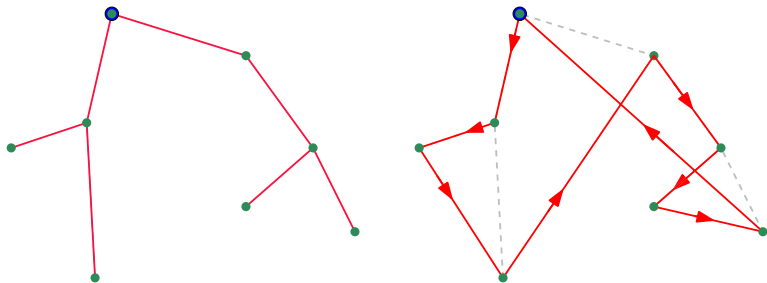
An approximation algorithm provides a *constant-factor approximation* (for TSP) if a constant  $c \in \mathbb{R}^+$  exists such that  $APX \leq c \cdot OPT$  holds for all inputs.

- Simple constant-factor approximations to ETSP:
  - Doubling-the-EMST heuristic:  $c = 2$ ; runs in  $O(n \log n)$  time.
  - Christofides' heuristic [1976]:  $c = 3/2$ ; runs in  $O(n^3)$  time.



## Approximate ETSP: Doubling-the-EMST Heuristic

- 1 Compute the Euclidean minimum spanning tree  $\mathcal{T}(S)$  of  $S$ .
- 2 Select an arbitrary node  $v$  of  $\mathcal{T}(S)$  as root.
- 3 Compute a (pre-order-like) traversal of  $\mathcal{T}(S)$  rooted at  $v$  to obtain a tour  $\mathcal{C}(S)$ .
- 4 By-pass points already visited, thus shortening  $\mathcal{C}(S)$ .
- 5 Apply 2-opt moves (at additional computational cost).

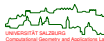


## Approximate ETSP: Doubling-the-EMST Heuristic

- Time complexity:  $O(n \log n)$  for computing the EMST  $\mathcal{T}(S)$ .
- Factor of approximation:  $c = 2$ .

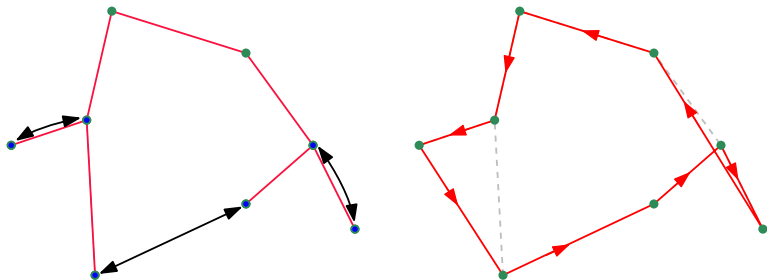
### Theorem 116

The doubling-the-EMST heuristic computes a tour on  $n$  points within  $O(n \log n)$  time that is at most 100% longer than the shortest tour.



## Approximate ETSP: Christofides' Heuristic

- 1 Compute the Euclidean minimum spanning tree  $\mathcal{T}(S)$  of  $S$ .
- 2 Get a minimum Euclidean matching  $\mathcal{M}$  on the vertices of odd degree in  $\mathcal{T}(S)$ .
- 3 Compute an Eulerian tour  $\mathcal{C}$  on  $\mathcal{T} \cup \mathcal{M}$ .
- 4 By-pass points already visited, thus shortening  $\mathcal{C}$ .
- 5 Apply 2-opt moves (at additional computational cost).



## Approximate ETSP: Christofides' Heuristic

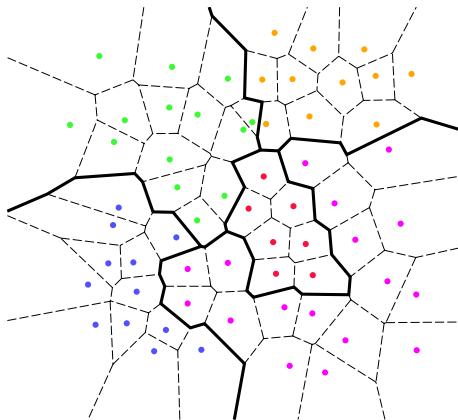
- Time complexity:  $O(n^3)$  for computing the Euclidean matching.
- Factor of approximation:  $c = \frac{3}{2}$ .

### Theorem 117

Christofides' heuristic computes a tour on  $n$  points within  $O(n^3)$  time that is at most 50% longer than the shortest tour.

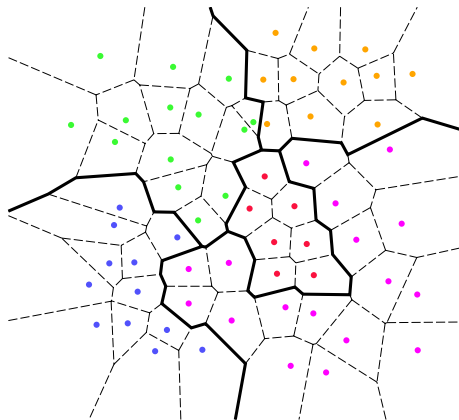
# Statistical Classification and Shape Estimation

- Given are sets of differently colored points in the plane. What is a suitable partition of the plane according to the colors of the points?
- Well-known idea: Compute the Voronoi diagram and color every Voronoi region with its point's color.



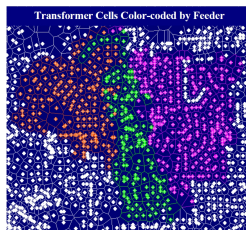
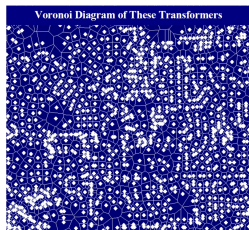
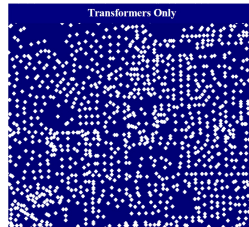
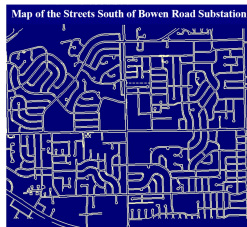
# Estimating Electrical Distribution Boundaries

- TXU Energy (Dallas, TX, USA):
  - Which area is serviced by a particular electric device?
  - How can we display (feeder-level) statistical information within a geographic context?



# Estimating Electrical Distribution Boundaries

- [Held&Williamson (2004)] generate distribution boundaries as boundaries of unions of Voronoi regions of basic devices (e.g., transformers) and integrate them into TXU's geographic information system.



# Natural-Neighbor Interpolation

## Problem: INTERPOLATION

**Given:** A set  $S$  of  $m + 1$  sites  $p_0, p_1, \dots, p_m \in \mathbb{R}^2$  with associated (scalar or vector-valued) “data”  $v_0, v_1, \dots, v_m$ , and  $q \in CH(S)$ .

**Compute:** An estimate  $f(q)$  of the data at  $q$ , obtained by interpolation of  $v_0, v_1, \dots, v_m$ .

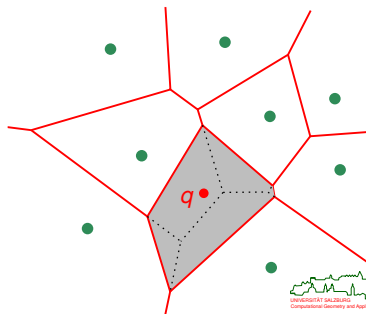
## Natural-neighbor interpolation (NNI)

[Sibson (1981)]: Use ratios of Voronoi areas as weights  $\lambda_i(q)$  in the interpolation:

$$f(q) := \sum_{i=0}^m v_i \cdot \lambda_i(q).$$

## Natural-neighbor extrapolation

[Bobach et al. (2009)]: NNI outside of convex hull.



# Natural-Neighbor Interpolation

## Definition 118 (NNI)

Consider a set  $S$  of  $m + 1$  sites  $p_0, p_1, \dots, p_m \in \mathbb{R}^2$  with associated (scalar or vector-valued) “data”  $v_0, v_1, \dots, v_m$ , and  $q \in CH(S)$ . Let  $S' := S \cup \{q\}$ . Then

$$f(q) := \sum_{i=0}^m v_i \cdot \lambda_i(q)$$

gives the interpolated data for  $q$  obtained by *natural-neighbor interpolation* (NNI), with

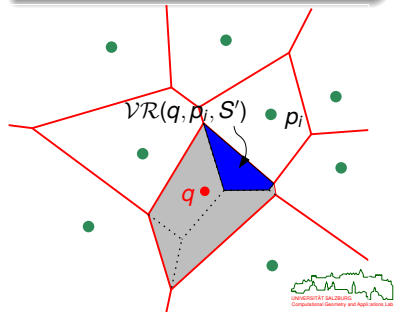
$$\lambda_i(q) := \frac{|\mathcal{VR}(q, p_i, S')|}{|\mathcal{VR}(q, S')|},$$

where  $|\mathcal{VR}(q, S')|$  denotes the area of the Voronoi region of  $q$  within  $S'$ , and  $|\mathcal{VR}(q, p_i, S')|$  corresponds to the area of the second-order Voronoi region of  $q$  and  $p_i$  within  $S'$ .

## Theorem 119

Sibson's NNI interpolant is

- $C^0$  if  $q \in S$ ,
- $C^1$  if  $q$  lies on a Delaunay circle of  $S$ , and
- $C^\infty$  otherwise.



# Improved Laser Sintering Based on Natural-Neighbor Interpolation

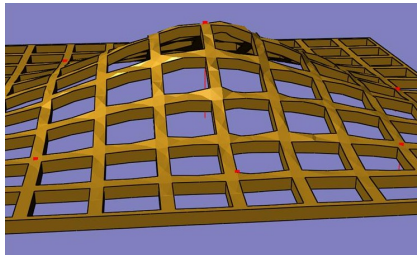
- Laser sintering is a manufacturing process used in rapid prototyping:
  - A laser is used to manufacture a part by sintering powder-based materials layer by layer.
  - Small-series production is possible.
  - Snap fits and living hinges can be produced.



Images courtesy of EOS GmbH

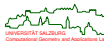
# Improved Laser Sintering Based on Natural-Neighbor Interpolation

- Major problem:
  - The laser-induced heating and subsequent cooling down of the material may cause the “warpage” phenomenon.
  - Warpage is the result of a change in the morphology of the molten powder: amorphous to part-crystalline.
  - Crystalline regions have a higher density than the amorphous regions, leading to a loss of volume.
  - Different layers undergo different loss in volume, leading to inter-layer tension.
  - This tension may result in a bimetallic effect: “curl”.



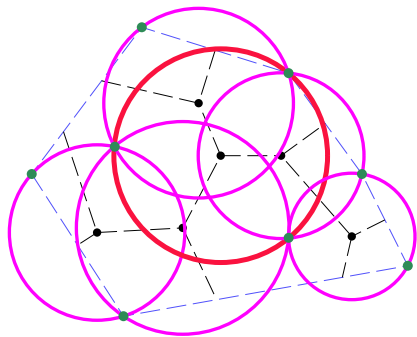
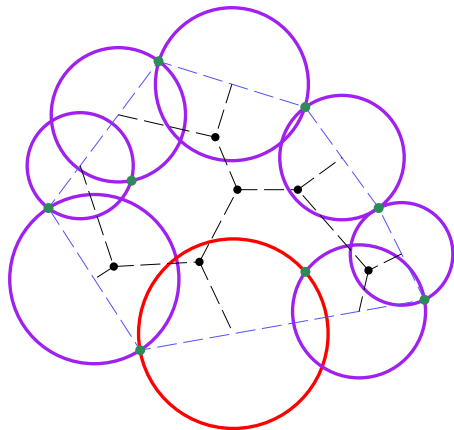
# Improved Laser Sintering Based on Natural-Neighbor Interpolation

- Bold idea: Apply a pre-deformation in order to manufacture an inversely deformed part!
- It seems natural to use interpolation — but how shall we interpolate vectors on the surface of a polyhedron?
- [Held&Pfligersdorffer (2009)]: Pre-deformation by means of approximate natural-neighbor interpolation (NNI) helps to reduce warpage by 90%.
- Pre-deformation works neatly for reasonably triangulated parts and a reasonable number of deformation vectors.



# Maximum Empty Circle

- 1 Restrict  $\mathcal{VD}(S)$  to  $CH(S)$ .
- 2 Determine the largest circle centered at an intersection of  $\mathcal{VD}(S)$  and  $CH(S)$ .
- 3 Determine the largest circle centered at an interior node of  $\mathcal{VD}(S)$ .
- 4 Pick the largest circle among those two categories of circles.



## Definition 120 (Hausdorff distance)

Let  $A, B$  be two non-empty subsets of  $\mathbb{R}^d$ . The *directed Hausdorff distance*,  $h(A, B)$ , from  $A$  to  $B$  (relative to the standard Euclidean distance  $d(., .)$ ) is defined as

$$h(A, B) := \sup_{a \in A} \left( \inf_{b \in B} d(a, b) \right).$$

The (*symmetric*) *Hausdorff distance*,  $H(A, B)$ , between  $A$  and  $B$  is defined as

$$H(A, B) := \max \{h(A, B), h(B, A)\}.$$

- Introduced by Felix Hausdorff in 1914.
- If both  $A$  and  $B$  are bounded then  $H(A, B)$  is guaranteed to be finite.
- For compact sets we can replace  $\inf$  by  $\min$  and  $\sup$  by  $\max$ .

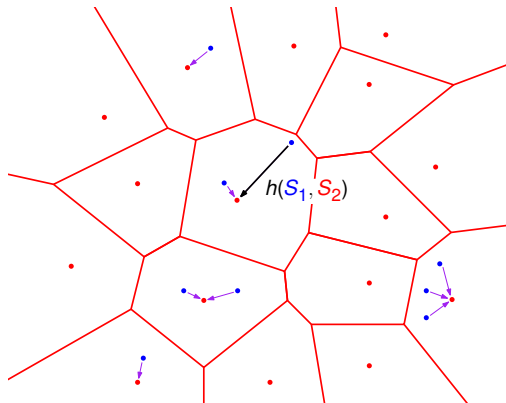
## Theorem 121

The Hausdorff distance between two finite sets  $S_1, S_2$  of points in  $\mathbb{R}^2$  can be computed in  $O(n \log n)$  time, where  $n := \max\{|S_1|, |S_2|\}$ .

# Hausdorff Distance

*Sketch of Proof of Theorem 121 :*

- 1 Consider sets  $S_1$  and  $S_2$  of blue and red points.
- 2 Compute  $\mathcal{VD}(S_2)$ .
- 3 Locate each point of  $S_1$  within the Voronoi regions of  $\mathcal{VD}(S_2)$ .
- 4 The maximum distance yields  $h(S_1, S_2)$ .



# Centroidal Voronoi Diagrams and Territorial Behavior

- *Tilapia mossambica* (Dt.: Weißkehl-Buntbarsch):
  - The male fishes dig nesting pits into sandy grounds.
  - The centers and corners of the pits are adjusted until the final configuration resembles a centroidal Voronoi diagram.

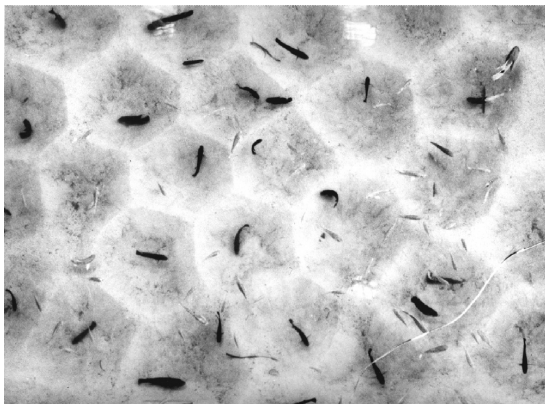
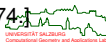


[Image credit: G. Barlow, "Hexagonal Territories", *Animal Behavior* 22:876–878, 1974]



## Evaporation as a Massively Parallel Algorithm?



- Salar de Atacama in the Chilean Andes: 3 000 km<sup>2</sup>, average elevation about 2 300 m asl., 3 500 milliliters annual evaporation, only a few milliliters of annual rainfall.

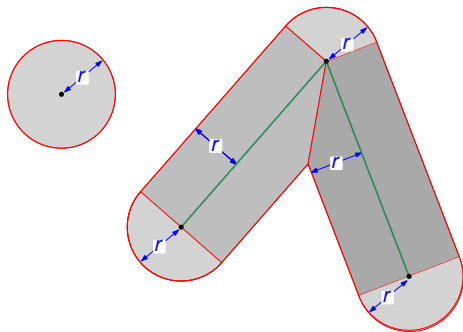


## Skeletal Structures

- Voronoi Diagram of Points, Line Segments and Circular Arcs
- Straight Skeleton
- Applications

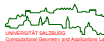
## Generalizing the Wavefront

- The wavefront of a point is a circle of radius  $r$ , for some non-negative value of  $r$ .
- The wavefront of a straight-line segment is a box with semi-circular caps.
- Of course, individual portions of the wavefront may interact again.
- It is natural to split up the wavefront into parts according to the input items that emitted them.



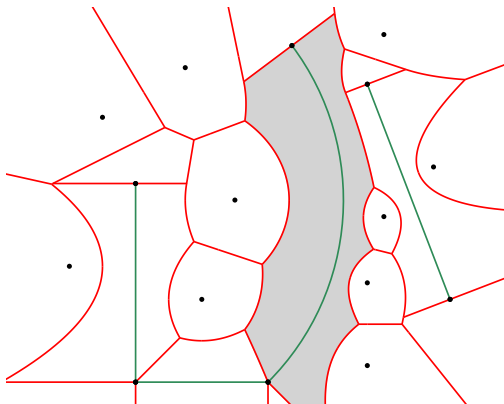
## Voronoi Diagram of Points, Line Segments and Arcs: Wavefront

- Consider a set  $S$  of  $n$  points, straight-line segments, and circular arcs (“sites”).
- For technical reasons we assume that all end-points of all segments and arcs are members of  $S$ . Furthermore, the segments and arcs are allowed to intersect only at common end-points. Such a set of sites is called “*admissible*”.
- Now perform a (generalized) wavefront propagation.



# Voronoi Diagram of Points, Line Segments and Arcs

- Intuitively, the Voronoi diagram of  $S$  partitions the Euclidean plane into regions that are closer to one site than to any other.
- Natural generalization of Voronoi diagrams of points, but Voronoi regions are now bounded by conics and need not be convex.



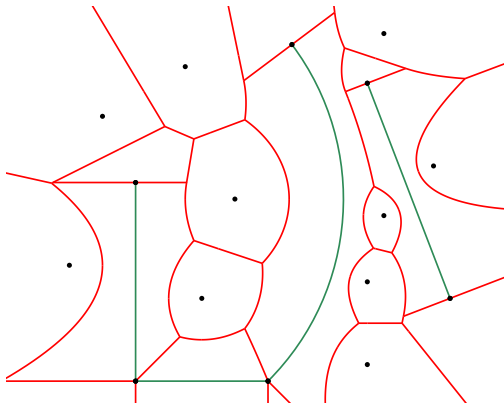
# Voronoi Diagram of Points, Line Segments and Arcs

## Problem: GENERALIZED VORONOI DIAGRAM

**Given:** Admissible set  $S$  of points, line segments and circular arcs in 2D.

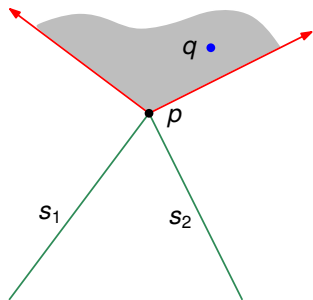
**Compute:** Voronoi diagram  $\mathcal{VD}(S)$  under the Euclidean distance  $d(\cdot, \cdot)$ .

- Formal definition requires some technicalities ... [Yap (1987), Held (1991)]

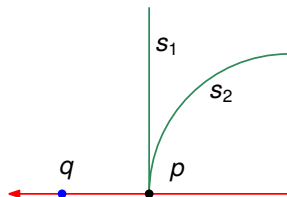


# Voronoi Diagram of Points, Line Segments and Arcs: Technical Problem

- Consider an admissible set  $S$  of  $n$  points, line segments and circular arcs as input sites in 2D, and two sites  $s_1, s_2 \in S$ .
- Problem: We need to avoid “two-dimensional” and “non-intuitive” bisectors.



$$d(q, p) = d(q, s_1) = d(q, s_2)$$

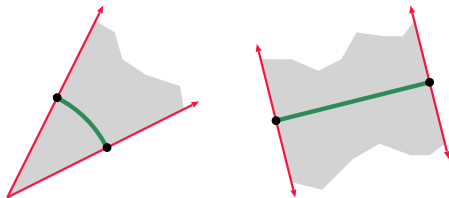


# Voronoi Diagram of Points, Line Segments and Arcs: Definitions

## Definition 122 (Cone of influence)

The *cone of influence*,  $CI(s)$ , of

- a circular arc  $s$  is the closure of the cone bounded by the pair of rays originating in the arc's center and extending through its endpoints;
- a straight-line segment  $s$  is the closure of the strip bounded by the normals through its endpoints;
- a point  $s$  is the entire plane.



# Voronoi Diagram of Points, Line Segments and Arcs: Definitions

## Definition 123 ((Generalized) Voronoi region)

The (*generalized*) Voronoi region of  $s_i \in S$  relative to  $S$  is defined as

$$\mathcal{VR}(s_i, S) := \text{cl}\{q \in \text{int CI}(s_i) : d(q, s_i) \leq d(q, S)\}.$$

- It is common to drop the attribute “generalized” if the meaning is clear.

## Definition 124 ((Generalized) Voronoi polygon)

The (*generalized*) Voronoi polygon of  $s_i \in S$  relative to  $S$  is defined as

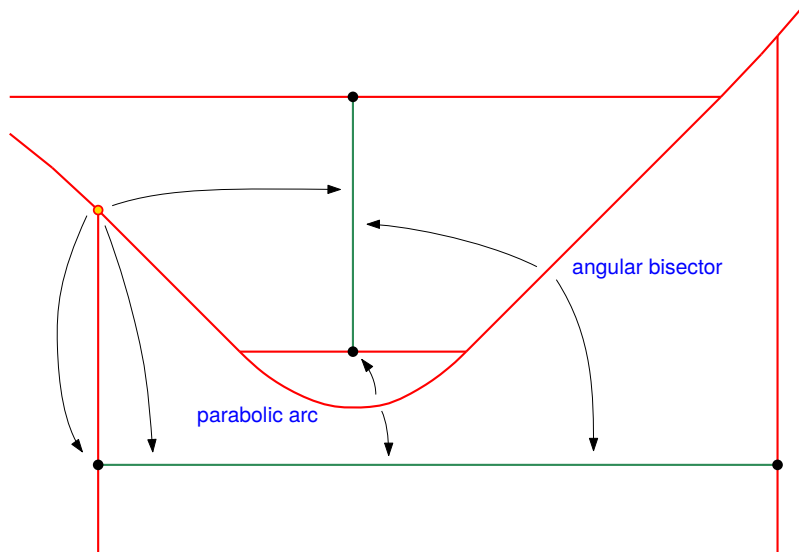
$$\mathcal{VP}(s_i, S) := \partial \mathcal{VR}(s_i, S).$$

## Definition 125 ((Generalized) Voronoi diagram)

The (*generalized*) Voronoi diagram of  $S$  is defined as

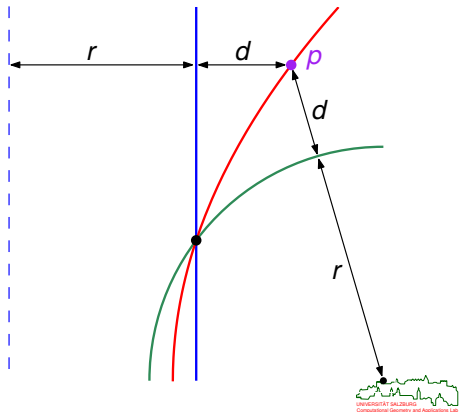
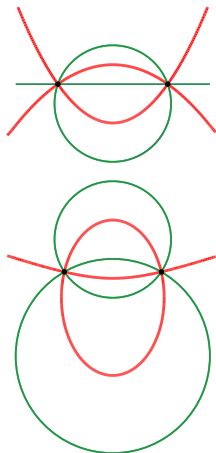
$$\mathcal{VD}(S) := \bigcup_{1 \leq i \leq n} \mathcal{VP}(s_i, S).$$

# Sample Voronoi Diagram Dissected



## Lemma 126

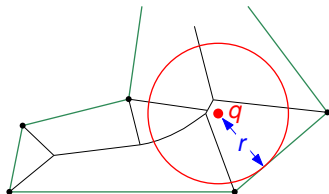
The structure  $\mathcal{VD}(S)$  is a planar graph and consists of  $O(n)$  parabolic, hyperbolic, elliptic and straight-line edges.



# Voronoi Diagram of Points, Line Segments and Arcs: Medial Axis

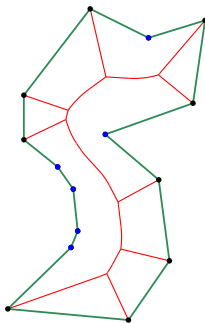
## Definition 127 (Clearance)

The *clearance* of a point  $q$  relative to  $S$  is the radius  $r$  of the largest disk (“*clearance disk*”) centered at  $q$  which does not contain any site of  $S$  in its interior.



## Definition 128 (Medial axis)

A point in the interior of a (multiply-connected) polygonal region belongs to the *medial axis* (MA) of the region if and only if its clearance disk touches the boundary in at least two disjoint points.



# Voronoi Diagram of Points, Line Segments and Arcs: State of the Art

## Theorem 129 (Fortune (1987))

The Voronoi diagram of  $n$  points and straight-line segments can be constructed in  $O(n \log n)$  time by means of a sweep-line algorithm.

## Theorem 130 (Yap (1987))

The Voronoi diagram of  $n$  points, straight-line segments and circular arcs can be constructed in  $O(n \log n)$  time by means of a divide&conquer algorithm.

## Theorem 131 (Aichholzer et alii (2009))

The Voronoi diagram of  $n$  points, straight-line segments and circular arcs can be constructed in  $O(n \log^2 n)$  expected time by means of randomization combined with a divide&conquer algorithm.

## Theorem 132 (Held&Huber (2009), based on Held (2001))

The Voronoi diagram of  $n$  points, straight-line segments and circular arcs can be constructed in  $O(n \log n)$  expected time by means of randomized incremental construction.

# Voronoi Diagram of Points, Line Segments and Arcs: State of the Art

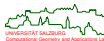
- Several other  $O(n \log n)$  expected-time algorithms for polygons and/or line segments . . .
- What about Voronoi diagrams of polygons? Can one achieve  $o(n \log n)$ ?

## Theorem 133 (Aggarwal et alii (1989))

The Voronoi diagram of a convex polygon can be constructed in linear time.

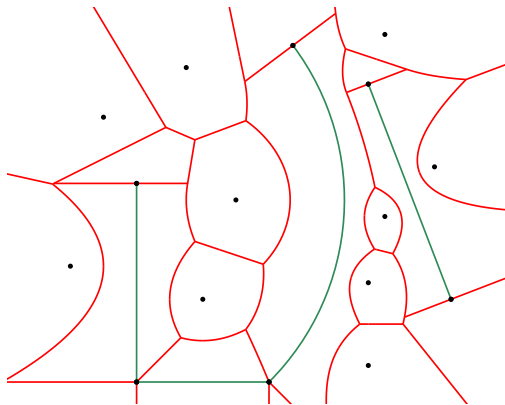
## Theorem 134 (Chin et alii (1999))

The Voronoi diagram of a simple polygon can be constructed in linear time.



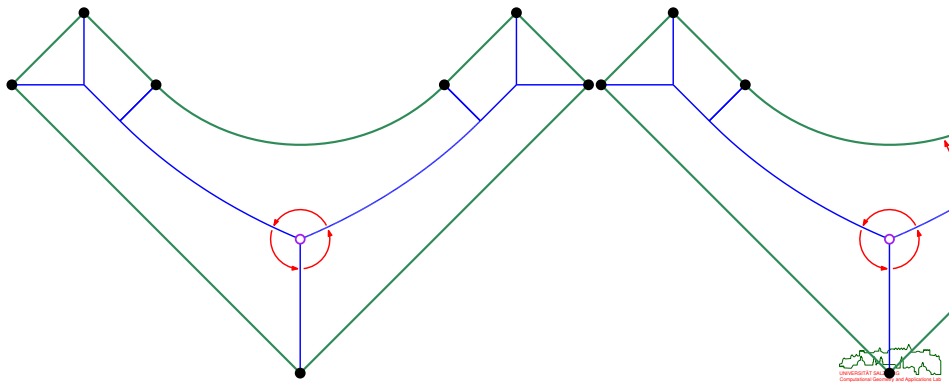
## Randomized Incremental Construction

- [Held (2001), Held&Huber (2009)]: Start with the vertices of  $S$ , and compute their Voronoi diagram. (E.g., use randomized incremental construction.) Insert segments, in random order, one after the other. Same for the arcs.



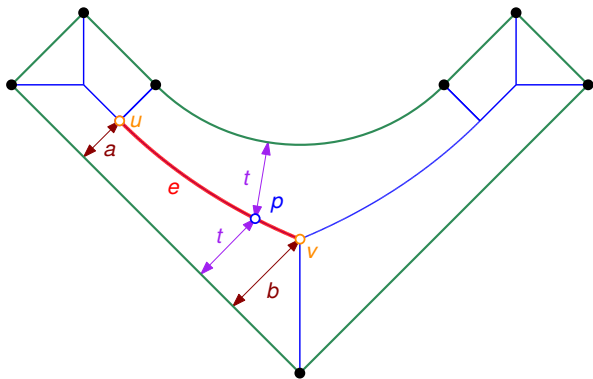
## Storing a Voronoi Diagram: Topological Data

- Any standard way to represent a planar graph is good enough to store the topology of a Voronoi diagram.
- E.g., we
  - store CCW pointers around all nodes,
  - store pointers to the two defining sites of every edge,
  - store pointers to the first and last edge of a site's Voronoi region.



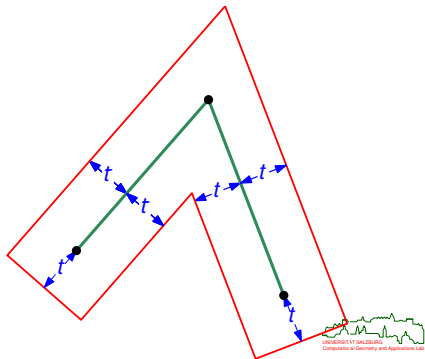
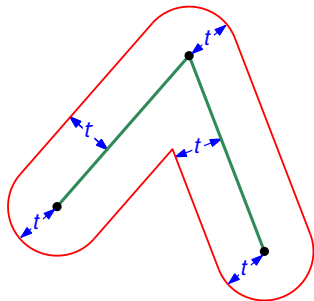
## Storing a Voronoi Diagram: Numerical Data

- We assign a clearance-based parameterization  $f: [a, b] \rightarrow \mathbb{R}^2$  to every edge  $e$ , where  $a$  is the minimum and  $b$  is the maximum clearance of points of  $e$ .
- The coordinates of a point  $p$  of  $e$  with clearance  $t$  are obtained by evaluating  $f$ : we have  $p = f(t)$ .



# Straight Skeletons: Constant-Radius vs. Mitered Wavefront

- Voronoi diagram: constant-radius wavefront.
- Straight skeleton: mitered wavefront.

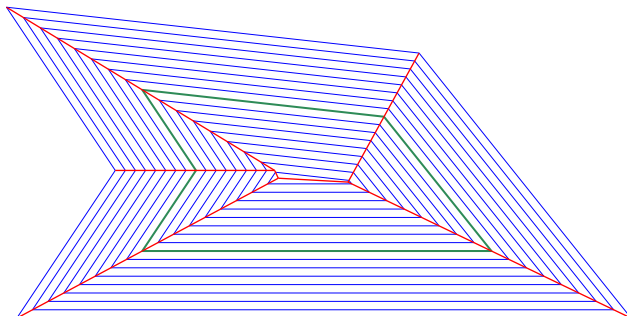


University of Salzburg  
Computer of Geometry and Applications Lab

# Straight Skeletons: Motivation

Aichholzer&Alberts&Aurenhammer&Gärtner (1995)

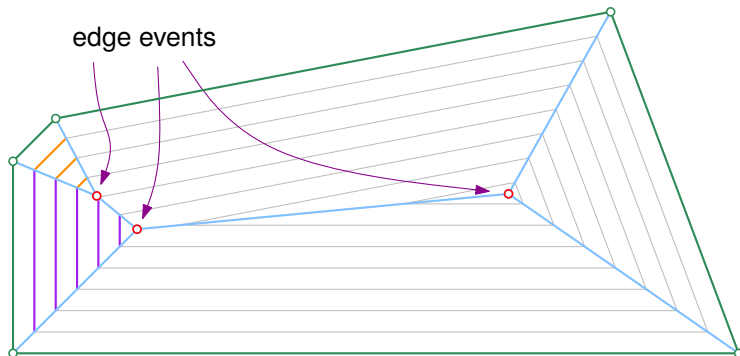
- Self-parallel mitered offsetting of input polygon  $\mathcal{P}$  yields wavefront  $\mathcal{WF}(\mathcal{P}, t)$  for offset distance  $t$ .
- Wavefront propagation: Shrinking process via continued self-parallel offsetting with unit speed, where offset distance  $t$  equals time.
- Straight skeleton  $SK(\mathcal{P})$  is union of traces of wavefront vertices.



# Change of Wavefront Topology

## Edge event

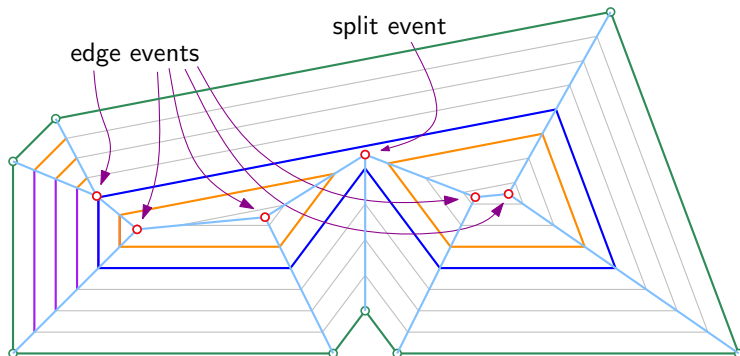
- Topology of wavefront  $\mathcal{WF}(\mathcal{P}, t)$  changes over time.
- *Edge event*: an edge of  $\mathcal{WF}(\mathcal{P}, t)$  vanishes.
- Such a change of topology of  $\mathcal{WF}(\mathcal{P}, t)$  corresponds to a *node* of  $SK(\mathcal{P})$ .



# Change of Wavefront Topology

## Split event

- Topology of wavefront  $\mathcal{WF}(\mathcal{P}, t)$  changes over time.
- *Split event*: Wavefront  $\mathcal{WF}(\mathcal{P}, t)$  splits into two parts.
- Also split events correspond to *nodes* of  $SK(\mathcal{P})$ .





## Definition 135

The *straight skeleton*  $SK(\mathcal{P})$  of a polygon  $\mathcal{P}$  is given by the union of traces of wavefront vertices of  $\mathcal{P}$  over the entire wavefront propagation process.

## Lemma 136

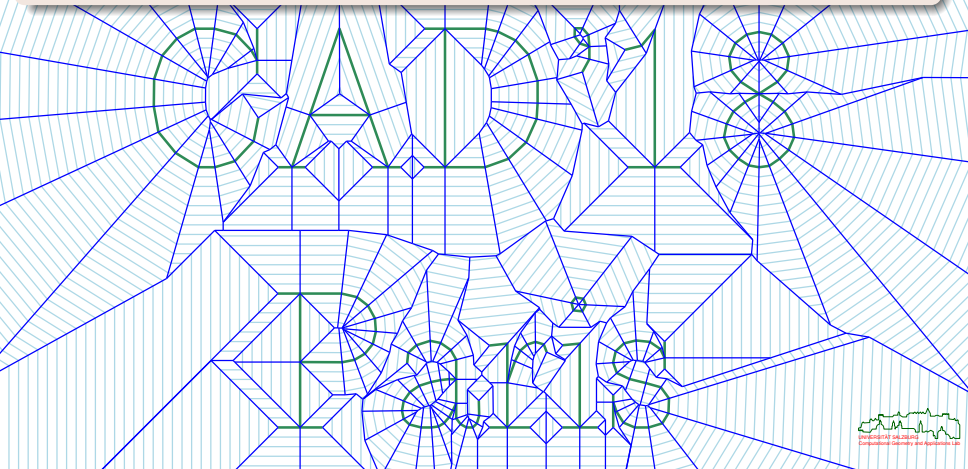
- 1 The topology of the wavefront  $WF(\mathcal{P}, t)$  changes with time/distance  $t$  due to edge and split events.
- 2 These events correspond to nodes of  $SK(\mathcal{P})$ .
- 3 No metric-based definition of straight skeletons exists.
- 4 If  $\mathcal{P}$  has  $n$  segments then  $SK(\mathcal{P})$  consists of  $O(n)$  nodes and  $O(n)$  straight-line edges.



# Straight Skeleton of a Planar Straight-Line Graph

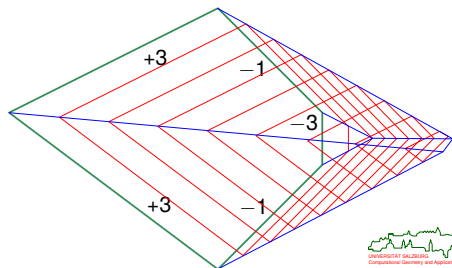
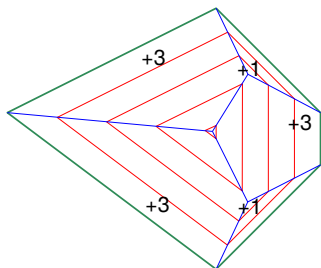
## Generalization to PSLGs

The definition of straight skeletons can be extended easily to arbitrary planar straight line graphs (PSLGs) within the entire plane, i.e., to a collection of straight-line segments that do not intersect except possibly at common endpoints.



# Weighted Straight Skeletons

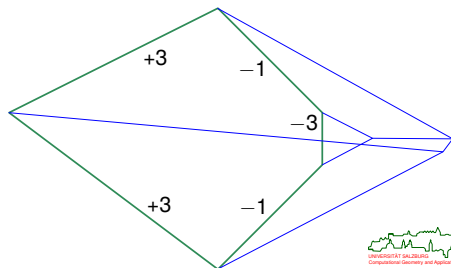
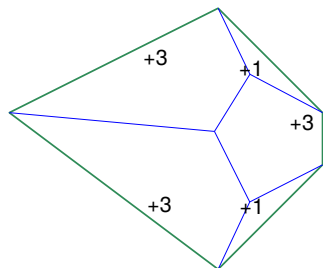
- Multiplicative weights: Edges move at different speeds, possibly even at negative speeds.
- [Barequet et alii (2008)]: Weighted straight skeletons in 2D can be used for computing a straight skeleton in the interior of a polyhedron in 3D.
- Which of the properties of the straight skeleton (planarity, tree structure, faces are monotone) carry over to weighted straight skeletons?



# Weighted Straight Skeletons

## Theorem 137 (Biedl et alii (2014))

The geometric, graph-theoretical, and combinatorial properties of multiplicatively weighted straight skeletons are identical to unweighted straight-skeletons if all weights are positive. If negative weights are allowed then the weighted straight skeleton of even a convex polygon may contain crossings and cycles.



## Straight Skeleton: State of the Art

### Theorem 138 (Aichholzer et alii (1995))

The straight skeleton of a simple  $n$ -gon with  $r$  reflex vertices can be computed in  $O(nr \log n)$  time.

### Theorem 139 (Aichholzer&Aurenhammer (1998))

A wavefront-propagation can be used to compute the straight skeleton of an  $n$ -vertex PSLG in  $O(n^3 \log n)$  time.

### Theorem 140 (Eppstein&Erickson (1999))

Efficient closest-pair data structures can be combined in a hierarchical fashion to achieve an  $O(n^{17/11 + \epsilon})$  time and space complexity for computing the straight skeleton of an  $n$ -vertex PSLG.

### Theorem 141 (Cheng&Vigneron (2007))

Based on  $1/\sqrt{r}$  cuttings, the straight skeleton of a simple  $n$ -gon with  $r$  reflex vertices can be computed in expected time  $O(n \log^2 n + r\sqrt{r} \log r)$ .

## Straight Skeleton: State of the Art

### Theorem 142 (Huber&Held (2012))

A straight-skeleton algorithm based on motorcycle-graph computations can be engineered to run in  $O(n \log n)$  time and  $O(n)$  space for practical  $n$ -vertex PSLGs. However, its worst-case complexity is  $O(n^2 \log n)$ .

### Theorem 143 (Palfrader&Held&Huber (2012))

A wavefront-propagation based on kinetic triangulations can be engineered to run in  $O(n \log n)$  time and  $O(n)$  space for practical  $n$ -vertex PSLGs. In particular, only  $O(n)$  flip events occur in practice. However, its worst-case complexity is  $O(n^3 \log n)$ .

### Theorem 144 (Biedl et alii (2014))

The weighted straight skeleton of an  $n$ -vertex convex polygon (with positive multiplicative weights) admits a non-procedural characterization and can be computed in  $O(n)$  time.

## Straight Skeleton: State of the Art

### Theorem 145 (Vigneron&Yan (2013))

A motorcycle-graph based algorithm allows to compute the straight skeleton of a non-degenerate polygon with  $n$  vertices and  $h$  holes in time  $O(n\sqrt{h+1} \log^2 n + n^{4/3+\varepsilon})$ , for any  $\varepsilon > 0$ . If all coordinates are  $O(\log n)$ -bit rationals then the straight skeleton of a simple polygon can be computed in  $O(n \log^3 n)$  expected time.

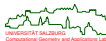
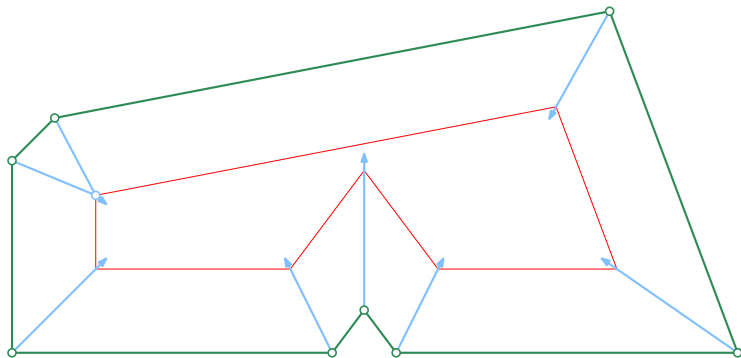
### Theorem 146 (Cheng&Mencel&Vigneron (2014))

A motorcycle-graph based algorithm allows to compute the straight skeleton of a non-degenerate polygon with  $n$  vertices, with  $r$  vertices being reflex, in time  $O(n \log n \log r + r^{4/3+\varepsilon})$ , for any  $\varepsilon > 0$ . For degenerate input the time increases to  $O(n \log n \log r + r^{17/11+\varepsilon})$ .

# Wavefront Propagation for Computing Straight Skeletons

## Basic idea

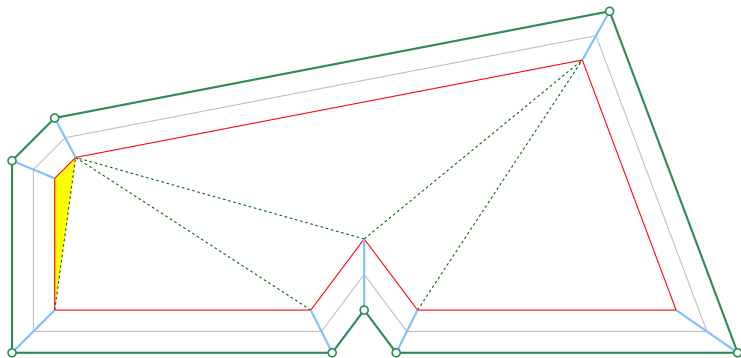
- Simulate the wavefront propagation.
- Problem: When will the next event happen? Which event?
- If we can solve this problem then we can construct straight skeletons.



# Triangulation-Based Algorithm

## Aichholzer&Aurenhammer (1998)

- Maintain a kinetic triangulation of (the interior of) the wavefront.
- Collapsing triangles witness edge and split events.
- A triangle collapses when its area becomes zero.

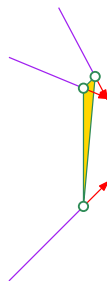


# Triangulation-Based Algorithm

## Algorithmic insight

Collapsing triangles witness edge and split events.

- Compute collapse times of triangles.
- That is, determine when the area of a triangle becomes zero.
- Maintain a priority queue of collapse events.
- Update triangulation and priority queue as required upon events.



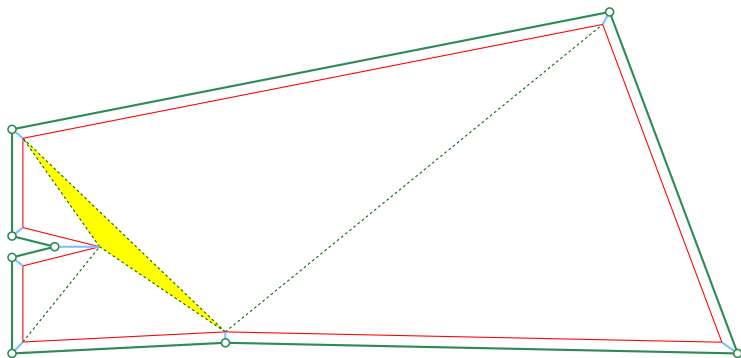
## Wavefront propagation based on kinetic triangulations ...

... allows to determine all events and to compute straight skeletons.

# Triangulation-Based Algorithm

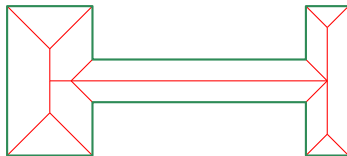
## Flip events

- Caveat: Not all collapses witness changes in the wavefront topology.
- Such collapses cannot be ignored!
- Rather these collapses need special processing: *flip events*.



## Implementation of Triangulation-Based Algorithm

- Long way to go from the theoretical sketch by Aichholzer&Aurenhammer (1998) to an actual implementation . . .
- [Palfrader&Held&Huber (2012)]: Need to avoid flip-event loops.
- [Palfrader&Held (2015)]: Need to handle degeneracies that cause multiple simultaneous events.
- [Palfrader&Held (2015)]: Need to detect and classify simultaneous events reliably on a standard floating-point arithmetic.



# Implementation of Triangulation-Based Algorithm: SURFER

## SURFER

Straight-skeleton algorithm, based on kinetic triangulations and standard floating-point arithmetic, implemented in C and named SURFER.

## Experimental result [Palfrader&Held (2015)]

SURFER runs in  $O(n \log n)$  time for  $n$ -vertex PSLGs. In particular, only a (small) linear number of flip events occur.

## How many flip events can occur in the worst case?

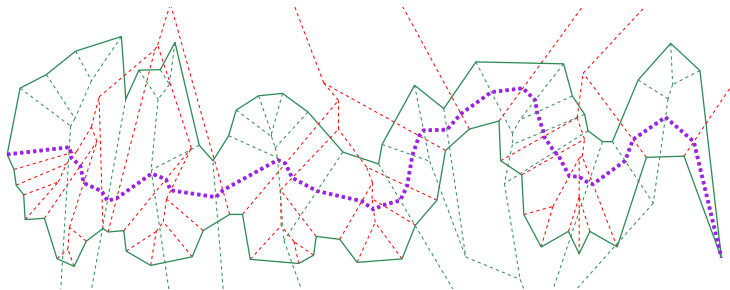
This is an open problem! Trivial upper bound is  $\Theta(n^3)$ , but only (highly contrived) inputs with  $\Theta(n^2)$  flips are known.

# Straight Skeleton of Monotone Polygons

- The (positively weighted) straight skeleton of a convex polygon can be computed in  $O(n)$  time. (Recall Thm. 144 by [Biedl et al. (2014)].)
- Can we also do better for other specific input classes?
- Yes!

## Theorem 147 (Biedl et alii (2015))

The straight skeleton of an  $n$ -vertex monotone polygon can be computed in  $O(n \log n)$  time.



# Origami and Cut-and-Fold Problems

## Theorem 148 (Demaine et alii (1999))

Every polygon can be cut out of a sheet of paper by one straight cut after adequate folding. The folding creases can be constructed by a straight-skeleton-based algorithm.

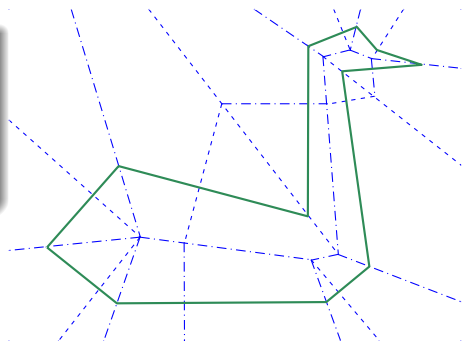
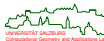


[Image courtesy of Erik Demaine]

- Other applications of straight skeletons comprise
  - design of pop-up cards [Sugihara (2013)];
  - shape reconstruction and contour interpolation [Oliva et alii (1996)];
  - computing centerlines of roads and area collapsing in GIS maps [Haurert&Sester (2008)].

## Unweighted and Weighted Offsets of Point

- The *unweighted offset area*  $\mathcal{O}A(p, r)$  of the point  $p$  of  $\mathbb{R}^2$  for offset value  $r \geq 0$  is the set of all points  $u$  of  $\mathbb{R}^2$  whose unweighted distance  $d(u, p)$  to  $p$  is at most  $r$ .
- The *weighted offset area*  $\mathcal{O}A_w(p, r)$  of the point  $p$  of  $\mathbb{R}^2$  for offset value  $r \geq 0$  and weight  $w(p) > 0$  is the set of all points  $v$  of  $\mathbb{R}^2$  whose weighted distance  $d_w(v, p)$  to  $p$  is at most  $r$ .
- For  $w(p) := 1$  we get standard offsetting.



# Unweighted and Weighted Offsets of Line Segment

- The *unweighted offset area*  $\mathcal{OA}(\overline{pq}, r)$  of the straight-line segment  $\overline{pq}$  for offset value  $r \geq 0$  is the set of all points  $u$  of  $\mathbb{R}^2$  whose minimum unweighted distance to a point  $v$  of  $\overline{pq}$  is at most  $r$ :

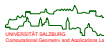
$$\mathcal{OA}(\overline{pq}, r) := \{u \in \mathbb{R}^2 : \min_{v \in \overline{pq}} d(u, v) \leq r\}$$

- This definition is generalized easily to circular arcs and to offsets of (curvilinear) polygons.

## Unweighted and Weighted Offsets of Line Segment

- Suppose that  $p$  has weight  $w(p) > 0$  and  $q$  has weight  $w(q) > 0$ , possibly with  $w(p) \neq w(q)$ . (In the figure,  $w(p) := 1$  and  $w(q) := 2$ .)
- For  $0 \leq \lambda \leq 1$ , the weight of a point  $(1 - \lambda)p + \lambda q$  on  $\overline{pq}$  is given by  $(1 - \lambda)w(p) + \lambda w(q)$ , i.e., by linear interpolation of the weights of  $p$  and  $q$ .
- Then the *variable-radius offset area*  $\mathcal{O}A_v(\overline{pq}, r)$  of the straight-line segment  $\overline{pq}$  for offset value  $r \geq 0$  is the set of all points  $u$  of  $\mathbb{R}^2$  whose minimum weighted distance to a (weighted) point  $v$  of  $\overline{pq}$  is at most  $r$ :

$$\mathcal{O}A_v(\overline{pq}, r) := \{u \in \mathbb{R}^2 : \min_{v \in \overline{pq}} d_w(u, v) \leq r\}$$



# Unweighted and Weighted Offsets of Line Segment

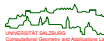
[Held&Huber&Palfrader (2016)]

The *variable-radius offset area*  $\mathcal{O}A_v(\overline{pq}, r)$  of the straight-line segment  $\overline{pq}$  for offset value  $r \geq 0$  is given by the convex hull of  $\mathcal{O}A_w(p, r) \cup \mathcal{O}A_w(q, r)$ . Thus,  $\mathcal{O}A_v(\overline{pq}, r)$  is bounded by up to two straight-line segments and up to two circular arcs.

# Unweighted and Weighted Offsets of Line Segment

[Held&Huber&Palfrader (2016)]

All supporting lines of segments of  $\mathcal{O}_{\mathcal{A}_V}(\overline{pq}, r)$  meet in a point  $p'$ .



# Minkowski Sum and Difference

- Let  $A, B$  be sets, and  $a, b$  denote points of  $A$  respectively  $B$ .
- We define the translation of  $A$  by the vector  $b$  as

$$A_b := \{a + b : a \in A\}.$$

- [Hadwiger (1950)]: The *Minkowski sum* of  $A$  and  $B$  is defined as

$$A \oplus B := \bigcup_{b \in B} A_b.$$

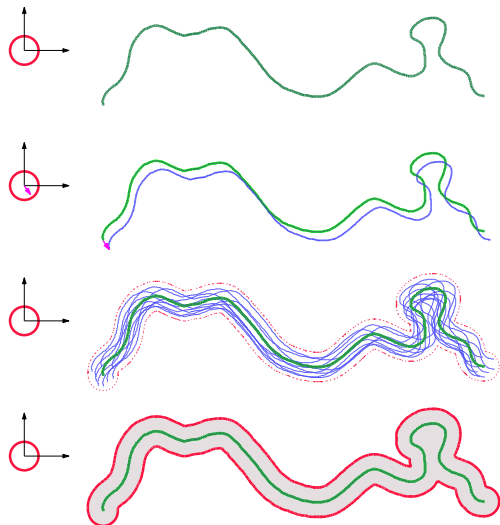
- [Hadwiger (1950)]: The *Minkowski difference* of  $A$  and  $B$  is defined as

$$A \ominus B := \bigcap_{b \in B} A_{-b}.$$

- Note: In general,  $(A \oplus B) \ominus B \neq A$ .

# Minkowski Sum for Offsetting

- Let  $A$  be a curve, and  $B$  be a circular disk centered at the origin. What is  $A \oplus B$ ?



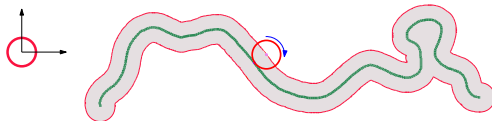
# Minkowski Sum for Offsetting

## Lemma 149

The Minkowski sum  $A \oplus B$  of a curve  $A$  and a circular disk  $B$  (with radius  $r$ ) centered at the origin is the area swept by a disk with radius  $r$  whose center is moved along  $A$ . That is, it is the (unweighted) offset area of  $A$  for offset distance  $r$ .

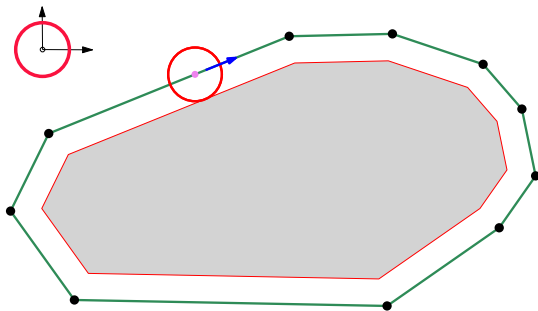
## Lemma 150

The boundary of the Minkowski sum  $A \oplus B$  of a curve  $A$  and a circular disk  $B$  (with radius  $r$ ) centered at the origin is traced out by the center of a disk with radius  $r$  that is “rolled” along  $A$ .



## Minkowski Difference for Offsetting

- Let  $A$  be a polygon, and  $B$  be a circular disk centered at the origin. What is  $A \ominus B$ ?



- Hence, it is the interior offset area of the polygon.
- Offsets, i.e., Minkowski sums and differences of an area  $A$  with a circular disk  $B$  centered at the origin, are also called *buffers* (in GIS) and *dilation/erosion* (in image processing).

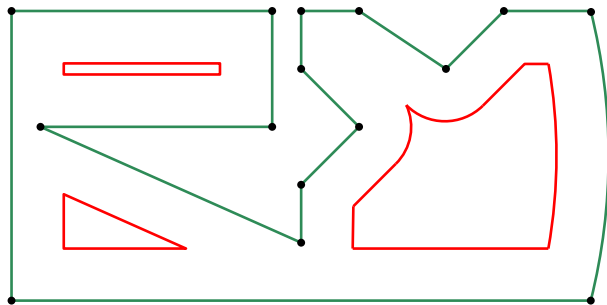
## Buffering in Geographical Information Systems

- Sample GIS application: Identify the portion of the territorial waters of Malta that is within some nautical miles of the baseline (coast) of Malta.



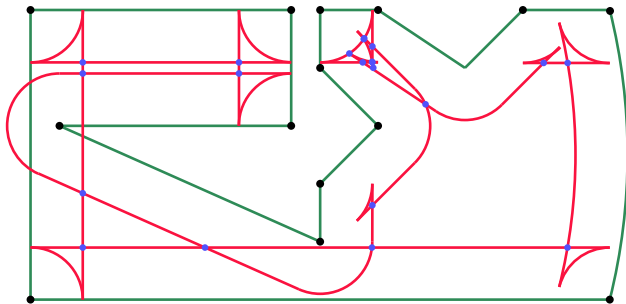
# Computation of Offset Patterns

- How can we compute offset patterns reliably and efficiently?
- Note: The boundary of an offset may contain circular arcs even if the input is purely polygonal.
- Note: Offsetting may cause topological changes!
- How can we compute even just one individual offset?



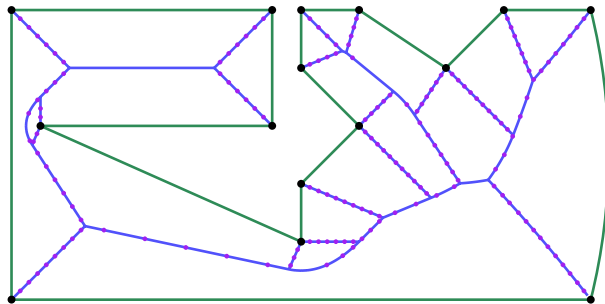
# Conventional Offsetting

- 1 First, one computes offset elements for every input element.
- 2 In order to get one closed loop, trimming arcs are inserted.
- 3 Next, all self-intersections are determined.
- 4 Finally, all incorrect loops of the offset are removed.

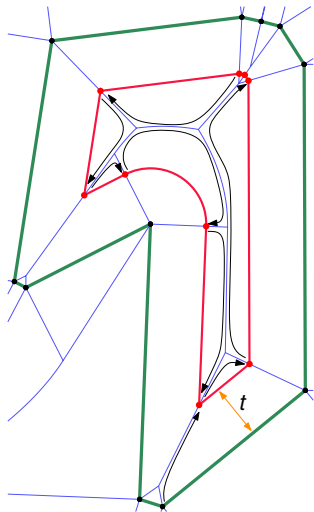


## Voronoi-Based Offsetting

- We start with analyzing the positions of the end-points of the offset segments.
- This looks familiar!
- Indeed, all end-points of offset segments lie on the Voronoi diagram!
- A linear-time scan of the Voronoi diagram reveals the end-points of one offset.



# Voronoi-Based Offsetting



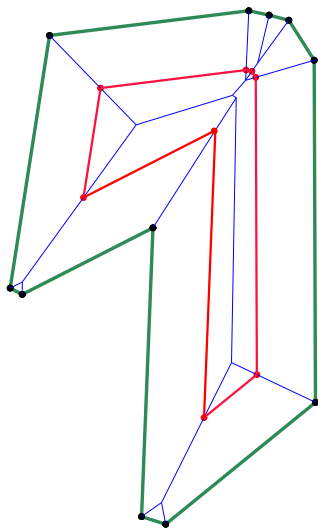
## Theorem 151 (Persson (1978), Held (1991))

Let  $S$  be an admissible set of sites, and  $t \in \mathbb{R}^+$ . If  $\mathcal{VD}(S)$  is known then all offset curves of  $S$  at offset  $t$  can be determined in  $O(n)$  time.

## Corollary 152

Let  $S$  be an admissible set of sites, and  $t \in \mathbb{R}^+$ . Then all offset curves of  $S$  at offset  $t$  can be determined in  $O(n \log n)$  time.

# Straight-Skeleton Based Mitered Offsetting



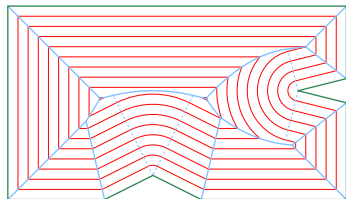
## Theorem 153 (Palfrader&Held (2014))

Let  $S$  a PSLG, and  $t \in \mathbb{R}^+$ . If  $SK(S)$  is known then all mitered offset curves of  $S$  at offset  $t$  can be determined in  $O(n)$  time.

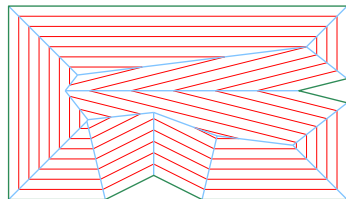
## Comparison of Offsets: Constant-Radius vs. Mitered Offsets

Held&Palfrader (2015)

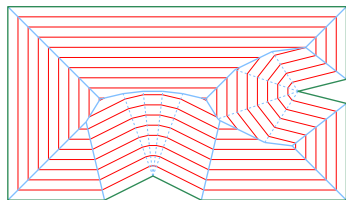
Computing just one mitered offset via an SK is faster than standard mitered offsetting.



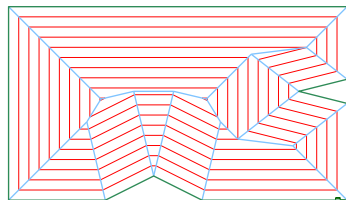
Voronoi diagram and rounded offsets



Straight skeleton and mitered offsets



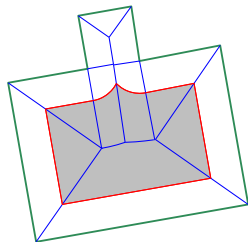
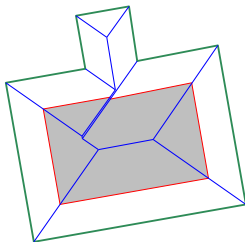
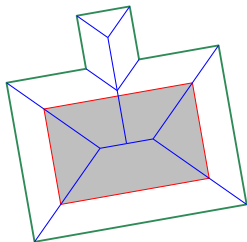
Linear axis and multi-segment bevels



Straight skeleton and beveled offsets

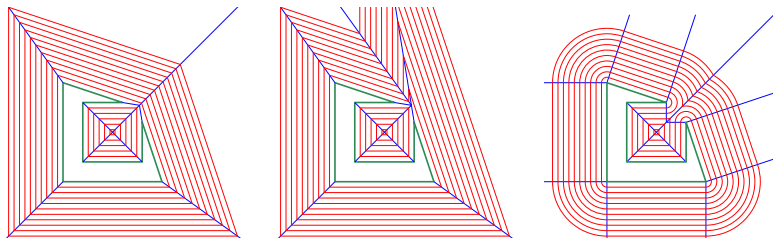
# Sensitivity of Straight Skeleton to Perturbations of the Input

- Even a small perturbation of the input may suffice to change the straight skeleton drastically.
- From left to right:
  - symmetric shape and its straight skeleton and mitered offset,
  - perturbed shape and its straight skeleton and mitered offset,
  - perturbed shape and its Voronoi diagram and constant-radius offset.



# Sensitivity of Straight Skeleton to Perturbations of the Input

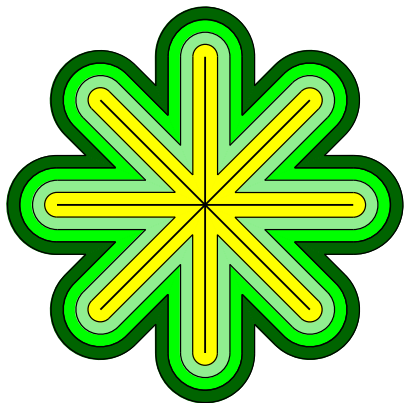
- Even a small perturbation of the input may suffice to change the straight skeleton and the resulting mitered offsets drastically.
- From left to right:
  - symmetric shape and its straight skeleton and mitered offsets,
  - perturbed shape and its straight skeleton and mitered offsets,
  - perturbed shape and its Voronoi diagram and constant-radius offsets.



# Variable-Radius Offsets: Brush Stroke

## Uniform pressure

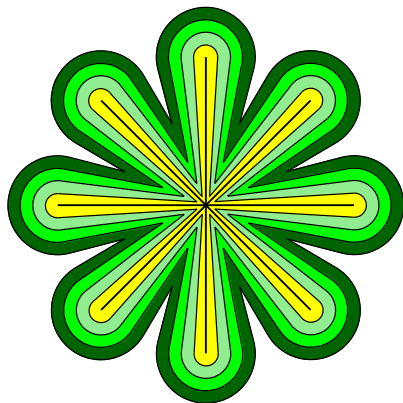
Constant uniform width of the shape.



constant-radius offset

## Non-uniform pressure

Varying width of the shape.



variable-radius offset

# Variable-Radius Offsets: Applications

## Brush stroke

Standard application in computer-assisted calligraphy.

## Shoe and garment design

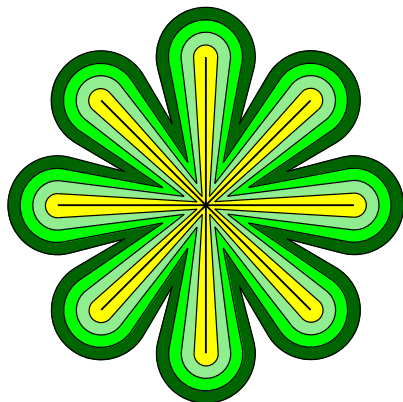
- Ornamentary stitches need not run in a perfectly parallel manner.
- Scaling a basic shape need not necessarily be uniform.

## Image manipulation

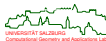
Patent “Retrograde Curve Filtering for Variable Offset Curves” granted to Adobe Inc. in April 2014.

## Non-uniform pressure

Varying width of the shape.



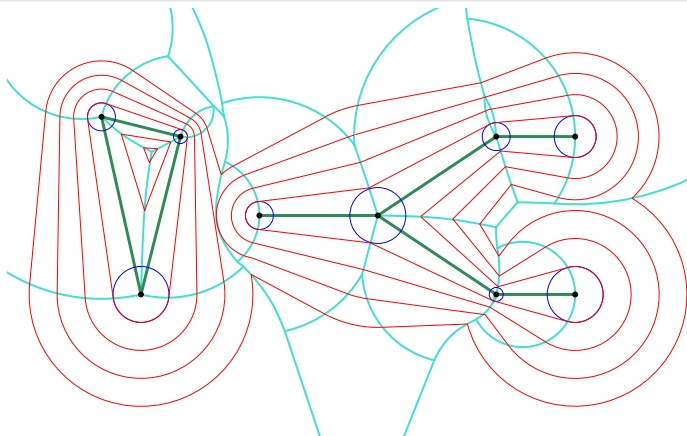
variable-radius offset



# Variable-Radius Offsets and Variable-Radius Voronoi Diagram

Held&Huber&Palfrader (2015)

Assign non-negative weights to the vertices of a PSLG, and interpolate weights linearly along segments. Then the variable-radius Voronoi diagram induced by the resulting weighted distance supports variable-radius offsets.

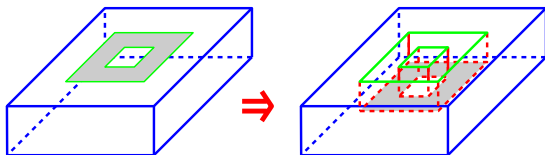


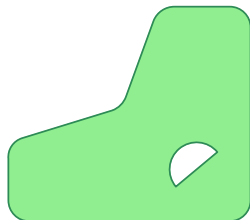
# Tool Paths for Pocket Machining

## Pocket Machining

**Pocket:** Interior recess that is cut into the surface of a workpiece.

**Tool:** Can be regarded as a cylinder that rotates.





## Geometry of a pocket

- 2D area,
- straight-line segments and circular arcs as boundary elements,
- may contain islands.

## Geometry of a tool

- circular disk.

## The goal is ...

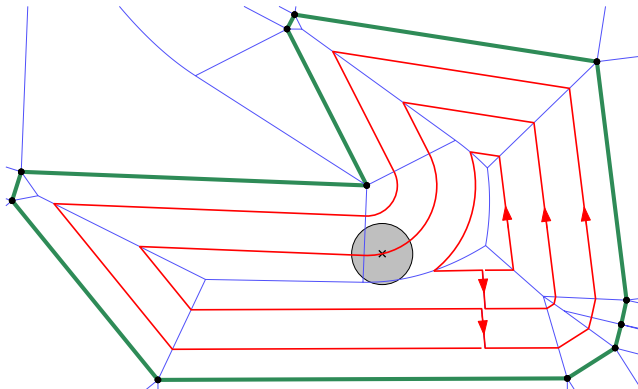
- ... to compute a “good” tool path.

- Similar path planning problems arise in many other applications that require “coverage” of an area by a disk-shaped object, e.g., layered manufacturing, spray painting, aerial surveillance.

# Voronoi-Based Generation of Tool Path

Persson (1978), Held (1991)

- Family of offset curves forms a tool path.
- Tool path computed by means of Voronoi diagram.



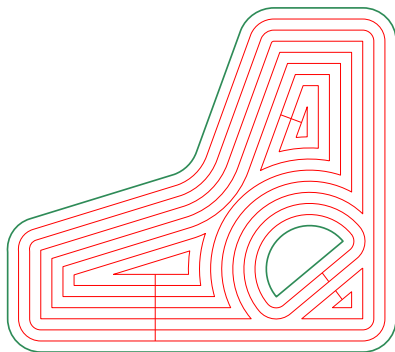
# Voronoi-Based Generation of Tool Path

## Pros of offset-based machining

- Offset curves can be computed easily (based on Voronoi diagram).
- Reasonably short tool path.

## Cons of offset-based machining

- Sharp corners.
- Highly varying material removal rate.
- Might require tool retractions.
- Not suitable for high-speed machining.

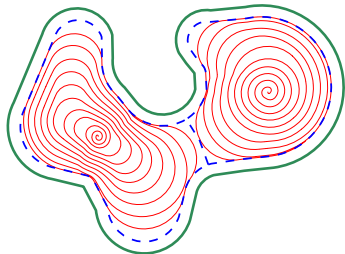
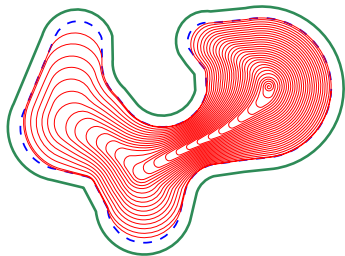


## High-speed machining (HSM)

Faster tool movement requires

- smooth tool paths,
- low variation of material removal rate.

# Voronoi-Based Generation of Smooth Spiral Paths



## Held&Spielberger (2009)

- Smooth spiral path.
- Handle general areas without islands.

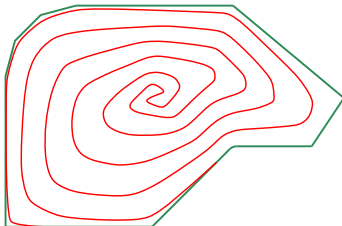
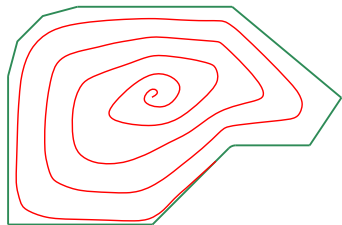
## Held&Spielberger (2013)

- Optimization of the start point of the spiral tool path.
- Decomposition of "complex" areas.
- Handle areas with islands.

## Algorithmic vehicle

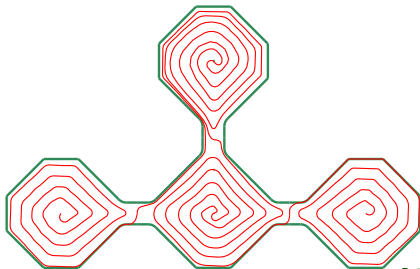
- Voronoi diagram of area boundary.

# Voronoi-Based Generation of Smooth Multi-Spiral Paths



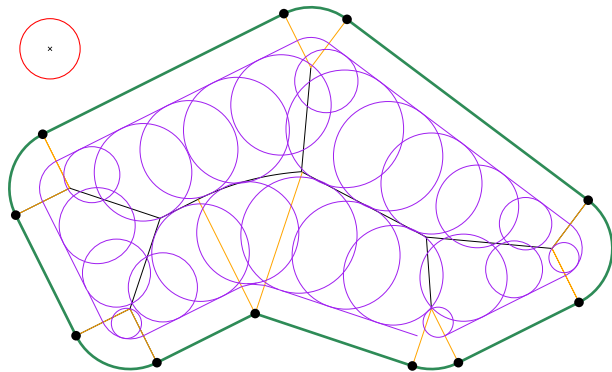
## Held&de Lorenzo (2018)

- Simplified approach to computing a smooth spiral path.
- Double spiral that starts and ends on the boundary.
- Double spirals linked to one multi-spiral path.



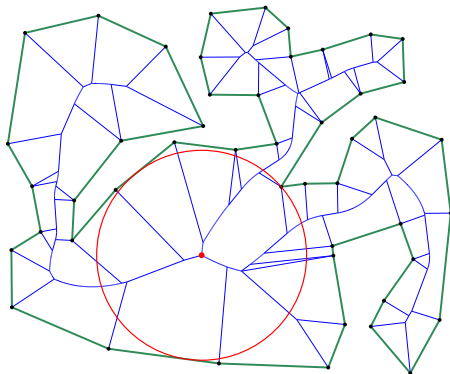
# Paths for High-Speed Machining

- [Elber&Cohen&Drake (2005)]: “Medial axis transform toward high-speed machining of pockets” (MATHSM). They use the medial axis of a pocket to compute clearance disks that form “machining circles”.
- The path is an alternating series of “machining circles” and tangential “transition elements” between pairs of machining circles.
- [Held&Pfeiffer (2024)]: MATHSM extended such that the engagement angle is controlled.



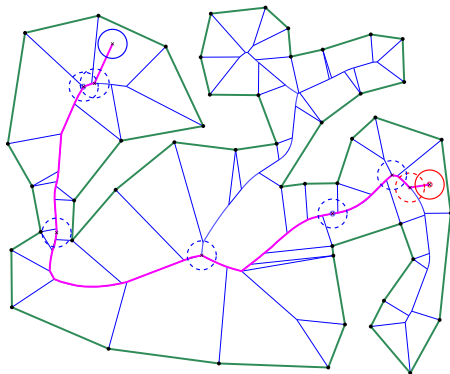
## Maximum Inscribed Circle

- Similarly to the computation of a maximum empty circle, scanning the Voronoi nodes interior to a polygon yields a maximum inscribed circle in  $O(n)$  time.



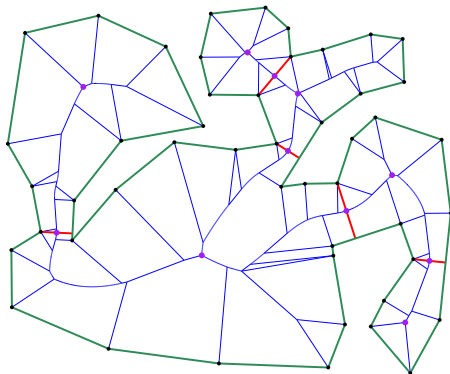
## Finding a Gouge-Free Path

- Can we move the disk within the polygon from the blue to the red position?
- [Ó'Dúnlaing&Yap (1985)]: Retraction method:
  - Project red and blue centers onto the Voronoi diagram.
  - Scan the Voronoi diagram to find a way from blue to red.
  - Make sure to check the clearance while moving through a bottleneck.
- Indeed, this disk can be moved from blue to red!



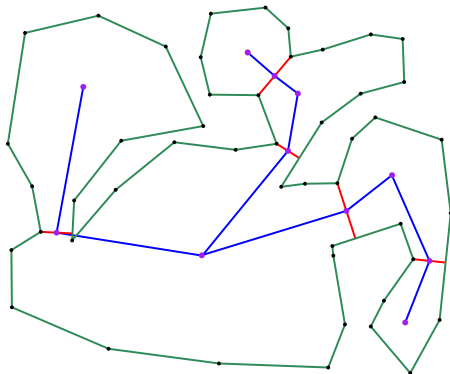
## Bottlenecks and Locally Inner-Most Points

- A linear-time scan of the VD reveals all bottlenecks and locally inner-most points.



## Bottlenecks and Locally Inner-Most Points

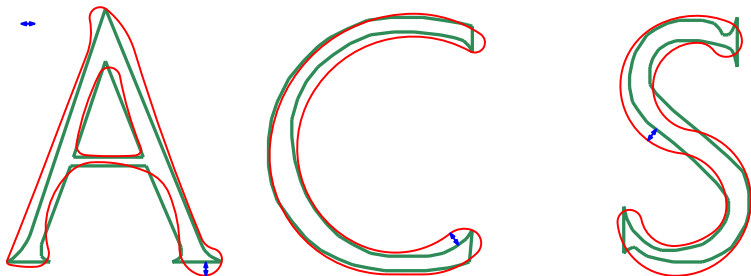
- To save time, a graph search is performed on the graph of offset-connected areas.



# Approximation of Polygonal Profiles

## Informal problem statement

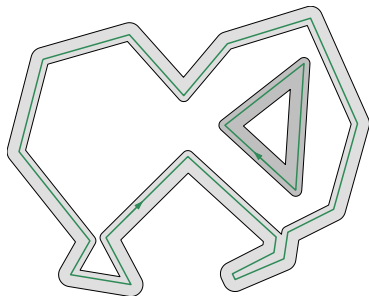
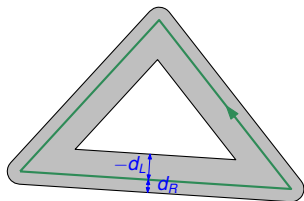
- For a set  $\mathcal{P}$  of planar (polygonal or curvilinear) profiles
- and an approximation threshold given,
- compute an approximation such that the approximation threshold is not exceeded.



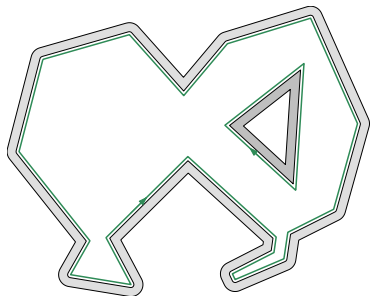
- Real-world applications: smoothing of tool paths, simplification of contours derived from scanning, recovery of “linearized” PCB data.

## Approximation: Specifying a Tolerance

- Intuitively, for an **input profile**  $P \in \mathcal{P}$  we seek a tolerance zone,  $\mathcal{TZ}(P, d_L, d_R)$ , of  $P$  with **left tolerance**  $d_L$  and **right tolerance**  $d_R$ .
- Non-trivial tolerances classified as
  - symmetric* if  $-d_L = d_R > 0$ ,
  - asymmetric* if  $d_L < 0 \leq d_R$  or  $d_L \leq 0 < d_R$ , and
  - one-sided* if  $d_L < d_R < 0$  or  $0 < d_L < d_R$ .



asymmetric with  $d_L < 0 < d_R$



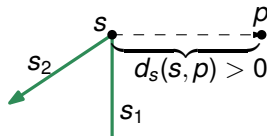
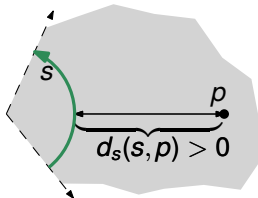
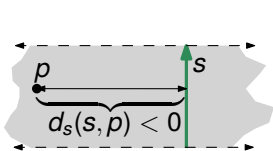
one-sided with  $0 < d_L < d_R$

# Signed Distance

## Definition 154 (Signed distance)

The *signed distance*,  $d_s(s, p)$ , of a point  $p \in \mathcal{CI}(s)$

- to an oriented straight-line segment or circular arc  $s$  of  $\mathcal{P}$  is given by the standard (Euclidean) distance of  $p$  to  $s$ , multiplied by  $-1$  if  $p$  is on the left side of the supporting line or circle of  $s$ ,
- to a vertex  $s$  of  $\mathcal{P}$  we take the standard distance between  $p$  and  $s$ , and multiply it by  $-1$  if the ray from  $s$  to  $p$  is locally on the left side of  $s_1$  and  $s_2$ , where  $s_1$  and  $s_2$  are the sites of  $\mathcal{P}$  that share  $s$  as a common vertex.



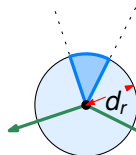
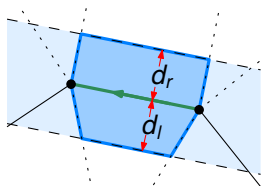
## Definition 155 (Tolerance zone)

The tolerance zone of a site  $s$  of  $\mathcal{P}$  is defined as

$$\mathcal{TZ}_{site}(s, \mathcal{P}, d_L, d_R) := \{p \in \mathcal{VR}(\mathcal{P}, s) : d_L < d_s(s, p) < d_R\}.$$

The tolerance zone of  $\mathcal{P}$  is defined as the union of all tolerance zones of all sites:

$$\mathcal{TZ}(\mathcal{P}, d_L, d_R) := \bigcup_{s \in \mathcal{P}} \mathcal{TZ}_{site}(s, \mathcal{P}, d_L, d_R).$$



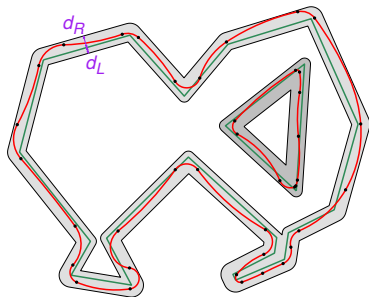
# Problem Statement

**Given:** Input

- Set  $\mathcal{P}$  of (open or closed) **polygonal profiles** that do not intersect pairwise;
- Left approximation tolerance  $d_L$  and right approximation tolerance  $d_R$ , with  $d_L < d_R$ .

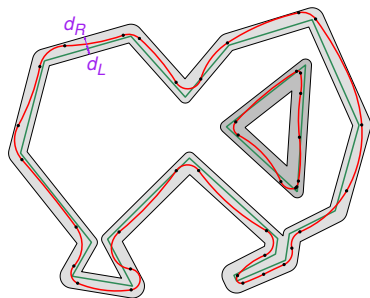
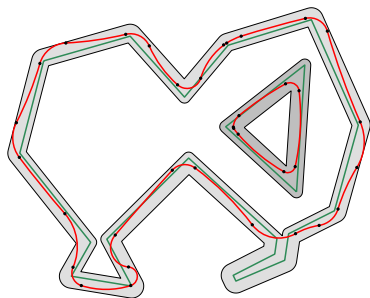
**Compute:** Approximation  $\mathcal{A}$  of  $\mathcal{P}$  such that

- $\mathcal{A}$  consists of  $G^k$  curves, for some  $k \in \mathbb{N}$ ,
- all curves of  $\mathcal{A}$  are simple and pairwise disjoint,
- $\mathcal{A} \subset \mathcal{TZ}(\mathcal{P}, d_L, d_R)$ ,
- $\mathcal{P} \subset \mathcal{TZ}(\mathcal{A}, -d_R, -d_L)$  if requested by user,
- topology of  $\mathcal{A}$  matches topology of  $\mathcal{P}$ .



## Tolerance Zone and Distance Measures

- Omitting the second condition  $\mathcal{P} \subset \mathcal{TZ}(\mathcal{A}, -d_R, -d_L)$  makes a difference!



## Tolerance Zone and Distance Measures

- Assume  $-d_L = d_R > 0$ . We have

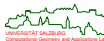
$$\mathcal{A} \subset \mathcal{TZ}(\mathcal{P}, -d_R, d_R) \wedge \mathcal{P} \subset \mathcal{TZ}(\mathcal{A}, -d_R, d_R) \implies H(\mathcal{A}, \mathcal{P}) \leq d_R,$$

where  $H(\mathcal{A}, \mathcal{P})$  denotes the Hausdorff distance between  $\mathcal{A}$  and  $\mathcal{P}$ .

- Assume  $-d_L = d_R > 0$ . If each approximation curve  $A \in \mathcal{A}$  is “monotone” relative to its corresponding input curve  $P \in \mathcal{P}$ , then

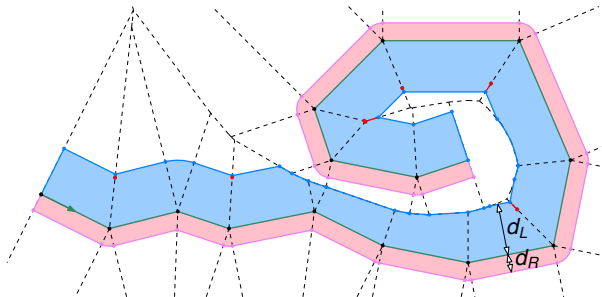
$$\mathcal{A} \subset \mathcal{TZ}(\mathcal{P}, -d_R, d_R) \wedge \mathcal{P} \subset \mathcal{TZ}(\mathcal{A}, -d_R, d_R) \implies \text{Fr}(A, P) \leq d_R,$$

where  $\text{Fr}(A, P)$  denotes the Fréchet distance between  $A$  and  $P$ , for each  $A \in \mathcal{A}$  and corresponding  $P \in \mathcal{P}$ .



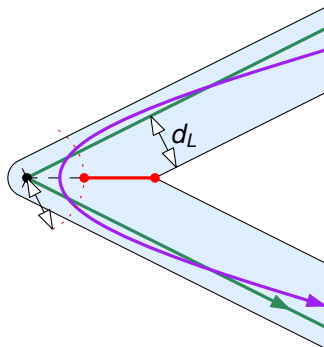
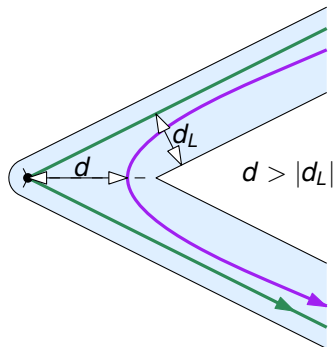
# VD-Based Computation of the Tolerance Zone

- [Held&Heimlich (2008), Held&Kaaser (2014)] use the Voronoi diagram of the input to compute the boundary of the tolerance zone.
- Tolerance zone computation for an input profile:
  - 1 Collect all nodes of Voronoi cells left of the profile.
  - 2 Skip nodes that are further away than  $d_L$  from the profile.
  - 3 Remove trees within the tolerance zone and add spikes.
  - 4 Repeat this procedure for the right side of the profile w.r.t.  $d_R$ .



## Offset Spikes

- How can we guarantee  $\mathcal{P} \subset \mathcal{TZ}(\mathcal{A}, -d_R, -d_L)$ ?
- *Offset spikes* ensure that the directed Hausdorff distance from the input to the approximation curve does not exceed the user-specified maximum tolerance.
- Spikes are formed by portions of the Voronoi diagram; they can be computed in linear time.



## Results on Voronoi-Based Approximation

### Theorem 156 (Held&Heimlich (2008))

Let  $n$  denote the number of vertices of a set  $\mathcal{P}$  of polygonal profiles. Then a  $G^1$  biarc approximation or a polygonal approximation, within an (asymmetric) user-specified tolerance that preserves the topology of  $\mathcal{P}$ , can be computed in  $O(n \log n)$  time.

### Theorem 157 (Maier&Pisinger (2013))

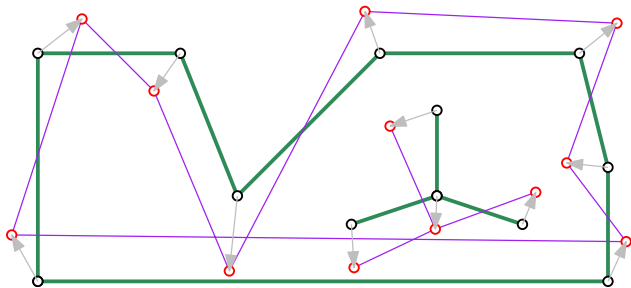
Let  $n$  denote the number of vertices of one closed polygon  $P$ , and assume that a tolerance zone is given. Then a  $G^1$  biarc approximation of  $P$  that uses the minimum number of biarcs (relative to the tolerance zone) can be computed in  $O(n^3)$  time.

### Theorem 158 (Held&Kaaser (2014))

Let  $n$  denote the number of vertices of a set  $\mathcal{P}$  of polygonal profiles. Then a  $C^2$  approximation by uniform cubic B-splines within an (asymmetric) user-specified tolerance that preserves the topology of  $\mathcal{P}$  can be computed in  $O(n \log n)$  time.

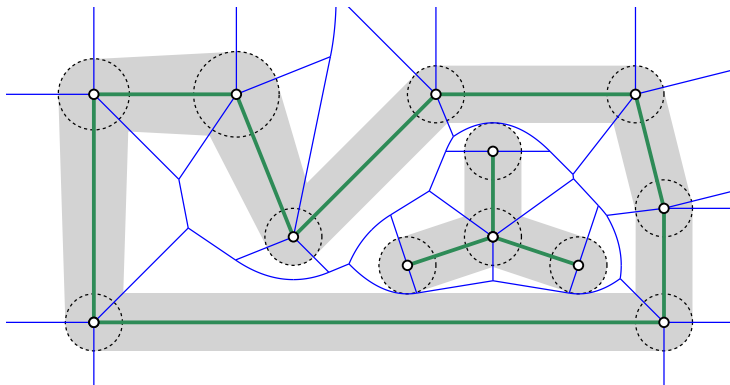
# Topology-Preserving Watermarking of Vector Graphics

- Watermarking techniques for vector graphics dislocate vertices in order to embed imperceptible, yet detectable, statistical features into the input data.
- Obvious problem: One needs to guarantee that the introduction of a watermark preserves the input topology.



# Topology-Preserving Watermarking of Vector Graphics

- [Huber et al. (2014)] compute for each vertex a disk-shaped maximum perturbation region (MPR), based on the Voronoi diagram of the input.
- Perturbing the vertices within their MPRs causes the edges to stay within their hoses and allows to preserve the input topology.
- This scheme can be extended to cover straight-line segments and circular arcs.



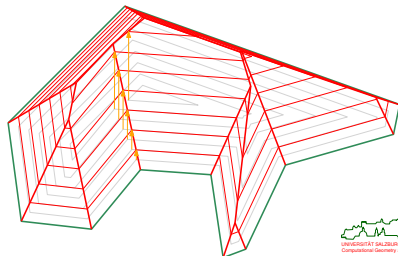
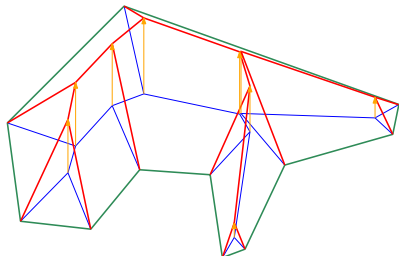
# Straight Skeleton: Roof Model

## Roof model via lifted wavefronts

We lift a wavefront  $\mathcal{WF}(P, t)$  of  $P$  for the orthogonal boundary clearance  $t$  to z-coordinate  $t$ : We get  $\mathcal{WF}(P, t) \times \{t\}$ .

## Roof model

Alternatively, a point  $p$  of the straight skeleton of polygon  $P$ , with coordinates  $(p_x, p_y)$ , is lifted to a point in 3D with coordinates  $(p_x, p_y, t)$  if the orthogonal boundary clearance of  $p$  is  $t$ .



# Straight Skeleton: Properties of Roof Model

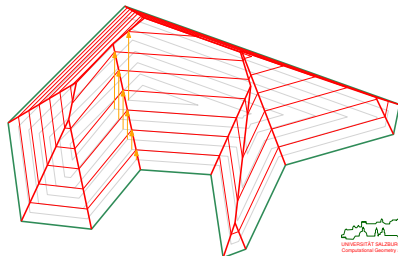
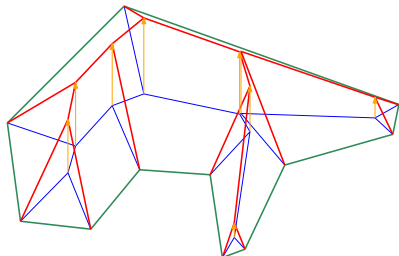
## Properties

- The *roof*

$$\mathcal{R}(P) := \bigcup_{t \geq 0} (\mathcal{WF}(P, t) \times \{t\})$$

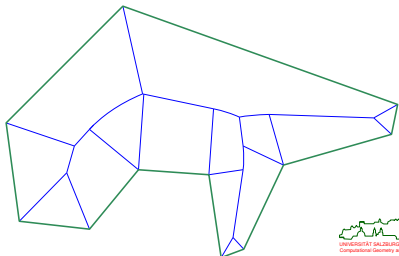
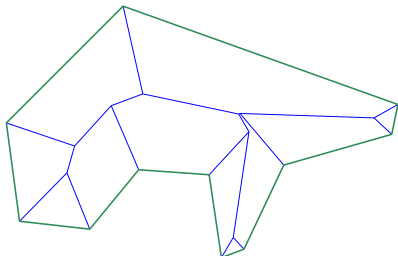
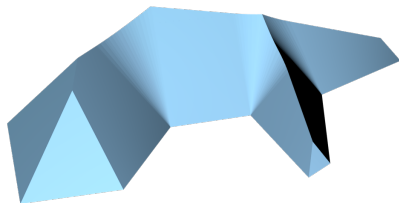
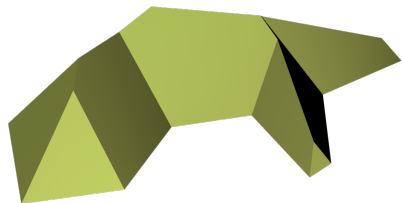
is a piecewise-linear and continuous surface.

- It is monotone relative to the  $xy$ -plane.



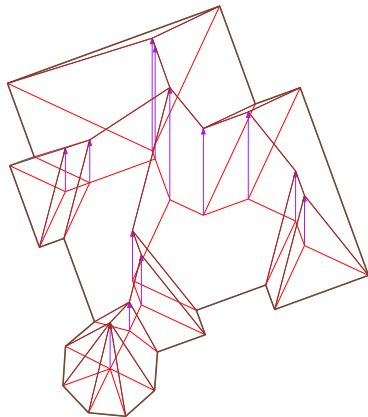
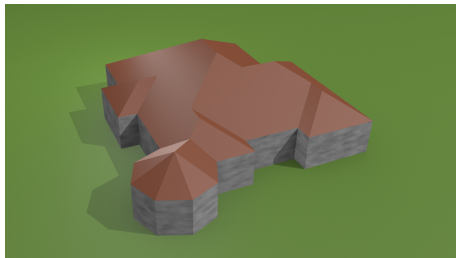
## Straight Skeleton and Voronoi Diagram: Roof Model

- The same lifting approach can also be applied to Voronoi diagrams, thereby generating a roof for a Voronoi diagram.



# Roofs as Skeletal Structures Lifted to 3D

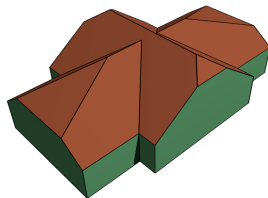
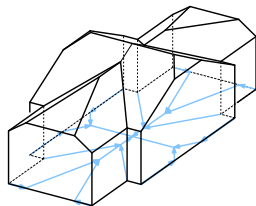
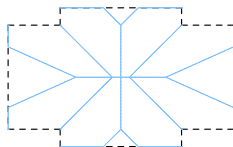
- Footprint. Straight skeleton. Lift to 3D. Roof.



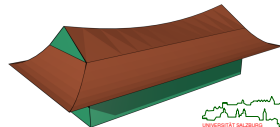
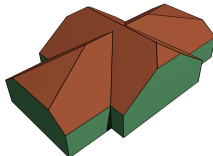
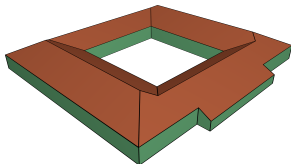
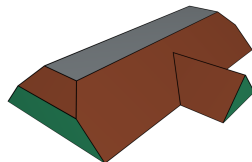
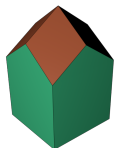
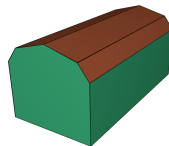
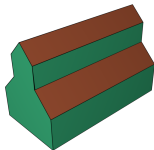
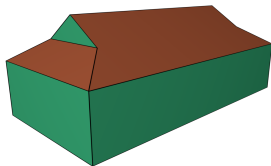
# Complex Roofs for Urban Modeling and Reconstruction

Held&Palfrader (2016)

Additive and multiplicative weights support the automatic generation of realistic complex roofs based on the footprints of buildings.



# Complex Roofs for Urban Modeling and Reconstruction

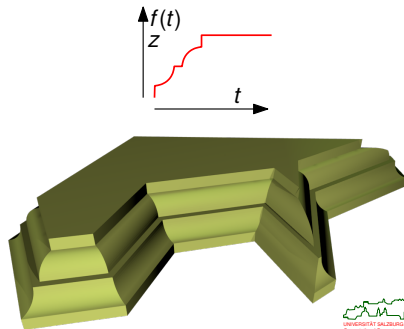
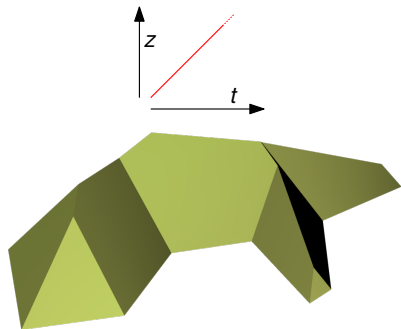


# Generalizing the Roof Based on Straight Skeleton

## Generalized Roof

We use a (continuous) height “function”  $f$  to obtain a scalar field on  $P$ , thereby generalizing the roof  $\mathcal{R}(P)$  to a surface  $\mathcal{T}_f(P)$ :

$$\mathcal{T}_f(P) := \bigcup_{t \geq 0} (\mathcal{WF}(P, t) \times \{f(t)\}).$$

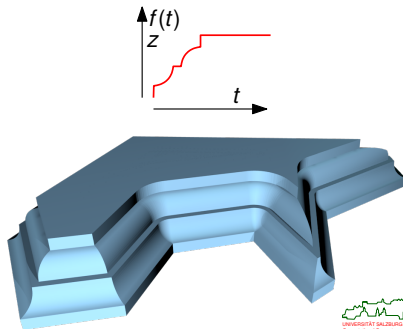
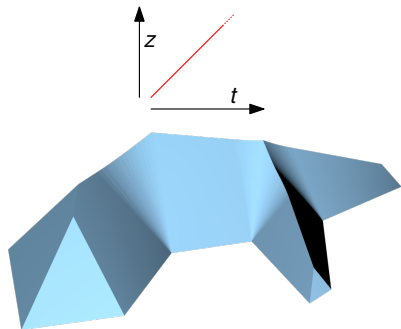


# Generalizing the Roof Based on Voronoi Diagram

## Generalized Roof

We use a (continuous) height “function”  $f$  to obtain a scalar field on  $P$ , thereby generalizing the roof  $\mathcal{R}(P)$  to a surface  $\mathcal{T}_f(P)$ :

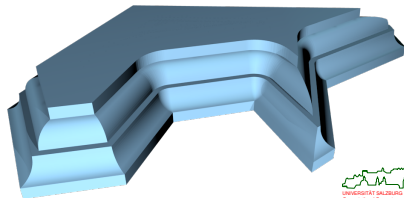
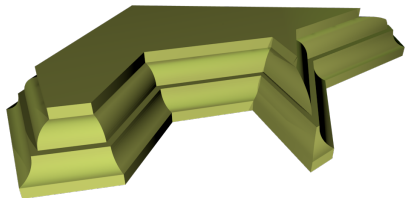
$$\mathcal{T}_f(P) := \bigcup_{t \geq 0} (\mathcal{WF}(P, t) \times \{f(t)\}).$$



# Straight Skeleton: Properties of Generalized Roofs

## Properties

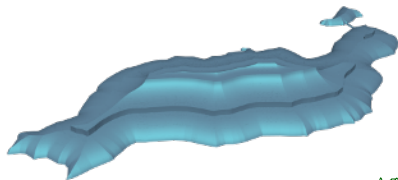
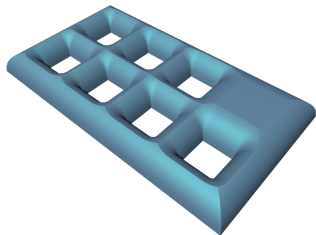
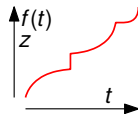
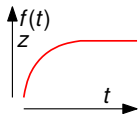
- The generalized roof  $\mathcal{T}_f(P)$  is monotone relative to the  $xy$ -plane.
- If  $f$  is continuous then also  $\mathcal{T}_f(P)$  is continuous.
- A face of  $\mathcal{T}_f(P)$  is a ruled surface if it is incident to an edge of  $P$ , and a surface of revolution if it is incident to a reflex vertex.



# Complex Chamfers and Fillets

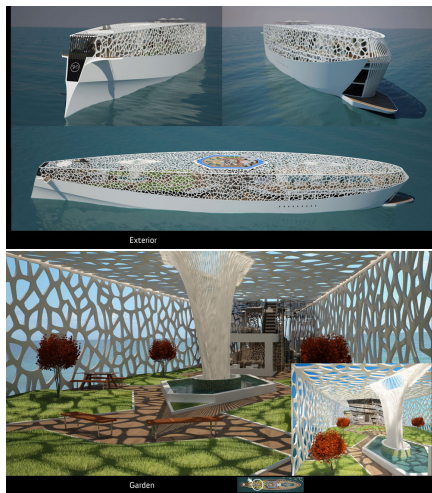
Held&Palfrader (2018)

Such a generalization of the function that “lifts” a Voronoi diagram or (weighted) straight skeleton to 3D supports the generation of complex chamfers and fillets.



# Voronoi Diagrams in Structural Design

- CNN (16-Aug-2011): “Stunning superyacht design inspired by nature’s hidden patterns”.



[Images courtesy of Hyun-Seok Kim]

## 7

## Triangulations

- Basics
- Computing Constrained Triangulations
- Triangulations in 3D
- Applications of Triangulations

## Definition 159 (Triangulation of a point set)

A *triangulation* of a set  $S$  of  $n$  points of  $\mathbb{R}^2$  is a subdivision of the convex hull  $CH(S)$  into triangles such that

- 1 the set of vertices of the triangles matches  $S$ ,
- 2 no pair of triangles intersects except in a common vertex or edge.

## Definition 160 (Triangulation of a polygon)

A *polygon triangulation* is a subdivision of a (simple plane) polygon  $P$  into triangles such that

- 1 the set of vertices of the triangles matches the vertices of  $P$ ,
  - 2 no pair of triangles intersects except in a common vertex or edge.
- Similarly for points/polyhedra in  $\mathbb{R}^3$  and a subdivision into tetrahedra.
  - For  $d > 3$  it is standard to resort to the terms “simplex” and “simplicial complex” to define triangulations in  $\mathbb{R}^d$ .

## What is a Good Triangulation?

- Let  $S$  be a set of  $n$  points in  $\mathbb{R}^2$ . Several options to demand additional properties for a triangulation of  $S$ .

### Definition 161 (Locally Delaunay)

A triangulation  $\mathcal{T}(S)$  of  $S$  is *locally Delaunay* if for every pair of adjacent triangles  $\Delta(a, b, c)$  and  $\Delta(a, c, d)$  of  $\mathcal{T}(S)$  the Delaunay triangulation of  $a, b, c, d$  includes these two triangles.

### Lemma 162 (Fortune (1992))

A triangulation of  $S$  is a Delaunay triangulation of  $S$  if and only if it is locally Delaunay.

### Lemma 163 (Sibson (1978))

The minimum internal angle of the triangles of  $DT(S)$  is maximum over all triangulations of  $S$ .

### Lemma 164 (Lambert (1994))

The (arithmetic) mean inradius of the triangles of  $DT(S)$  is maximum over all triangulations of  $S$ .

# What is a Good Triangulation?

## Definition 165 (Hamiltonian triangulation)

A triangulation of  $S$  is a *Hamiltonian triangulation* if the dual graph of the triangulation admits a Hamiltonian path.

## Lemma 166 (Arkin et alii (1996))

A Hamiltonian triangulation of  $S$  can be computed in  $O(n \log n)$  time.

## Definition 167 (Minimum-weight triangulation)

A triangulation of  $S$  is a *minimum-weight triangulation* (MWT) if the sum of the lengths of the triangulation edges is minimum over all triangulations.

## Theorem 168 (Mulzer&Rote (2006))

Computing a minimum-weight triangulation is  $\mathcal{NP}$ -hard.

## Theorem 169 (Remy&Steger (2009))

For any  $\varepsilon > 0$ , a minimum-weight triangulation can be approximated with approximation factor  $1 + \varepsilon$  in time  $2^{O((\log n)^c)}$  for some fixed  $c \in \mathbb{R}^+$ .

## Counting Triangulations

- No tight bounds are known for the minimum and the maximum number of (different straight-edge) triangulations that  $n$  points in 2D may admit.
- For 20 points, the best known minimum is 20 662 980, and the best known maximum is 918 462 742 512 [Aicholzer et alii (2001–2003)].

### Lemma 170 (Goldbach&Euler (1751), Lamé (1838))

If  $(n + 2)$  points are in convex position then the number of different triangulations is given by the  $n$ -th Catalan number  $C_n$ .

### Lemma 171 (Sharir&Sheffer (2009))

Every set of  $n$  points in the plane admits at most  $30^n$  different triangulations.

### Lemma 172 (Aicholzer et alii (2016))

Every set of  $n$  points — GPA! — in the plane admits at least  $\Omega(2.631^n)$  triangulations.

### Lemma 173 (Dumitrescu et alii (2010))

There exist sets of  $n$  points in the plane which admit at least  $\Omega(8.65^n)$  triangulations.

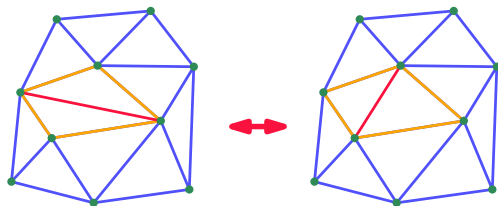
# Triangulations are Related via Edge Flips

## Definition 174 (Edge flip, Dt.: Kantenaustausch)

An *edge flip* is a local operation on a triangulation that replaces one diagonal of a convex quadrilateral (formed by two neighboring triangles) with the other diagonal.

## Lemma 175 (Bern&Eppstein (1992))

$O(n^2)$  edge-flipping operations suffice to transform any triangulation of  $n$  points (in  $\mathbb{R}^2$ ) into a Delaunay triangulation.



# Triangulations are Related via Edge Flips

## Lemma 176 (Lubiw&Pathak (2012))

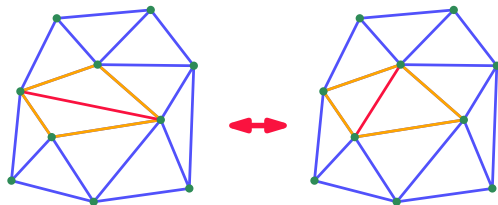
Minimizing the flip distance between triangulations of point sets is  $\mathcal{NP}$ -hard.

## Lemma 177 (Aichholzer&Mulzer&Pilz (2013))

Minimizing the flip distance between triangulations of a polygon is  $\mathcal{NP}$ -hard.

## Lemma 178 (Pilz (2014))

Minimizing the flip distance between triangulations of point sets is APX-hard; i.e., no polynomial-time constant factor approximation exists unless  $\mathcal{P} = \mathcal{NP}$ .

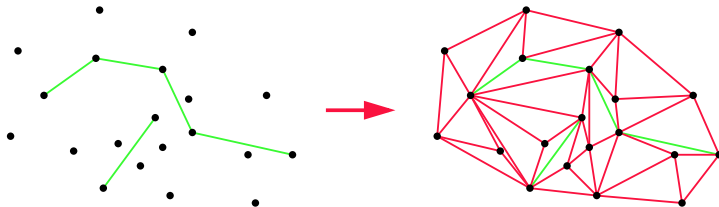


# Constrained Triangulation

## Definition 179 (Constrained triangulation)

A triangulation  $\mathcal{T}$  forms a *constrained triangulation* of an admissible set  $S$  of vertices and line segments in  $\mathbb{R}^2$  if

- 1  $\mathcal{T}$  is a triangulation of the convex hull of all vertices of  $S$ ,
- 2 all line segments of  $S$  are edges of  $\mathcal{T}$ .

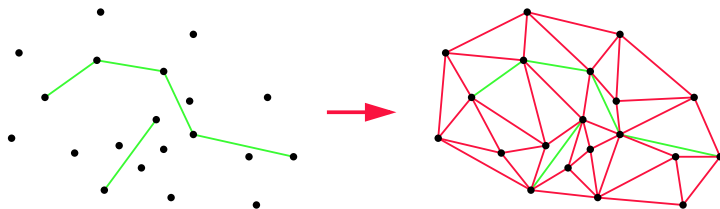


# Constrained Delaunay Triangulation

## Definition 180 (Constrained Delaunay triangulation)

A triangulation  $\mathcal{T}$  forms a *constrained Delaunay triangulation* (CDT) of an admissible set  $S$  of vertices and line segments if

- 1  $\mathcal{T}$  is a constrained triangulation of  $S$ , and
- 2 no triangle  $\Delta$  of  $\mathcal{T}$  contains a vertex of  $S$  in its circumcircle that is visible from  $\Delta$ .

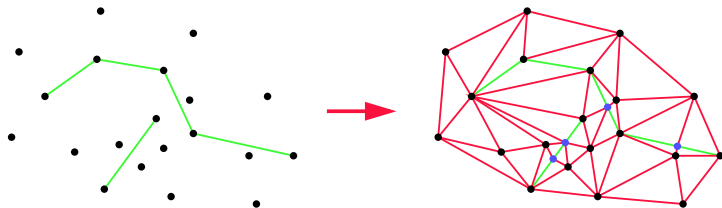


# Conforming Triangulation

## Definition 181 (Conforming triangulation)

A triangulation  $\mathcal{T}$  forms a *conforming triangulation* of an admissible set  $S$  of vertices and line segments if

- 1  $\mathcal{T}$  is a triangulation of the convex hull of all vertices of  $S$  and (possibly) of some additional Steiner points,
- 2 all line segments of  $S$  are represented by unions of edges of  $\mathcal{T}$ .



# Computing Constrained Triangulations

## Definition 182 (Diagonal)

For vertices  $p$  and  $q$  of a simple polygon  $P$ , the line segment  $\overline{pq}$  forms a *diagonal* of  $P$  if  $\overline{pq}$  lies completely in the interior of  $P$ , except for the vertices  $p$  and  $q$ .

## Lemma 183

Every simple polygon with  $n \geq 4$  vertices contains a diagonal.

## Corollary 184

Every simple polygon with  $n$  vertices can be partitioned into  $n - 2$  triangles by inserting  $n - 3$  appropriate diagonals.

## Lemma 185

A regularization procedure can be used to partition a simple polygon with  $n$  vertices in  $O(n \log n)$  time into a set of monotone polygons.

## Corollary 186

A simple polygon with  $n$  vertices can be triangulated in  $O(n \log n)$  time.

# Computing Constrained Triangulations

## Theorem 187 (Chazelle (1991))

A simple polygon with  $n$  vertices can be triangulated in optimal  $O(n)$  time.

## Corollary 188 (Chazelle (1991))

In  $O(n)$  time we can check whether a polygon is simple.

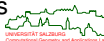
## Theorem 189 (Clarkson&Tarjan&Wyk (1989), Seidel (1991))

A simple polygon with  $n$  vertices can be triangulated in expected  $O(n \log^* n)$  time by means of randomization.

## Theorem 190 (Amato&Goodrich&Ramos (2001))

A simple polygon with  $n$  vertices can be triangulated in expected  $O(n)$  time by means of randomization.

- The algorithms by Chazelle and Amato et alii are considered impractical.
- The implementation of Seidel's algorithm by Narkhede&Manocha (1995) is surprisingly slow.



# Computing Constrained Delaunay Triangulations

## Theorem 191 (Chew (1989))

A constrained Delaunay triangulation of an admissible set  $S$  of  $n$  vertices and straight-line segments can be computed in optimal  $O(n \log n)$  time.

## Theorem 192 (Chin&Wang (1998))

A constrained Delaunay triangulation of a simple polygon with  $n$  vertices can be computed in optimal  $O(n)$  time.

- The algorithm by Chin&Wang is far too complicated to be of practical relevance.

# Polygon Triangulation via Ear-Clipping

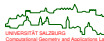
## Definition 193 (Ear)

Three consecutive vertices  $(u, v, w)$  of a simple polygon  $P$  form an *ear* of  $P$  if  $\overline{uw}$  constitutes a diagonal of  $P$ .

## Lemma 194 (Meisters (1975))

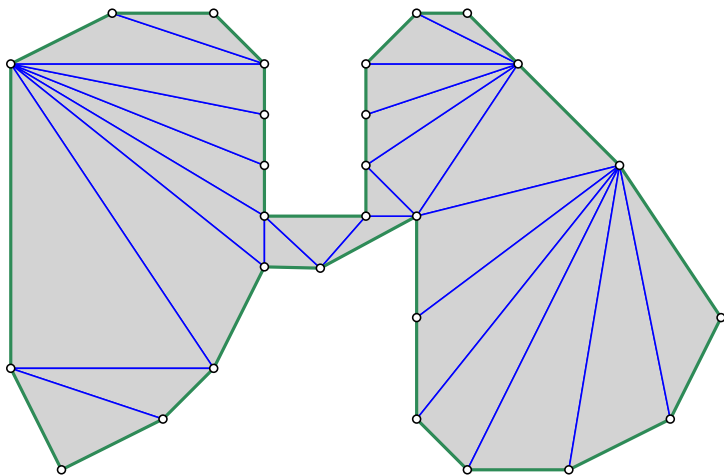
Every simple polygon with four or more vertices has at least two non-overlapping ears.

- Simple triangulation algorithm:
  - Find an ear of  $P$  and clip it.
  - Repeat the ear clipping until only one triangle is left.
- An ear-clipping operation transforms an  $n$ -gon into an  $(n - 1)$ -gon.



## Animation of Ear Clipping

- Find an ear, and clip it. Keep clipping ears, until triangulation is finished.

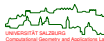


# Polygon Triangulation via Ear-Clipping

- Complexity of naïve algorithm:  $O(n^3)$ .
  - $O(n)$  time to check whether a triple of consecutive vertices forms an ear.
  - $O(n)$  many checks to find next ear.
  - $O(n)$  many ears needed.
- Observation: The clipping of one ear can change the earity status of at most two other triples of vertices of  $P$ .
- Thus, the overall complexity can be reduced to  $O(n^2)$ .

## Lemma 195

Ear clipping computes a triangulation of a simple  $n$ -gon in  $O(n^2)$  time.



# Polygon Triangulation via Ear-Clipping

## Lemma 196

Three consecutive vertices  $(u, v, w)$  of  $P$  form an ear of  $P$  if and only if

- 1  $v$  is a convex vertex,
- 2 the triangle  $\Delta(u, v, w)$  contains no reflex vertex of  $P$ , except for  $u$  or  $w$  if they are reflex.

## Corollary 197

Ear clipping computes a triangulation of a simple  $n$ -gon in  $O(n \cdot r)$  time, where  $r$  is the number of its reflex vertices.

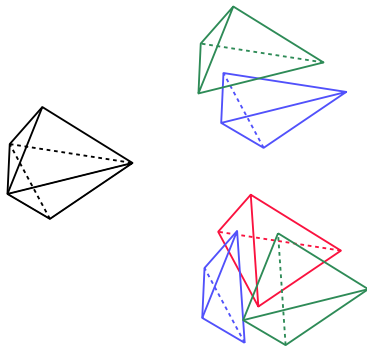
- [Held (2001)]: A triangulation algorithm based on ear-clipping and geometric hashing can be engineered to run in near-linear time, beating implementations of theoretically better algorithms on thousands of synthetic and real-world data sets.  
→ “Fast Industrial-Strength Triangulation” (FIST).
- [Eder&Held&Palfrader (2018)]: A coarse-grain parallelization of FIST’s ear-clipping algorithm achieves a speedup of about 2–3 for four threads and about 3–4 for eight threads. Also parallel edge flipping to obtain a CDT is possible.



## Caveats for 3D Triangulations: Number of Tetrahedra

### Theorem 198

The number of tetrahedra contained in a triangulation of points in  $\mathbb{R}^3$  may vary.



### Theorem 199

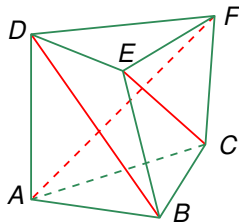
A triangulation of  $n$  points in  $\mathbb{R}^3$  can have  $\Theta(n^2)$  many tetrahedra.

## Caveats for 3D Triangulations: Does a Triangulation Exist?

### Theorem 200

Not every polyhedron can be triangulated.

*Proof:* The triangle  $\Delta(D, E, F)$  of Schönhardt's polyhedron (Math. Annalen, 1928) is rotated relative to  $\Delta(A, B, C)$ , causing the three red edges  $BD$ ,  $CE$  and  $AF$  to become reflex.  $\square$



### Theorem 201 (Ruppert&Seidel (1992))

It is  $\mathcal{NP}$ -complete to determine whether a polyhedron requires Steiner points for triangulation. (And this result holds even for star-shaped polyhedra!)

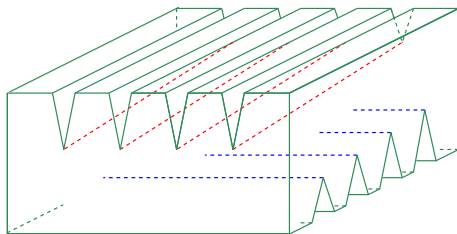
### Theorem 202 (Barequet et al. (1996))

It is  $\mathcal{NP}$ -complete to determine whether a non-plane polygon in  $\mathbb{R}^3$  has a non-intersecting triangulation.

# Caveats for 3D Triangulations: Many Steiner Points Required

## Theorem 203 (Chazelle (1984))

There exist polyhedra with  $n$  vertices that require  $\Omega(n^2)$  Steiner points.

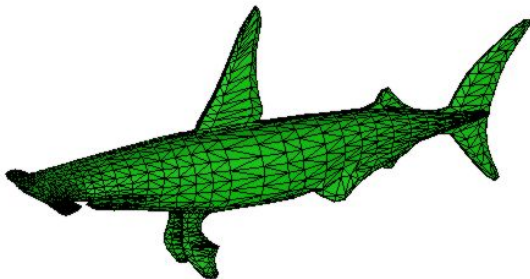


## Theorem 204 (Chazelle&Palios (1990))

Every simple polyhedron with  $n$  vertices and  $r$  reflex edges can be triangulated using  $O(n + r^2)$  Steiner points and a total of  $O(n + r^2)$  tetrahedra.

# Rendering

- Graphics hardware is best at handling triangles rather than more general geometric primitives. Thus, the surfaces of 3D models need to be triangulated.
- Euler's Theorem applies to the faces, edges and vertices of a polyhedron.

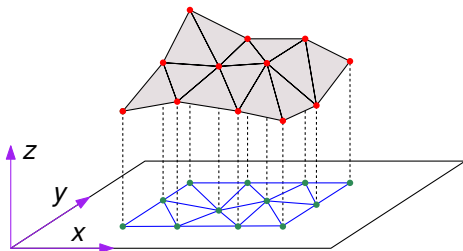


## Caveat

3D polyhedral models used for graphics purposes tend to exhibit all types of “problems”!

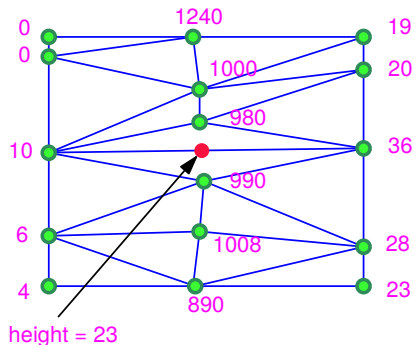
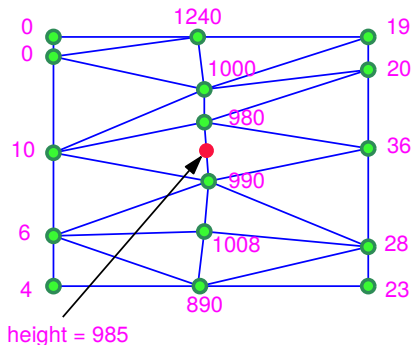
# Triangulated Irregular Network

- Given is a set of sample points on a 3D terrain. How can we model the actual terrain surface by interpolating those points?
- Natural approach:
  - Project the points onto 2D (by discarding their  $z$ -coordinate).
  - Compute a triangulation  $\mathcal{T}$  of the projected points.
  - Lift  $\mathcal{T}$  back to 3D.
- Known to the GIS community as *triangulated irregular network* (TIN).



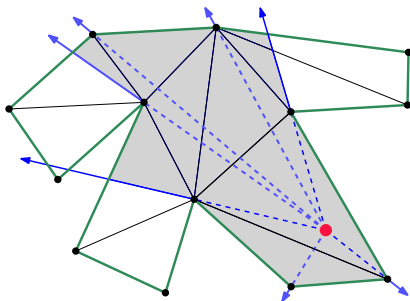
# Triangulated Irregular Network

- Note: The shape of the terrain depends heavily on the 2D triangulation!



## Visibility Determination Within Triangulated Environments

- Which portion of the green polygon is visible from the red point?
- We start with an arbitrary triangulation of the polygon.
- The triangle that contains the red point is illuminated.
- Neighboring triangles are illuminated and new visibility rays generated.
- All triangles which are at least partially visible have been traversed.



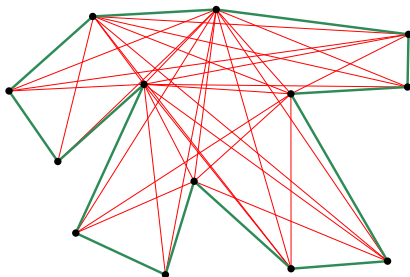
# Visibility Graph

## Definition 205 (Visibility graph, Dt.: Sichtbarkeitsgraph)

The *visibility graph* inside an  $n$ -gon  $P$  consists of the vertices of  $P$  as nodes which are connected by edges if the vertices can see each other.

## Theorem 206 (Ghosh&Mount (1991))

The full visibility graph inside an  $n$ -gon can be computed in time  $O(|E| + n \log n)$ , where  $|E|$  is the size of the visibility graph.



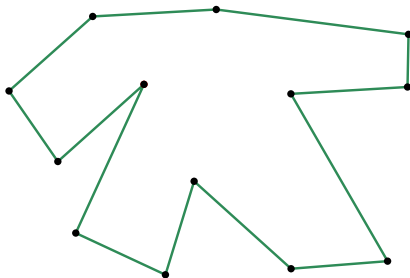
# Guarding an Art Gallery

## Problem: ARTGALLERYPROBLEM

**Given:** A simple polygon  $P$ .

**Select:** A minimum number of vertices of  $P$  such that every point of  $P$  can be seen from at least one of the vertices selected.

- Posed by Klee in 1973.
- The problem is  $\mathcal{NP}$ -hard.

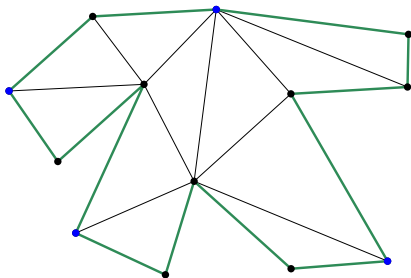


## Guarding an Art Gallery

### Theorem 207 (Chvátal (1975))

To guard a simple polygon with  $n$  vertices,  $\lfloor n/3 \rfloor$  guards are always sufficient and sometimes necessary.

*Sketch of Proof by Fisk (1978):* Consider an (arbitrary) triangulation of the polygon. One can show that the vertices of the triangulation graph are 3-colorable. Of course, vertices of one color form a valid set of guards. Hence, the color with the fewest vertices yields a valid set of at most  $\lfloor n/3 \rfloor$  guards. □



# Minimum Convex Decomposition

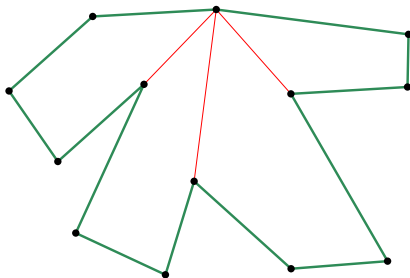
## Problem: MINIMUM CONVEX DECOMPOSITION

**Given:** A simple polygon  $P$ .

**Compute:** A minimum number of polygonal convex areas whose vertices match the vertices of  $P$ , whose interiors are disjoint and whose union equals  $P$ .

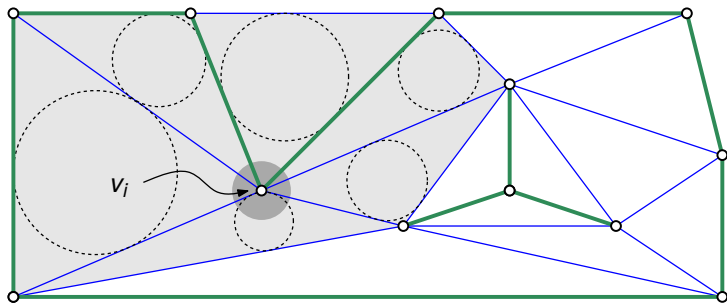
## Theorem 208 (Hertel&Mehlhorn (1983))

If a triangulation of  $P$  is given then an approximate convex decomposition with at most four times the minimum number of convex pieces can be obtained in linear time.



# Topology-Preserving Watermarking of Vector Graphics

- [Huber et al. (2014)] compute for each vertex a disk-shaped maximum perturbation region (MPR), based on the radii of the inscribed circles of a constrained triangulation of the input.
- Perturbing the vertices within their MPRs causes the edges to stay within their hoses and allows to preserve the input topology.
- This scheme can be extended to 3D.



## Robustness Problems and Real-World Issues

- Theory and Practice
- Introduction to Robustness Problems
- Approaches to Achieving Robustness
- Improving the Reliability of Floating-Point Code
- Real-World Applications and Experiences

## Theory and Practice

- Voronoi diagrams of points and segments and/or arcs are easy to understand, but notorious for being difficult to implement reliably. No surprise that very few decent Voronoi codes are known.
- The situation is similar for many other algorithms of computational geometry. That is, there is a gap between theory and practice . . .

### Benjamin Brewster (“The Yale Literary Magazine” 1882)

In theory, there is no difference between theory and practice. In practice, there is.

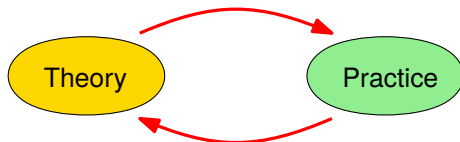
### Marie von Ebner-Eschenbach (1893)

Theorie und Praxis sind eins wie Seele und Leib, und wie Seele und Leib liegen sie größtenteils miteinander in Streit.

### Jan L.A. van de Snepscheut

The difference between theory and practice is larger in practice than the difference between theory and practice in theory.

What we'd need . . .



**Ayn Rand (Russian-born American writer and philosopher)**

Those who say that theory and practice are two unrelated realms are fools in one and scoundrels in the other.

**Folklore ☺**

Theory is when you know everything but nothing works. Practice is when everything works but no one knows why. However, we combine theory and practice: Nothing works and no one knows why.

# Floating-Point Arithmetic

- Computers employ floating-point arithmetic to perform real arithmetic.
- No matter how many bits are used, floating-point arithmetic represents a number by a fixed-length binary mantissa and an exponent of fixed size. E.g., according to the IEEE 754 standard, we have 23 bits for the mantissa and 8 bits for the exponent in case of 32-bit floats, and 52 bits and 11 bits in case of 64-bit doubles.
- Thus, only a finite number of values within a finite sub-interval of  $\mathbb{R}$  can be represented accurately; all other values have to be rounded to the closest number that is representable.
- The IEEE 754 standard for floating-point arithmetic knows four different rounding modes. The first mode is the default; the others are called directed roundings.

**Round to Nearest**

**Round towards 0**

**Round towards  $+\infty$**

**Round towards  $-\infty$**

## Chuck Allison

Floating-point numbers are not real numbers  $[\dots]$ . Real numbers have infinite precision and are therefore continuous and non-lossy; floating-point numbers have limited precision, so they are finite, and they resemble “badly behaved” integers, because they are not evenly spaced throughout their range.



# Floating-Point Errors

- There are two sources of error for floating-point computations: input error and round-off error.

**Input error:** It arises from reading/assigning a value to a floating-point variable.

- It is well-known that  $\frac{1}{3}$  cannot be represented by a finite sum of powers of 10.
- Similarly, 0.1 cannot be represented by a finite sum of powers of 2!
- What do we get if we assign  $2^{24} + 1 = 16777217$  to a 32-bit float? We get 16777216!
- Integers between  $2^n$  and  $2^{n+1}$  round to a multiple of  $2^{n-23}$  when assigned to a float.

**Round-off error:** It arises from rounding results of floating-point computations during an algorithm.

- E.g.,  $\sqrt{2}$  cannot be represented exactly since  $\sqrt{2}$  is an irrational number.
- While one can instruct the C command `printf` to print, say, 57 digits after the decimal separator, one will “only” get the digits of the closest value that is representable:

$$1/3 = 0.333333333333333314829616256247390992939472198486328125000$$

$$1/10 = 0.100000000000000005551115123125782702118158340454101562500$$



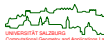
## Machine Precision

- The round-off error is bounded in terms of the *machine precision*,  $\varepsilon$ , which is the smallest value satisfying

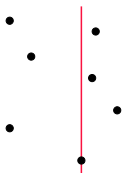
$$|fp(a \circ b) - (a \circ b)| \leq \varepsilon |a \circ b|$$

for all floating-point numbers  $a, b$  and any of the four operations  $+, -, \cdot, /$  instead of  $\circ$ , for which  $a \circ b$  does not cause an underflow or an overflow.

- On IEEE-754 machines,  $\varepsilon = 2^{-23} \approx 1.19 \cdot 10^{-7}$  for floats, and  $\varepsilon = 2^{-52} \approx 2.22 \cdot 10^{-16}$  for doubles.
- On some exotic platform,  $\varepsilon$  can be determined approximately by finding the smallest positive value  $x$  such that  $1 + x \neq 1$ .
- Note: Some compilers promote floats to doubles!



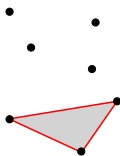
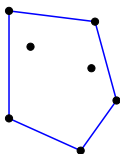
## Sorting



coordinate comparison

$$x_2 - x_1 > 0?$$

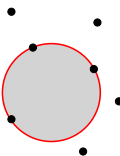
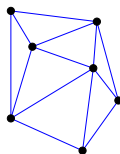
## Convex Hull



sidedness test

$$\begin{vmatrix} x_1 & y_1 & 1 \\ x_2 & y_2 & 1 \\ x_3 & y_3 & 1 \end{vmatrix} > 0?$$

## Delaunay Triangulation

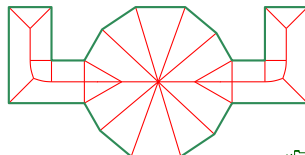


incircle test

$$\begin{vmatrix} x_1 & y_1 & x_1^2 + y_1^2 & 1 \\ x_2 & y_2 & x_2^2 + y_2^2 & 1 \\ x_3 & y_3 & x_3^2 + y_3^2 & 1 \\ x_4 & y_4 & x_4^2 + y_4^2 & 1 \end{vmatrix} > 0?$$

# Degeneracy

- Degeneracies are caused by the special position of two or more geometric objects. E.g.:
  - Two line segments that overlap partially rather than being disjoint or intersecting in a point.
  - Polygon edges that are parallel.
  - A Voronoi node of degree greater than three.
- Note: Degeneracies may be intentional, and real-world data should be assumed to be degenerate!
- The net result of degeneracies is a vastly increased number of so-called *special cases*.



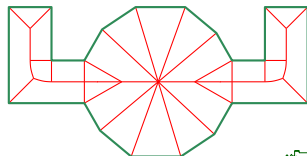
## Degeneracy Versus Numerical Precision

- How can we handle the special cases correctly?
- How can we even be sure that all special cases have been modeled?
- Typically, a degeneracy occurs if a predicate evaluates to zero.
- And, typically, predicates are evaluated by floating-point arithmetic.

**If a predicate evaluates to a value close to zero ...**

Is it a special case or simply a numerical inaccuracy??

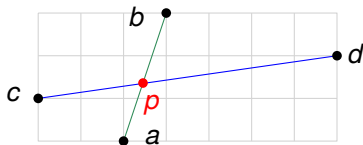
- The mere fact that a degeneracy cannot be classified reliably on a floating-point arithmetic complicates matters significantly.



## Sample Robustness Problem: Failure of Basic Mathematical Implications

- Suppose that we are given two line segments  $\overline{ab}$  and  $\overline{cd}$  in the plane such that

$$c_x < a_x < b_x < d_x \quad a_y < c_y < d_y < b_y.$$



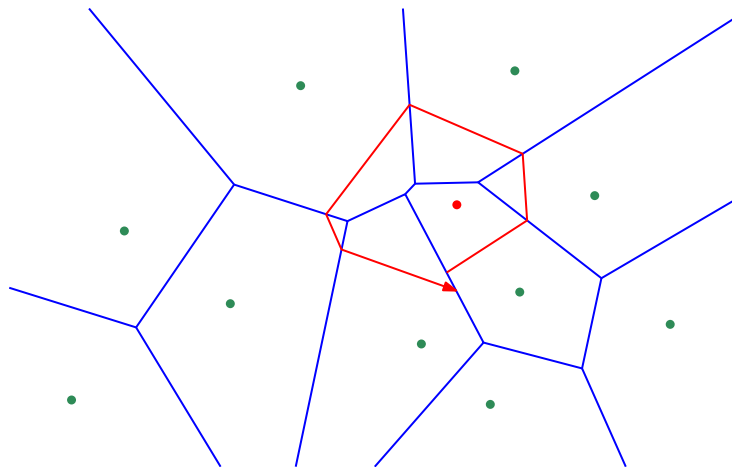
- It is easy to see that the two line segments intersect, without  $a$  or  $b$  lying on  $\overline{cd}$  and without  $c$  or  $d$  lying on  $\overline{ab}$ . In particular, the line segments cannot overlap. Hence, the two line segments intersect in a point.
- Let  $p := \overline{ab} \cap \overline{cd}$ . Are the following inequalities guaranteed to be true?

$$a_x < p_x < b_x \quad a_y < p_y < b_y \quad c_x < p_x < d_x \quad c_y < p_y < d_y$$

- Yes in theory, but no on a floating-point arithmetic!

## Sample Robustness Problem: Lack of Global Consistency

- Local consistency need not imply global consistency.



## Sample Robustness Problem: Incorrect Orientation Predicate

- [Kettner et alii 2006] study the standard determinant-based orientation predicate on IEEE 754 floating-point arithmetic to check the sidedness of  $(p_x + x \cdot u, p_y + y \cdot u)$  relative to two points  $q, r$ , for  $0 \leq x, y \leq 255$  and with  $u := 2^{-53}$ :

$$\text{sign det} \begin{pmatrix} p_x + x \cdot u & p_y + y \cdot u & 1 \\ q_x & q_y & 1 \\ r_x & r_y & 1 \end{pmatrix} \left\{ \begin{array}{l} > \\ = \\ < \end{array} \right\} 0 ?$$

- The resulting  $256 \times 256$  array of signs (as a function of  $x, y$ ) is color-coded: A yellow (red, blue) pixel indicates collinear (negative, positive, resp.) orientation.
- The black line indicates the line through  $q$  and  $r$ .
- Note the sign inversions!

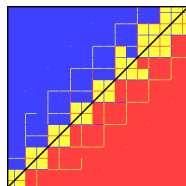
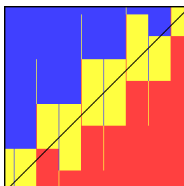
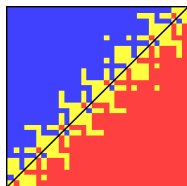
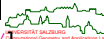


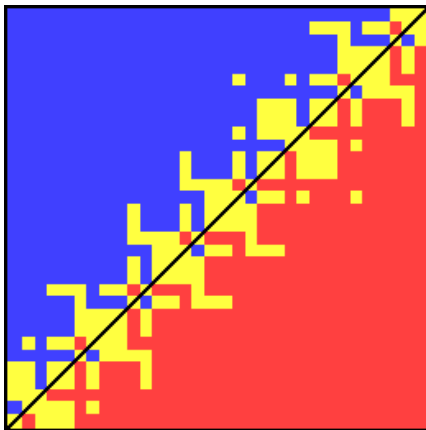
[Image credit: [www.mpi-inf.mpg.de/~kettner/proj/NonRobust/](http://www.mpi-inf.mpg.de/~kettner/proj/NonRobust/)]



## Sample Robustness Problem: Incorrect Orientation Predicate

- [Kettner et alii 2006]: A yellow (red, blue) pixel indicates collinear (negative, positive, resp.) orientation.

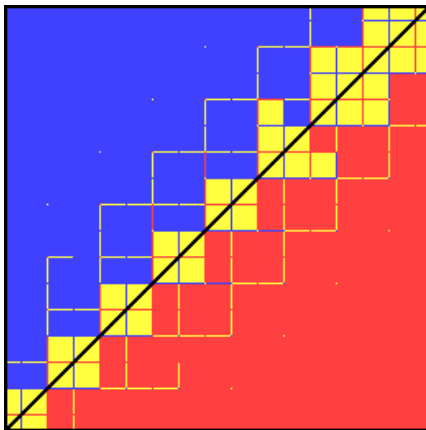
$$p := \begin{pmatrix} 0.5 \\ 0.5 \end{pmatrix} \quad q := \begin{pmatrix} 12 \\ 12 \end{pmatrix} \quad r := \begin{pmatrix} 24 \\ 24 \end{pmatrix}$$



## Sample Robustness Problem: Incorrect Orientation Predicate

- [Kettner et alii 2006]: A yellow (red, blue) pixel indicates collinear (negative, positive, resp.) orientation.

$$p := \begin{pmatrix} 0.5 \\ 0.5 \end{pmatrix} \quad q := \begin{pmatrix} 8.800000000000000007 \\ 8.800000000000000007 \end{pmatrix} \quad r := \begin{pmatrix} 12.1 \\ 12.1 \end{pmatrix}$$



# Approaches to Improving Robustness

- Several approaches have been proposed in recent years:
  - Error analysis.
  - Exact arithmetic (on integers, rationals, or even algebraic numbers).
  - Exact geometric computing.
  - Floating-point filters.
  - Symbolic perturbation.
  - Epsilon thresholds and sophisticated tolerancing.
- No agreement on the best approach . . .
- All methods have shortcomings, typically also limited applicability — or they suffer from inefficiency!

## Exact Arithmetic

- Input is assumed to be exact.
- Compute the numerical value of every predicate exactly, based on exact number types.
- Exact computation is possible if all numerical values are algebraic. (This is the case for most current problems in computational geometry.)
- Note: We may no longer assume that each arithmetic operation takes constant time!
- Note: Constructors complicate the situation significantly!

# Exact Number Types

**Bigint:** Arbitrary-precision integers.

- Usually based on Karatsuba's multiplication algorithm, with  $\Theta(b^{\log_2 3}) \equiv \Theta(b^{1.58\dots})$  complexity for multiplying  $b$ -bit numbers.
- See, e.g., GNU's GMP library <http://gmplib.org/>.

**Bigrational:** Quotients of bigints.

- Standard rational arithmetic.
- It is important to reduce fractions frequently.
- Euclid's algorithm can be used for finding common factors.
- See, e.g., GMP's `mpq_t` number type.

**Algebraic numbers:** Roots of polynomials with bigint coefficients.

- Complexity of deciding equality grows with the number of operators allowed.
- [Caviness (1967)] proved undecidability of functional equivalence for moderately complicated terms.

**Homogeneous coordinates:** Not exactly a number type.

- Can often be used to avoid divisions.
- It is important to reduce fractions frequently.
- Most predicates can be expressed directly in terms of homogeneous coordinates.



# Exact Geometric Computing

- Do we really need exact arithmetic for solving geometric problems?
- Not quite! Or, at least, not always! → Exact geometric computing (EGC).
- Input is assumed to be exact.
- Basic idea: Make sure that the sign of every predicate is evaluated correctly.
- Error analysis is needed to come up with *root bounds*: A positive number  $r$  forms a root bound for a predicate  $p$  if  $|p(x)| > r$  guarantees that the evaluation of  $p$  for  $x$  yields the correct sign.
- Main problems:
  - Arbitrary-precision arithmetic is needed.
  - Tight root bounds are difficult to obtain.
  - Constructors may cause the bit-length to grow tremendously.
- The use of floating-point filters may help to keep the increase in CPU time consumption a bit more moderate:
  - Work with floating-point arithmetic and check whether it gives the right answer.
  - Resort to extended-precision or exact arithmetic if the answer is incorrect.
  - Great example: Shewchuk's fine (and efficient!) CDT code "Triangle" [Shewchuk (1996)].
- Software libraries that provide support for EGC: CORE, CGAL, and Mörig's `RealAlgebraic` data type.

- Aka: Simulation of simplicity [Edelsbrunner&Mücke (1990)].
- Basic idea: Perturb input such that no degeneracies occur.
- Roughly, each coordinate  $x$  is replaced by  $x + f(\varepsilon)$ , where  $\varepsilon$  is unknown but very small and the perturbation function  $f$  is simple, e.g, a polynomial.
- Symbolic perturbation transforms the result of a numerical predicate into a polynomial in  $\varepsilon$ , whose sign is given by the sign of the first non-zero coefficient.
- For several important types of predicates perturbation functions can be chosen such that all degeneracies are resolved.
- Main problems:
  - Exact arithmetic is required for evaluating the predicates.
  - Constructors are often disallowed.
  - Computational or combinatorial complexities may change substantially. E.g., the arrangement of  $n$  lines that intersect in one common point has  $\Theta(n)$  complexity whereas an arrangement of the perturbed lines will have  $\Theta(n^2)$  complexity.
  - The output computed does not correspond to the actual input.
  - Intentional degeneracies in the input are “resolved”, too!
  - Similar to EGC codes, it is extremely difficult to interface a code based on SoS with a code based on conventional floating-point arithmetic.

## Epsilon Thresholds

- Topological decisions are based on the results of floating-point computations, which are prone to round-off errors.
- Threshold-based comparison:

$$(a =_{\epsilon} b) : \iff (|a - b| \leq \epsilon),$$

for some positive value of  $\epsilon$ .

### Caveat!

Threshold-based comparisons are not transitive:  $a =_{\epsilon} b$  and  $b =_{\epsilon} c$  need not imply  $a =_{\epsilon} c$ .

- This gap between theory and practice once again has important and severe consequences for the actual coding practice when implementing geometric algorithms:

### No guarantee for success!

- 1 The correctness proof of a mathematical algorithm does not extend to the program, and the program can fail on seemingly appropriate input data.
- 2 Local consistency need not imply global consistency.

## Standard Tricks for Achieving Reliable Floating-Point Code

- Try to perform all numerical computations relative to the original input data.
- All floating-point computations need to be consistent! In particular, make sure that different calls of the same function with the “same” input will yield exactly the same output. E.g., when computing  $3 \times 3$  determinants, we need

$$\begin{aligned}\det(p, q, r) &= \det(q, r, p) = \det(r, p, q) \\ &= -\det(q, p, r) = -\det(p, r, q) = -\det(r, q, p).\end{aligned}$$

- Do not resort to multiple precision thresholds! At most two thresholds: One to avoid divisions by zero, and another threshold to catch “nearly zero” numbers.
- Epsilon-based comparisons need to be relative to the absolute values of the numbers to be compared, or the input has to be scaled (by performing shifts!) to fit into the unit square/cube prior to the actual computation.
- Use iterations as back-up for analytical solutions to equations. If at all possible, use methods that bracket the solution sought!
- Algebraically equivalent terms need not be equally reliable on a floating-point arithmetic. E.g., consider the quadratic equation  $x^2 + px + q = 0$  and compare

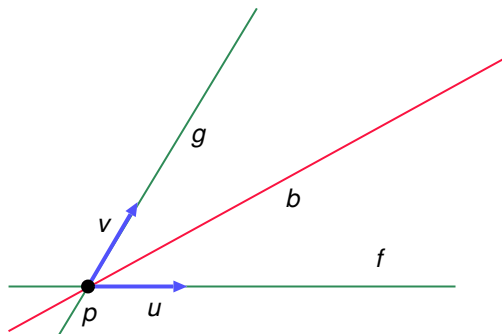
$$\left\{ \begin{array}{l} x_1 := -\frac{1}{2}(p + \sqrt{p^2 - 4q}) \\ x_2 := -\frac{1}{2}(p - \sqrt{p^2 - 4q}) \end{array} \right\} \quad \text{to} \quad \left\{ \begin{array}{l} x_1 := -\frac{1}{2}(p + \text{sign}(p)\sqrt{p^2 - 4q}) \\ x_2 := q/x_1 \end{array} \right\}$$

if  $|q|$  is small.



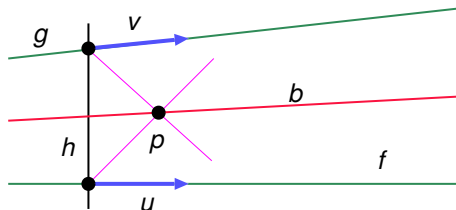
## Case Study: Computing Voronoi Bisectors

- Algorithm for computing a bisector  $b$  between two lines  $f$  and  $g$  which are not parallel:
  - Compute their point of intersection:  $p$ .
  - Compute unit direction vectors  $u$  and  $v$  of  $f, g$ .
  - Then a parametrization of  $b$  is given by  $p + t \cdot (u + v)$ .
- This “natural” approach to computing  $b$  becomes completely infeasible if  $f$  and  $g$  are nearly parallel. (In that case the computation of  $p$  will become very unreliable!)



## Case Study: Computing Voronoi Bisectors

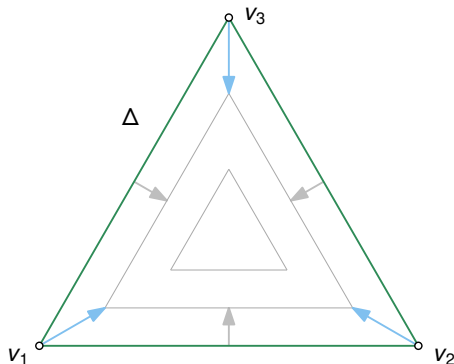
- Algorithm for computing a bisector  $b$  between two lines  $f$  and  $g$  which are roughly parallel:
  - Compute a line  $h$  that is normal on  $f$ .
  - Compute the bisector  $b_1$  between  $h$  and  $f$ , and the bisector  $b_2$  between  $h$  and  $g$ .
  - Compute their point of intersection:  $p$ .
  - Compute unit direction vectors  $u$  and  $v$  of  $f, g$ .
  - Then a parametrization of  $b$  is given by  $p + t \cdot (u + v)$ .



- Note: All intersections are defined by pairs of lines that are roughly perpendicular.

## Case Study: Collapse Time of Kinetic Triangle

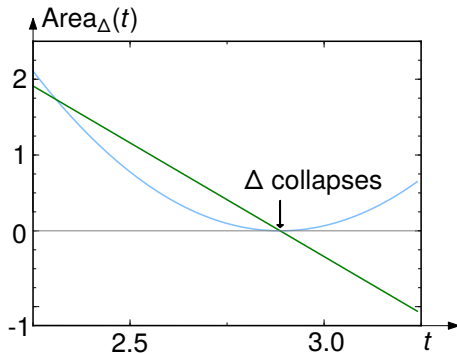
- Suppose that all three vertices  $v_1$ ,  $v_2$ ,  $v_3$  of a triangle  $\Delta$  move along straight-line paths (modeled as functions of time), and that we are interested in knowing when the triangle collapses. (That is, when it has zero area.)



- How can we determine the time(s) of collapse?

## Case Study: Collapse Time of Kinetic Triangle

- Which option is better?
  - 1 Check the signed area of the triangle, e.g., as obtained by means of determinant computations.
  - 2 Check the signed distance of a kinetic vertex to its opposite edge.

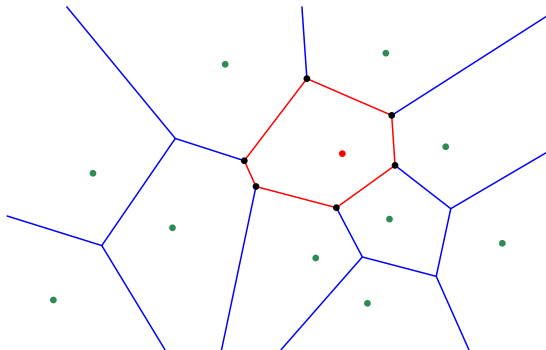


# Topology-Oriented Computation

- First used by Sugihara et alii [1992, 2000].
- Basic idea:
  - 1 Define topological criteria that the output has to meet.
  - 2 Use floating-point computations to choose among different geometric set-ups if two or more set-ups fulfill all topological criteria.
- Main problem: For many problems it is difficult to formulate meaningful topological criteria.
- Sample application: When inserting a new site into a Voronoi diagram (during an incremental construction), the portion of the old Voronoi diagram to be deleted forms a tree.

# Topology-Oriented Computation

- The portion of the Voronoi diagram to be deleted forms a tree.
- We start at the closest Voronoi node and scan the Voronoi diagram for nodes to be deleted, making sure that no cycle occurs.
- All Voronoi nodes found by this scan are deleted, and their incident bisectors are shortened appropriately.
- All that remains to be done is to compute the new Voronoi nodes, which form the corners of the new Voronoi polygon, and to link them in cyclic order.



## Relaxation of Epsilon Thresholds

- Common practice: Use epsilon thresholds for comparisons with respect to zero.
- The test “ $x = 0$ ?” is replaced by the test “ $|x| \leq \epsilon$ ?”, for some positive value of  $\epsilon$ .
- Just what is an appropriate value for  $\epsilon$ ?
- Asking the user of a geometric code to choose an appropriate precision threshold comes close to asking for witch-craft.
- To make the situation worse, experience tells me that one fixed precision threshold will rarely suffice to handle all sorts of different input data.
- Alternate approach:
  - A natural lower bound  $\epsilon_{min}$  for a suitable threshold is given by the machine precision of the machine used.
  - The user specifies the maximum distance that two points (out of the unit square) may be apart in order to allow the code to treat them as one point. This yields an upper bound  $\epsilon_{max}$ .
  - The code varies  $\epsilon$  at its own discretion, always attempting to succeed with the smallest  $\epsilon$  possible, i.e., with maximal precision.

# Relaxation of Epsilon Thresholds

## Algorithm *Typical Computational Unit*

1.  $\varepsilon = \varepsilon_{min}$ ; (\* set epsilon to maximum precision \*)
2. **repeat**
3.    $x = \text{ComputeData}(\varepsilon)$ ; (\* compute some data \*)
4.    $\text{success} = \text{CheckConditions}(x, \varepsilon)$ ; (\* check topological/numerical conditions \*)
5.   **if** ( not success ) **then**
6.      $\varepsilon = 10 \cdot \varepsilon$ ; (\* relaxation of epsilon threshold \*)
7.     reset data structures appropriately;
8.   **until** ( success OR  $\varepsilon > \varepsilon_{max}$  );
9.    $\varepsilon = \varepsilon_{min}$ ; (\* make sure to reset epsilon \*)
10. **if** ( not success ) **then**
11.    $\text{illegal} = \text{CheckInput}()$ ; (\* check locally for soundness of input \*)
12.   **if** ( illegal ) **then**
13.     clean data locally; (\* fix the problem in the input data \*)
14.     restart computation from scratch;
15.   **else**
16.      $x = \text{DesperateMode}()$ ; (\* time to hope for the best \*)

## Desperate Mode

- What shall we do if computing  $x$  would require an invalid operation, e.g., a division by zero or taking the square root of a negative number?
- After all,  $x$  may be needed for subsequent computations! E.g., if a new Voronoi node is to be inserted into the Voronoi diagram then the code may subsequently need to access the coordinates of this node.
- Desperate mode: Replace “correct” or “optimum” by “best possible”.
  - Do not use any operation which is not defined for all floating-point numbers.
  - Any violation of a topological condition is “cured” by forcing its validity. E.g., a cycle of Voronoi nodes can be broken by inserting a new dummy node on one of the edges of the cycle.
  - If numerical data does not fulfill all numerical conditions then accept the data whichever meets most of them.
- Net result: A code that resorts to desperate mode will never get stuck, crash or loop. (Well, at least in theory . . .)
- Whether or not the output still is of practical use despite of desperate mode depends on the application and the type of problem that caused desperate mode.
- Personal experience: Desperate mode works remarkably well for “incremental” algorithms!

## Desperate Mode and Epsilon Relaxation: Caveats

- The relaxation of epsilon thresholds does not come for free: Repeatedly computing some data will increase the CPU time consumption.
- Always attempt to perform a computation as it would be performed normally, irrelevant of whether or not desperate mode was used once before.
- Keep track of how often your code resorts to an actual relaxation: Frequent use of epsilon relaxation is a hint that the numerical reliability of your code is less than ideal.

### Warning

The availability of such a multi-phase recovery process can easily conceal genuine algorithmic flaws or bugs!

### Important advice

Always test your code with desperate mode being disabled! Robustness without desperate mode is a must for *all* tests on *your* test data!

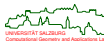
## Adding an MPFR Backend

- GNU's MPFR library ([www.mpfr.org](http://www.mpfr.org)) is a C library for multiple-precision floating-point computations.
- Canonical adaptations:
  - Precision threshold  $\varepsilon$  needs to depend on MPFR precision.
  - [Held&Huber (2013)] use a heuristic formula:

$$\varepsilon := \varepsilon_{\text{fp}} \cdot 2^{-100 \cdot (\sqrt{\text{prec}/53} - 1)},$$

where  $\varepsilon_{\text{fp}}$  is the machine precision.

- Subtle problem encountered: `mpfr_set_default_prec` does not change existing variables.
  - Global variables are not adjusted.



## Real-World Data

- Real-world data often means no quality at all:
  - raster-to-vector conversions,
  - data cleaned up manually or “visually”,
  - data preprocessed by some dubious program of unknown origin,
  - data comes from “an important customer” or from “God knows where”.
- As a consequence:
  - all sorts of degeneracies,
  - self-intersections,
  - tiny gaps in supposedly closed contours.

### Advice

Be prepared for troubles — general position must not be assumed!

### If the implementation ends up in an invalid algorithmic state ...

Is it due to

- a bug in the implementation,
- a genuine numerical problem, or
- invalid input data?



## Data size:

- Data sizes vary substantially from a few hundred segments/arcs in a machining application to a few million segments in a GIS application, or even tens of millions of segments/arcs in the PCB business if arcs are approximated by segments.

## Efficiency requirements:

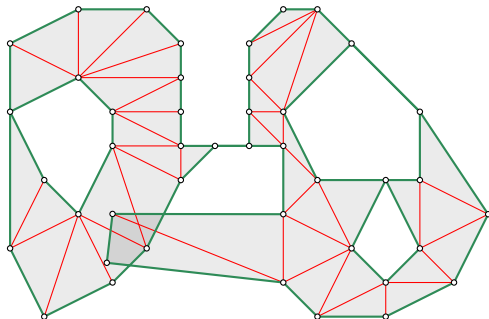
- Efficiency requirements vary substantially from real-time map generation on a smart phone to minutes of CPU time allowed on some high-end machine.
- In general, linear space complexity and a close-to-linear time complexity is expected.

## Parallelization requirements:

- Exactly one inquiry concerning GPU-based codes so far.
- Only moderate interest in multi-core computing and multi-threaded implementations.

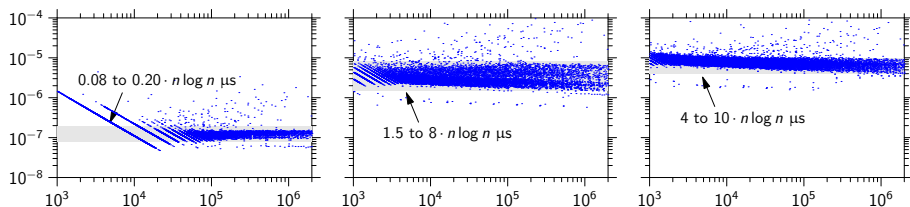
# Software for Triangulating Polygons: FIST

- [Held (2001)]: FIST triangulates polygons with holes in 2D and 3D,
  - based on ear-clipping and
  - multi-level geometric hashing to speed up computation.
- Handles
  - degenerate input,
  - self-overlapping input,
  - self-intersecting input,
  - Steiner points.
- No Delaunay triangulation, but heuristics to generate “decent” triangles.
- Runs in close-to-linear time in practice.
- ANSI C code based on IEEE 754 floating-point arithmetic, with careful engineering to ensure reliability. Thread-safe.
- [Eder&Held&Palfrader (2018)]: Heuristics for coarse-grain parallelization.
- Typical applications in industry: Triangulation of (very) large GIS datasets, triangulation of “planar” faces of 3D models.



## Experimental Results for Triangulations

- 21 175 polygons with and without holes.
- Six arithmetic configurations:
  - fistFp, fistShew, fistCore, fistMp{53, 212, 1000}
- Conclusion:
  - Shewchuck's predicates have negligible impact on speed.
  - fistMp\* about 24 times slower than fistFp.
  - fistCore about 50 times slower than fistFp.



Runtime per seconds divided by  $n \log n$ , for fistFp, fistMp212, fistCore.

## Held&Mann (2011)

### Correctness of FIST triangulations with floating-point arithmetic?

- Verification code:
  - Bentley-Ottmann algorithm, implemented with exact `mpq_t` from GMP.
- **Scenario 1:**
  - We interpret `0.1` in input files as  $\frac{1}{10}$ .
  - 4.9% of all results faulty, uniformly across all non-CORE configurations.
    - Including `fistShew`.
  - But: Error only visible at huge zoom factors.
- **Scenario 2:**
  - We take `0.1` as closest floating-point number using `atof()`.
  - No errors found!

## Conclusion

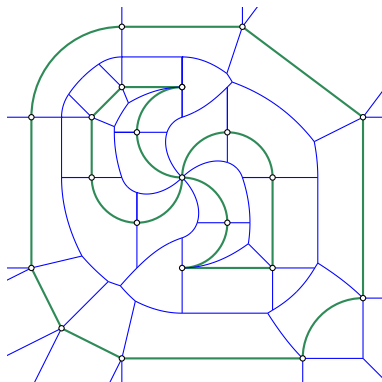
Non-exactness need not be a practical issue in pure floating-point applications.



- Segment-Delaunay-Graph implemented within CGAL by [Karavelas (2004)].
- Input:
  - Points and straight-line segments;
  - Input sites may intersect arbitrarily;
  - No support for circular arcs.
- Incremental construction.
- Complexity:
  - $O((n + m) \log^2 n)$  expected time, where  $n$  is the number of sites and  $m$  is the number of intersections.
  - $O((n + m) \log n)$  in practice.
- CPU-time consumption is claimed to be mostly insensitive to the number type used.

# Software for Computing Voronoi Diagrams: VRONI and ARCVRONI

- [Held (2001), Held&Huber (2009)]: VRONI/ARCVRONI computes Voronoi diagrams
  - of points, straight-line segments and circular arcs (input “sites”),
  - based on randomized incremental construction and a topology-oriented approach.
- Also computes
  - maximum-inscribed circle,
  - medial axis, and
  - offset curves.
- Complexity:
  - $O(n)$  space complexity, where  $n$  is the number of sites.
  - $O(n \log n)$  expected time.
- Based on standard IEEE 754 floating-point arithmetic, with careful engineering, epsilon relaxation and desperate mode.
- Typical applications in industry: generation of tool paths (e.g., for machining or sintering), generation of buffers in GIS applications.



## Codes tested:

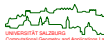
- CGAL 3.8 (cgvdEx, cgvdFp):
  - `CORE::Expr` as predicate kernel.
  - `Segment_Delaunay_graph_filtered_traits_2` template parameter to the underlying segment Delaunay graph class.
  - Graphics disabled, input stream-lined, own timing routine added.
  - Compiled with `g++ -O2`.
- VRONI 6.0 (vroniFp, vroniMp{53, 212, 1000}):
  - Also compiled with `g++ -O2`.

## Test platform:

- 3.33GHz i7 CPU X 980; 24GB RAM; 64bit Ubuntu.
- All timings given in CPU microseconds.

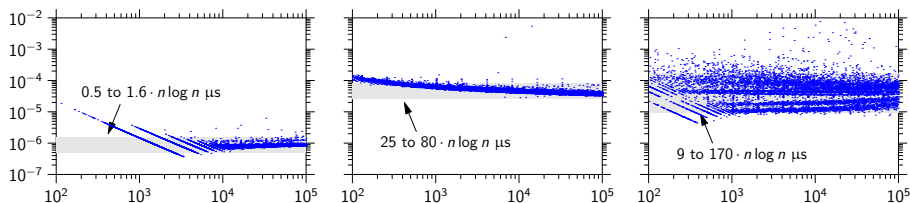
## Test data:

- Synthetic and real-world data; circular arcs approximated by polygonal chains.
- 18 787 data sets tested, with  $200 \leq \#(\text{segs}) \leq 100\,000$ .



# Experimental Results for Voronoi Diagrams

- Conclusion:
  - vroniFp about 50–60 times faster than vroniMp\*.
  - vroniFp about 20–100 times faster than cgvd\*.
  - cgvdFp only 1.5 times faster than cgvdEx.
    - Crashed on 937 datasets due to floating-point exception.
  - On average, cgvdEx is slightly faster than vroniMp\*.
    - cgvdEx timings vary by a factor of 20.
    - A few cgvdEx results were numerically clearly wrong.



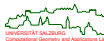
Runtime per seconds divided by  $n \log n$ , for vroniFp, vroniMp212, cgvdEx.

## Experimental Results for Voronoi Diagrams

- [Held&Mann (2011)]: Implemented a verifier based on GMP's `mpq_t` data type.
- Brute-force all-pairs distance computations used.
- Hence, verification was limited to small inputs with up to 2 000 segments.

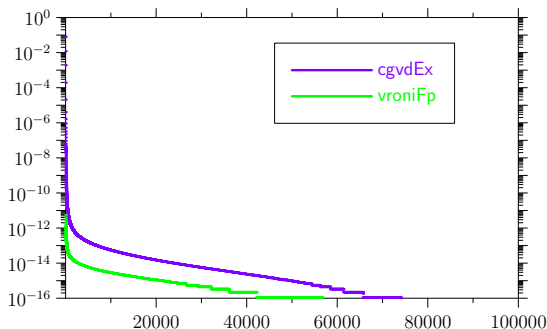
**Deviation:** Difference in the distances of a node to its defining sites.

**Violation:** Another site is closer to a node than defining sites.



# Experimental Results for Voronoi Diagrams

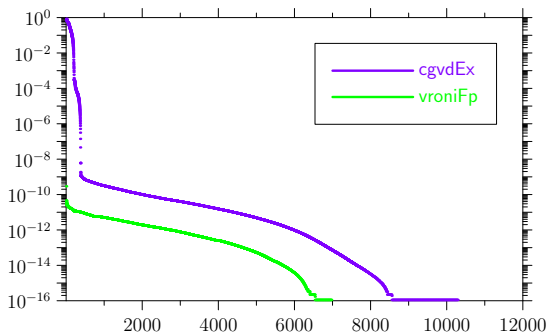
- Deviation: Difference in the distances of a node to its defining sites.



	VRONI	CGAL
maximum:	$7.25 \cdot 10^{-8}$	$8.04 \cdot 10^{-1}$
median:	$2.22 \cdot 10^{-16}$	$3.10 \cdot 10^{-15}$

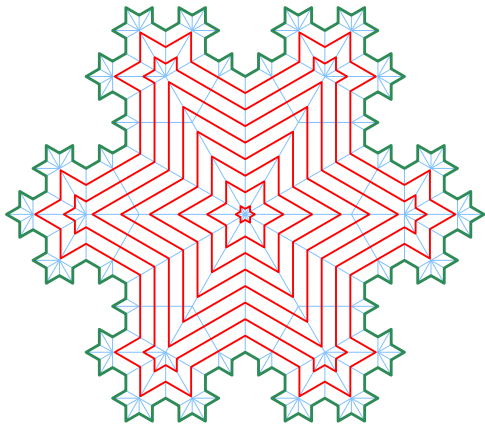
# Experimental Results for Voronoi Diagrams

- Violation: Another site is closer to a node than defining sites.



	Vroni	CGAL
maximum:	$1.75 \cdot 10^{-6}$	$9.14 \cdot 10^{-1}$
median:	$3.87 \cdot 10^{-14}$	$3.94 \cdot 10^{-12}$

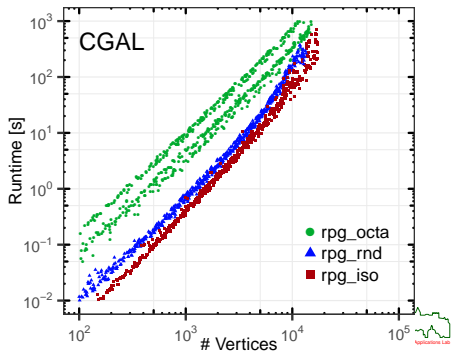
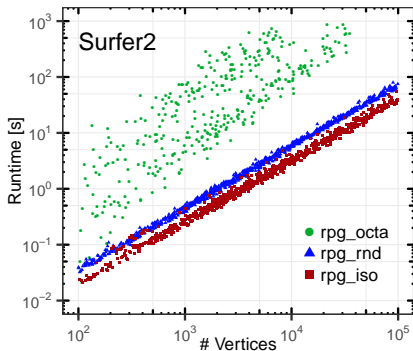
- [Held&Palfrader (2012–2020)]: SURFER, SURFER2
  - compute straight skeletons of planar straight-line graphs,
  - simulate the wavefront propagation based on kinetic triangulations.
- SURFER also computes mitered offset curves.
- SURFER2 handles weighted straight skeletons, too.
- Complexity:
  - $O(n)$  space complexity, where  $n$  is the number of segments.
  - $O(n \log n)$  average time complexity,  
 $O(n^3 \log n)$  worst-case time complexity.
- SURFER is based on standard IEEE 754 floating-point arithmetic.
- SURFER2 is based on exact geometric computing.



# Experimental Results for Straight Skeletons

## Eder&Held&Palfrader (2020)

- SURFER2: Based on CGAL's exact-predicates-exact-constructions algebraic kernel with square root, which is backed by CORE's `Core::Expr` exact number type.
- CGAL 5.0: Based on exact-predicates-inexact-constructions algebraic kernel.

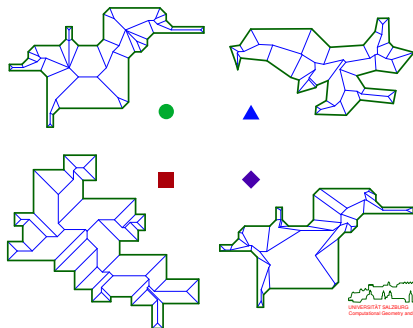
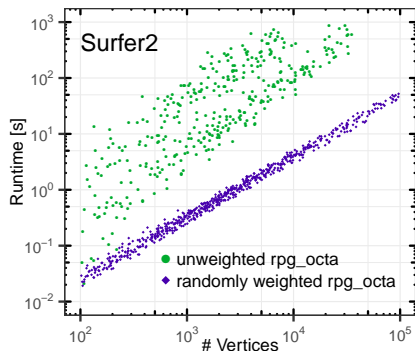


# Experimental Results for Straight Skeletons

Eder&Held&Palfrader (2020)

Multiple events that occur simultaneously have a significant impact on the practical runtime of SURFER2 if the `CORE::Expr` number type is used!

- That is, using the `CORE::Expr` number type forces one to abandon the concept of unit-cost comparisons!



# The End!

I hope that you enjoyed this course, and I wish you all the best for your future studies.

